HIGH-THROUGHPUT ASSAYS FOR BIOTIN PROTEIN LIGASE : A NOVEL ANTIBIOTIC TARGET

by

Belinda Ng Ling Nah, BSc in Industrial Biology (Hons)

A thesis submitted to the University of Adelaide in fulfillment of the requirement for the degree of Master of Science

School of Molecular & Biomedical Science
The University of Adelaide
Adelaide, South Australia, 5005

January 2009

TABLE OF CONTENTS

ABSTRACT

Antibiotics are defined as chemical substances that inhibit or limit the growth of microorganisms. Since the second world war, antibiotics have been widely used to reduce the morbidity and mortality associated with serious bacterial infections caused by organisms such as *Staphylococcus aureus*. However, it has become increasingly difficult to treat bacterial infections due to the emergence of antibiotic resistant strains. The first clinical case of drug resistant bacteria was observed in *S. aureus* in 1947, just four years after the mass production of penicillin. Since then, resistance has been reported to every antibiotic ever employed. According to the Centres for Disease Control and Prevention of the United States, more than 70% of hospital-acquired infections show resistance to at least one commonly used antibiotic. Coupled with the paucity of therapeutic agents in the pipeline, there is now an urgent demand for new antibiotics. One of the strategies employed to combat drug resistant bacteria requires new chemical entities that work through novel drug targets for which there is no pre-existing resistance. This thesis focuses on the essential metabolic enzyme biotin protein ligase (BPL) as one such new drug target.

BPL is the enzyme responsible for covalently attaching the cofactor biotin prosthetic group onto the biotin-dependent enzymes such as the carboxylases, decarboxylases and transcarboxylases. Enzymatic biotinylation proceeds via a two-step reaction whereby biotinyl-5'-AMP is synthesized from biotin and ATP before the biotin moiety is transferred onto the side chain of one specific lysine present in the active site of the biotin-dependent enzyme. One example of an important biotin-dependent enzyme is acetyl CoA carboxylase (ACC). ACC catalyzes the first committed step in fatty acid

biosynthesis. Through genetic studies, it has been demonstrated that BPL activity is essential for bacterial survival.

The aim for this project was to develop a convenient, high-throughput assay to measure BPL activity. This assay would permit 1) quantitative kinetic analysis of ligands and inhibitors and 2) screening of compound libraries for new BPL inhibitors. We propose that BPL inhibitors can be developed into new antibiotic agents. The novel BPL assay was developed employing fluorescence polarization (FP). FP is a light based technique which uses plane polarized light for the detection of tumbling motion of fluorescent molecules in solution. As polarization of the emitted light is relative to the apparent molecular mass of the fluorophore, this technique can be use for quantitation of changes in molecular mass of target molecules. This enabled 1) rapid kinetic analysis, 2) a minimal number of handling steps, 3) no washing steps and 4) automation by robotics.

A first generation assay was developed for *Escherichia coli* BPL using peptide 85-11 that has been shown to be a convenient substrate. Following the BPL reaction, biotinylated peptides will form large molecular mass complexes with avidin. The amount of product could then be quantitated using FP. Here, kinetic analysis of MgATP (K_m 0.25 ± 0.01 mM) and biotin (K_m 1.45 ± 0.15 μM) binding produced results consistent with published data. We validated this assay with inhibition studies with end products of the BPL reaction, AMP and pyrophosphate, and a compound, biotinol-5'-AMP. Statistical analysis, performed upon both intraassay and interassay results (n = 30), showed the coefficient of variance to be <10% across all data sets. Furthermore, the Z' factors between 0.5 and 0.8 demonstrated the utility of this technology in high-throughput applications. However, the use of peptide 85-11, a substrate specific to *E. coli* BPL, does limit the application of this methodology to *E. coli*.

In the second generation FP assay, I adapted this technology for *S. aureus* BPL by employing the biotin domain of *S. aureus* pyruvate carboxylase. Insertion of a fluorescein label was achieved by first engineering a cysteine residue into the domain by site directed mutagenesis then incubation with fluorescein-5'-maleimide. A series of mutants was created to investigate optimal positioning of the label into the substrate. Furthermore, the minimal size of the functional domain was determined. Our data showed that the placement of the fluorescein label is an important aspect of this project. Using this approach, I identified that a 90 amino acid domain with the label at position 1134 was optimal. Kinetic analysis of ligand binding showed *Sa*BPL had a K_m for biotin at 3.29 ± 0.37 µM and K_m for MgATP at 66 ± 16.08 µM. This was in good agreement with data obtained from our previous assay measuring ^{3}H-biotin incorporation. Inhibitor studies with pyrophosphate and analogues of biotin and biotinyl-5'-AMP further validated the assay.

Various studies have shown cross-species biotinylation activities by a diverse range of BPLs. Therefore, using this methodology with a biotin domain as the substrate potentially provides a convenient assay for all BPLs.

STATEMENT OF ORIGINALITY

This thesis contains no material that has been accepted for the award of any other degree or diploma in any university or other tertiary institution and, to the best of my knowledge and belief, contains no material that has been previously published or written by another person, except where due reference has been made in the text.

I consent to this thesis, when deposited in the University library, being made available for loan and photocopying, subject to the provisions of the Copyright Act 1968.

.....

Belinda Ng Ling Nah

ACKNOWLEDGEMENTS

I would like to take this opportunity to express my deepest gratitude and appreciation to all the wonderful people who are directly and indirectly involved in the completion of this study:-

First of all, I would like to thank my supervisors, Assoc. Prof. Grant Booker and Dr. Steven Polyak for giving me the opportunity to participate in this research. Your dedication, priceless advice and time spent are very much appreciated. I humbly acknowledge the breadth of perspective and experience that I have gained, professionally and personally, under your guidance.

Thanks also to Prof. John Wallace who is always ready to impart his knowledge and experience. To all the past and present members of the BPL team – Assoc. Prof. Mathew Wilce (Monash University), Prof. Andrew Abell, Dr. Daniel Pedersen, Dr. Renato Morona, William, Kevin, Nicole, Lisa, Lingusa and Daniel – thank you for the helpful discussion and valuable advice on matters regarding BPL. Your efforts had contributed tremendously to the success of this work. Iain and Cvetan – really appreciate your help and advice pertaining *in-silico* screening and FP assay. To the other members of Booker Lab (Hui, Philippa, Ethan and John) and Wallace lab (Dr. Briony, Clair, Carlie, Shee Chee and Kerrie), thank you all for making this such an enjoyable journey for me. Your caring nature and friendship has made my time in Australia an experience that far surpassed my expectation, one of which I will never forget.

I would also like to acknowledge the Sarawak Government and Sarawak Biodiversity Centre for giving me this tremendous opportunity. Without their funding and support, it will be impossible for me to further my studies here in Adelaide.

Above all, my biggest thanks to my family especially *Papa* and *Mummy*. For as long as I remember, you are always there to provide me with all the support, encouragement and help I could ever ask for. Your unceasing love and care has shaped me to be the person I am today. "*Che*" and Hui, thanks for constantly keeping me in your prayer. Not forgetting a special thanks to Yew Zion. Thank you for your unyielding love, support, understanding and patience all this while. There is no word to express my gratitude for what you all have done for me.

Last but none the least, I would like to thank all my relatives and friends especially Michele and Mei Mei, and those I have failed to mention here. Your support, care and encouragement have kept me going when things are not going well. I am truly blessed to have you all as part of my life.

"Praise God for all His grace and blessings!"

LIST OF FIGURES

LIST OF TABLES

LIST OF PUBLICATIONS

Refereed journal :

Ng, B., Murchland, I., Abell, A. D., Wilce, M. C., Wallace, J. C., Polyak, S. W. and Booker, G. W. (2008) "Engineered biotin domains as fluorescent substrates for biotin protein ligase," *Analytical Biochemistry* - Submitted

Ng, B., Polyak, S. W., Bird, D., Bailey, L., Wallace, J. C. and Booker, G. W. (2008) "*Escherichia coli* biotin protein ligase: characterization and development of a high-throughput assay," *Analytical Biochemistry* 376 (1): 131-136

Conference abstracts :

Ng, B., Pendini N.R., Tieu W., Kuan K., Morona R., Abell A., Wilce M.C.J., Wallace J.C., Polyak S.W. and Booker G.W. (2008) Discovery of biotin protein ligase as a novel class of antibiotic. *University of Adelaide, School of Molecular and Biomedical Sciences Research Symposia* pos 12

Ng, B., Pendini N.R., Tieu W., Kuan K., Morona R., Abell A., Wilce M.C.J., Wallace J.C., Polyak S.W. and Booker G.W. (2008) Discovery of biotin protein ligase as a novel class of antibiotic. *ComBio2008* pos WED-024

Ng, B., Pendini, N., Tieu, W., Kuan, K., Morona, R., Wallace, J. C., Wilce, M., Abell, A., Booker, G. W. & Polyak, S. W. (2008) Inhibitor of biotin protein ligase: a novel class of antibiotics for the treatment of *Staphylococcus aureus. Australian Society for Medical Research SA division Scientific Meeting*

Ng, B., Bird, D., Wallace, J. C., Booker, G. W. & Polyak, S. W. (2008) *Escherichia coli* biotin protein ligase: Development and validation of a high throughput assay. *Australian Society for Medical Research SA division Scientific Meeting* pos 11

Ng, B., Bird, D., Wallace, J. C., Booker, G. W. & Polyak, S. W. (2008) *Escherichia coli* biotin protein ligase: Development and validation of a high throughput assay. *Proc. Lorne Conference on Protein Structure and Function* pos 362

Ng, B., Bird, D., Wallace, J. C., Booker, G. W. & Polyak, S. W. (2007) Biotin protein ligase: A novel antibiotic target. *South Australian Division AUSBIOTECH Students Association Student Awards.* **Finalist

Ng, B., Bird, D., Wallace, J. C., Booker, G. W. & Polyak, S. W. (2007) *Escherichia coli* biotin protein ligase: Development and validation of a high throughput assay. *University of Adelaide, School of Molecular and Biomedical Sciences Research Symposia.*

LIST OF ABBREVIATION

ACC	acetyl CoA carboxylase
Amp	ampicillin
AMP	adenosine monophosphate
Amp^R	ampicillin resistant
ATP	adenosine triphosphate
BCA	bicinchoninic acid
BCCP	biotin carboxyl carrier protein
BirA	biotin inducible repressor A
BLAST	basic local alignment search tool
BME	β-mercaptoethanol
bp	base pair
BPL	biotin protein ligase
BSA	bovine serum albumin
BtnOH-AMP	biotinol-5'-AMP
°C	degree Celsius
C-	carboxyl-
$CaCl_2$	calcium chloride
Cpd	compound
CTP	cytidine triphosphate
cv	column volume
CV	coefficient of variation
DMSO	dimethyl sulfoxide
DNA	deoxynucleotide triphosphate
dNTPs	deoxynucleotide triphosphates
DTT	dithiothreitol
ECL	enhanced chemiluminescence
EDTA	ethylene diamine tetra-acetic acid
Fl-	fluorescently labeled
FP	fluorescence polarization
FPLC	fast protein liquid chromatography

GST	glutathione-S-transferase
GTP	guanosine triphosphate
HCl	hydrochloric acid
HEPES	4-(2-hydroxyethyl)-1-piperazine-ethanesulphonic acid
hr	hour
HRP	horseradish peroxidase
IC_{50}	inhibition concentration at 50% activity
Int	intensity
IPTG	isopropyl β-D-1-thiogalactopyranoside
ITP	inosine triphosphate
kb	kilobase pair
KCl	potassium chloride
kDa	kilo dalton
K_i	inhibition constant
K_M	Michaelis-Menten constant
KPO_4	potassium phosphate
LB	luria broth
m	metre
µ	micron
M	molar
mA	milliampere
Mg	magnesium
MIC	minimal inhibitory concentration
Min	minute, minutes
Mn	manganese
MOPS	3-morpholinopropanesulfonic acid
MS	mass spectrometry
MW	molecular weight
MWCO	molecular weight cut-off
n	nano
N-	amino-
NMR	nuclear magnetic resonance
OD_x nm	optical density at x nm wavelength
p	pico

P	polarization unit
PBS	phosphate buffered saline
PC	pyruvate carboxylase
PCR	polymerase chain reaction
PDB	protein data bank
*Ph*BPL	*Pyrococcus horikoshii* biotin protein ligase
PMSF	phenylmethylsulfonylfluoride
PVDF	polyvinyl difluoride
RNA	ribonucleic acid
rpm	revolutions per minute
RT	room temperature
*Sa*BPL	*S. aureus* biotin protein ligase
*Sa*PC	*S. aureus* pyruvate carboxylase biotin domain
SDS	sodium dodecyl sulphate
SDS-PAGE	sodium dodecyl sulphate polyacrylamide gel electrophoresis
sec	second
SEM	standard error of the mean
Std. dev.	standard deviation
TBS	tris buffered saline
TBS-T	tris buffered saline and 0.1% (v/v) Tween-20
TEMED	N,N.N,N'N'-tetramethylethylene-diamine
Tris	2-amino-2-hydroxymethylpropane-1,3-diol
TTP	thymidine triphosphate
Tween-20	polyoxyethylene-sorbitan monolaurate
U	units (active)
UTP	uridine triphosphate
UV	ultra violet
Vmax	maximum velocity
WB	Western blot
WT	wild type
*y*BPL	yeast (*S. cerevisiae*) biotin protein ligase
ΔmP	milli polarization unit difference between apo and holo substrate

CHAPTER 1

INTRODUCTION

CHAPTER 1 INTRODUCTION

1.1 NEEDS FOR NEW ANTIBIOTICS

The intensive use of antibiotics in human and veterinary medicine as well as exploitation of antibiotics in agriculture have been linked to the emergence and wide spread of antibiotic resistant bacteria (Khachatourians, 1998; Levy, 1998; Mazel and Davies, 1999; Chander *et. al.*, 2007). The first penicillin resistant *Staphylococcus aureus* strain was reported only three years after the discovery of penicillin in the 1940s. Since then many more drug resistant strains have been uncovered. In recent years, there has been a relentless increase in the occurrence of antibiotic resistance in many common bacterial pathogens (Levy, 1998; Talbot *et. al.*, 2006).

Infection by multidrug resistant bacteria is driving up health care costs due to longer hospital stays and more expensive treatment. According to the Centers for Disease Control and Prevention, over $4 billion was spend on medical costs associated with antibiotic-resistant microorganisms annually in the United States alone. In some cases, these infections lead to severe disability and even death. Some of the life-threatening bacterial species, for example *Enterococcus faecalis*, *Mycobacterium tuberculosis* and *Pseudomonas aeruginosa*, are resistant to more than 100 of the antibiotics available today (Levy, 2005).

The world is in an adverse circumstance whereby there is low supply of novel antibiotics in the development pipeline. In 2006, only one new antimicrobial compound was filed for FDA approval with 12 in late phase clinical trials. Most of these compounds are derivatives of existing classes with only two of these targeting a novel mechanism (Talbot *et. al.*, 2006). Furthermore, there is a significant reduction in the number of major

pharmaceutical companies engaged in the discovery and development of antimicrobial drugs (Wenzel, 2004).

There is a significant unmet medical need that must be addressed. One of the effective approaches to combat drug resistance is to identify new chemical entities that inhibit novel targets for which there is no pre-existing resistance. Here, we focus on the essential metabolic enzyme, biotin protein ligase (BPL) as one such target. As will be discussed, BPL is intimately linked to the fatty acid biosynthesis pathway (Campbell and Cronan, 2001) that is integral for cellular membrane biogenesis and maintenance. The establishment of cerulenin, thiolactomycin, triclosan and isoniazid as antibiotics that are directed to various enzymes in fatty acid synthesis (Clardy *et. al.*, 2006) have validated this pathway as a potential drug target (Campbell and Cronan, 2001; McDevitt *et. al.*, 2002). Genetic studies have demonstrated that both BPL and acetyl CoA carboxylase (ACC) activities are essential for survival of *Escherichia coli* (Barker and Campbell, 1981a; Chapman-Smith *et. al.*, 1994; Gerdes *et. al.*, 2003), *Staphylococcus aureus* (Payne *et. al.*, 2007) and *Streptococcus pneumoniae* (Thanassi *et. al.*, 2002).

1.2 BIOTIN

Biotin was first isolated as a yeast growth factor from egg yolk by Kogl and Tonnis in 1936 (Kogl and Tonis, 1936) and the structure was first determined by du Vigneaud *et. al.* in 1942 (du Vigneaud *et. al.*, 1942; Melville *et. al.*, 1942). Biotin (also known as vitamin H) is a water soluble vitamin belonging to the B complex family (vitamin B7). The best understood role for biotin is as an enzyme cofactor which will be discussed later.

Microorganisms and some plant species have the ability to synthesize biotin. In contrast, humans and other mammals lack this ability and, therefore, must obtain biotin from exogenous sources. Most of our biotin requirement can be supplied by intestinal microflora, although biotin can be obtained from dietary sources. The highest level of dietary biotin can be found in egg yolk and meat organs such as liver and kidney but it is low in meats, vegetables and fruits. Dietary biotin can exist either in a free or protein-bound form. Protein-bound biotin is digested by gastrointestinal proteases and peptidases to biocytin (*N*-biotinyl-L-lysine) and biotin-containing short peptides which are eventually converted to free biotin by the action of biotinidase (Lampen *et. al.*, 1941). Like other micronutrients, this vitamin is absorbed in the jejunum of the small intestine (Dakshinamurti *et. al.*, 1987). An alternative source of biotin for higher organisms is widely believed to be derived from the colonic microflora although there are controversies on absorption of biotin in the intestine. Several studies have shown that although bacterial biotin synthesis may be substantial, its form and location limits its bioavailability in higher organisms (Dakshinamurti *et. al.*, 1987; McMahon, 2002).

1.3 BIOTIN-DEPENDENT ENZYMES

Biotin-dependent enzymes are ubiquitous in nature. All biotin-dependent enzymes require biotin as a cofactor to catalyze various carboxyl transfer reactions (Samols *et. al.*, 1988; Knowles, 1989). The reaction mechanism occurs in two partial steps carried out at separate sub-sites. Biotin is required to shuttle carboxyl groups between these two sites (Wood, 1977; Samols *et. al.*, 1988).

Reactions involving biotin enzymes can be subdivided into three classes namely carboxylation, decarboxylation and transcarboxylation. All eukaryotic biotin enzymes

catalyse Class I carboxylation reactions (Samols *et. al.*, 1988). Here, bicarbonate, ATP and free divalent metal ions such as Mg^{2+} are required to transfer carbon dioxide onto an acceptor metabolite (Climent and Rubio, 1986; Knowles, 1989; Attwood and Wallace, 2002). The Class II enzymes, decarboxylases, are restricted to anaerobic bacteria (Samols *et. al.*, 1988; Jitrapakdee and Wallace, 2003). During decarboxylation, sodium ions (Na^{+}) are pumped across the membrane against a concentration gradient. This reaction serves as an important energy transducer for nutrient accumulation or ATP synthesis in the bacteria (Samols *et. al.*, 1988; Jitrapakdee and Wallace, 2003). Transcarboxylase is the only known member of the Class III enzyme. The transcarboxylase from *Propionibacterium shermanii* exists as a multisubunit enzyme composed of 30 polypeptides (Samols *et. al.*, 1988; Jitrapakdee and Wallace, 2003). Here, a carboxyl group is transferred from one metabolite onto another.

1.4 BIOTIN DOMAINS

Biotinylation is a relatively rare post-translational modification in cells as only between one and five biotinylated protein species are found in organisms (Cronan, 1990). In most prokaryotes, yeast and mammals a single biotin protein ligase is responsible for all protein biotinylation. This is possible due to the presence of a conserved biotin-accepting domain in all the biotin-requiring enzymes. Sequence comparison of biotin domains between different species shows that these domains are highly conserved across species (Figure 1.1). The structural conservation was demonstrated through superimposable domain structures of various species (Pendini *et. al.*, 2008b). This is further proven in cross-species biotinylation activities demonstrated by a diverse range of biotin protein ligases (McAllister and Coon, 1966; Cronan, 1990; Leon-Del-Rio and Gravel, 1994; Tissot *et. al.*, 1996).

Figure 1.1 : Comparison of sequence alignment of the biotin domains from various organisms. Residues forming β-strands of *E. coli* BCCP (Athappilly and Hendrickson, 1995) are shown with arrows. The biotinylated lysine residue is marked ❋ . Shading indicates residues highly conserved in all biotin domains compared.

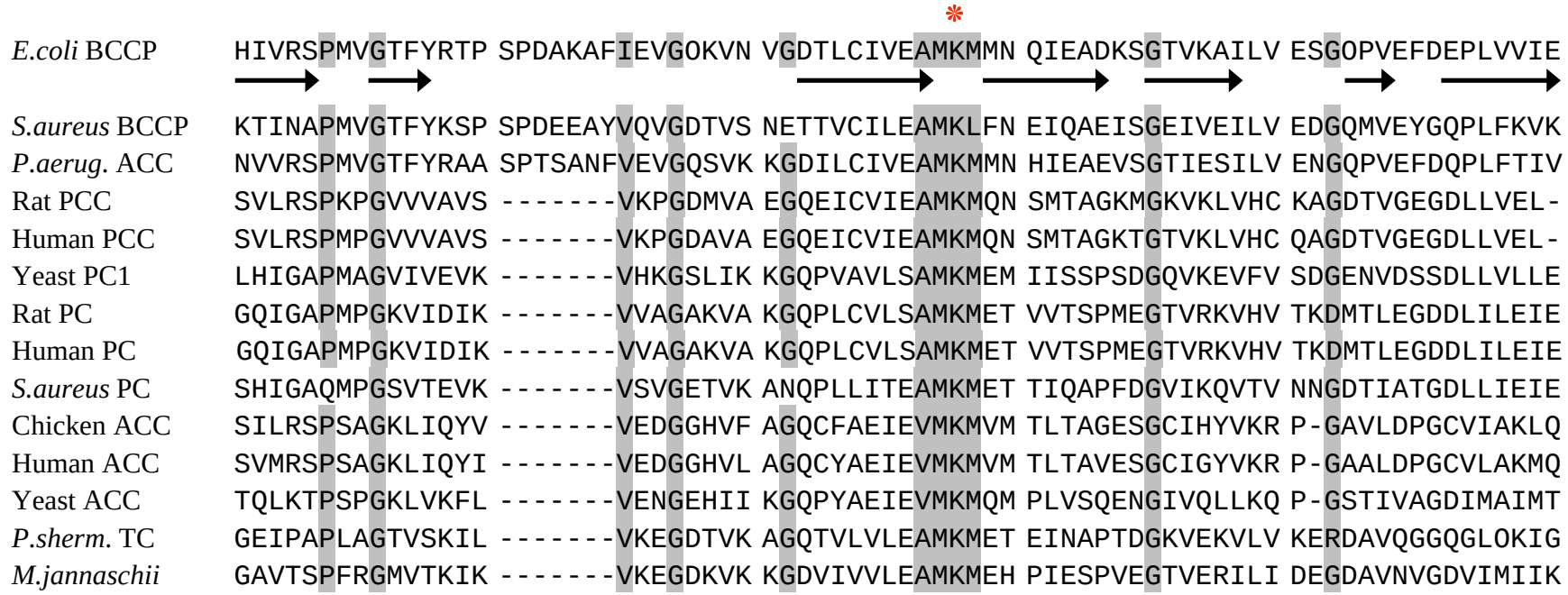
*
E.coli BCCP HIVRSPMVGTFYRTP SPDAKAFIEVGQKVN VGDTLCIVEAMKMMN QIEADKSGTVKAILV ESGQPVEFDEPLVVIE
S.aureus BCCP KTINAPMVGTFYKSP SPDEEAYVQVGDTVS NETTVCILEAMKLFN EIQAEISGEIVEILV EDGQMVEYGQPLFKVK
P.aerug. ACC NVVRSPMVGTFYRAA SPTSANFVEVGQSVK KGDILCIVEAMKMMN HIEAEVSGTIESILV ENGQPVEFDQPLFTIV
Rat PCC SVLRSPKPGVVVAVS -------VKPGDMVA EGQEICVIEAMKMQN SMTAGKMGKVKLVHC KAGDTVGEGDLLVEL-
Human PCC SVLRSPMPGVVVAVS -------VKPGDAVA EGQEICVIEAMKMQN SMTAGKTGTVKLVHC QAGDTVGEGDLLVEL-
Yeast PC1 LHIGAPMAGVIVEVK -------VHKGSLIK KGQPVAVLSAMKMEM IISSPSDGQVKEVFV SDGENVDSSDLLVLLE
Rat PC GQIGAPMPGKVIDIK -------VVAGAKVA KGQPLCVLSAMKMET VVTSPMEGTVRKVHV TKDMTLEGDDLILEIE
Human PC GQIGAPMPGKVIDIK -------VVAGAKVA KGQPLCVLSAMKMET VVTSPMEGTVRKVHV TKDMTLEGDDLILEIE
S.aureus PC SHIGAQMPGSVTEVK -------VSVGETVK ANQPLLITEAMKMET TIQAPFDGVIKQVTV NNGDTIATGDLLIEIE
Chicken ACC SILRSPSAGKLIQYV -------VEDGGHVF AGQCFAEIEVMKMVM TLTAGESGCIHYVKR P-GAVLDPGCVIAKLQ
Human ACC SVMRSPSAGKLIQYI -------VEDGGHVL AGQCYAEIEVMKMVM TLTAVESGCIGYVKR P-GAALDPGCVLAKMQ
Yeast ACC TQLKTPSPGKLVKFL -------VENGEHII KGQPYAEIEVMKMQM PLVSQENGIVQLLKQ P-GSTIVAGDIMAIMT
P.sherm. TC GEIPAPLAGTVSKIL -------VKEGDTVK AGQTVLVLEAMKMET EINAPTDGKVEKVLV KERDAVQGGQGLOKIG
M.jannaschii GAVTSPFRGMVTKIK -------VKEGDKVK KGDVIVVLEAMKMEH PIESPVEGTVERILI DEGDAVNVGDVIMIIK

The first biotin domain structure reported was of *E. coli* BCCP-87 determined by X-ray crystallography (Athappilly and Hendrickson, 1995) and NMR (Roberts *et. al.*, 1999) (Figure 1.2). In recent years, more structures have become available (reviewed in Pendini *et. al.*, 2008b). In biotin domains, the biotin prosthetic group is found to be covalently attached via a ε-amino group of one specific lysine (Lane and Lynen, 1963). This target residue occurs in a highly conserved Ala-Met-Lys-Met tetrapeptide (Samols *et. al.*, 1988), commonly found about 35 residues from the C-terminus of the carboxylase (Samols *et. al.*, 1988; Cronan, 1990). Several mutagenesis studies carried out on this sequence have shown that the flanking methionine is not essential for biotinylation (Shenoy *et. al.*, 1988; Shenoy *et. al.*, 1992; Leon-Del-Rio and Gravel, 1994; Reche *et. al.*, 1998; Polyak *et. al.*, 2001). However, these residues do affect carboxylation and carboxyl transfer reactions (Shenoy *et. al.*, 1988). Instead, it was the carboxy terminal sequence especially the key hydrophobic core residues that have been shown to reduce the efficiency of biotinylation (Murtif and Samols, 1987; Leon-Del-Rio and Gravel, 1994).

BPL recognizes the 60-90 amino acid domain with a minimum of 35-40 residues on either side of the biotin attachment site (Cronan, 1990; Shenoy *et. al.*, 1992). Further truncation or mutation of the residues that contribute to the hydrophobic core of the fold will abolish biotinylation (Murtif and Samols, 1987; Leon-Del-Rio and Gravel, 1994; Chapman-Smith *et. al.*, 1999). Interestingly, a minimal peptide of 14 residues (peptide 85-11) that efficiently mimics the function of the natural substrate, BCCP-87 has been reported. This peptide was shown to have an equivalent specificity constant (k_{cat} /K_M) indicating that the peptide was biotinylated at the same rate as BCCP (Beckett *et. al.*, 1999). However, this peptide bears no homology to a biotin domain and was found to be specific to *E. coli* BPL (BirA).

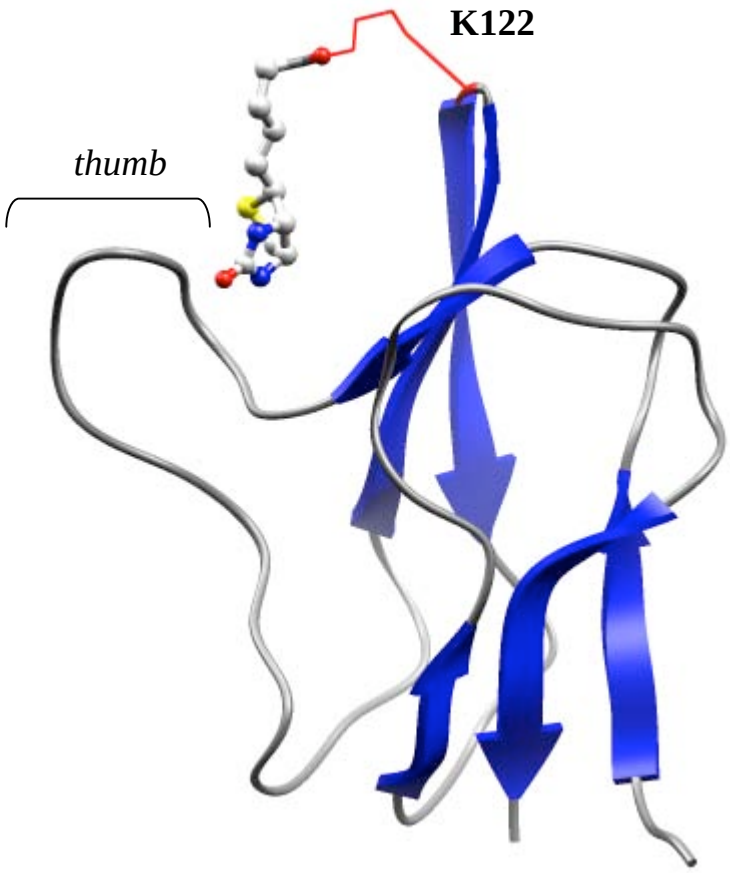

Figure 1.2 : X-ray crystallography structure of holo *E. coli* BCCP-87 in ribbon presentation. The biotin moiety, presented in ball and stick, is shown attached to lysine 122 (red) at the exposed hairpin loop of β-strands 4 and 5. The position of the "thumb" is indicated on the structure (Athappilly and Hendrickson, 1995).

1.5 BIOTIN PROTEIN LIGASE (BPL)

Biotin protein ligase (BPL), also known as the biotin inducible repressor (BirA) in *E. coli* and holocarboxylase synthetase in mammals, is the enzyme responsible for attaching the biotin prosthetic group onto the biotin-dependent enzymes. This process is carried out in a two-step reaction as shown in Figure 1.3.

In the first partial reaction, BPL catalyzes the formation of an active intermediate biotinyl-5'-AMP from inert biotin and ATP in the presence of Mg^{2+} ions. Studies by Xu *et. al.* have shown that the binding of biotin and ATP to BirA are in an ordered manner with biotin binding first (Xu and Beckett, 1994; Xu *et. al.*, 1995; Xu *et. al.*, 1996). In the second partial reaction, the biotin moiety is transferred to an apo-carboxylase (Christner *et. al.*, 1964) by forming a peptide bond with the ϵ amino group on the target lysine residue, resulting in the release of AMP.

1.6 MICROBIAL BPLS

To date, only the structures of BPL from the Gram-negative bacterium, *Escherichia coli* (Wilson *et. al.*, 1992; Weaver *et. al.*, 2001; Wood *et. al.*, 2006) and archeon *Pyrococcus horikoshii* (Bagautdinov *et. al.*, 2005; Bagautdinov *et. al.*, 2008) have been well characterized. Recently, the crystal structure of a Gram-positive bacterium, *Staphylococcus aureus* (Pendini *et. al.*, 2008c) has been reported. The coordinates for other BPL structures such as from *Mycobacterium tuberculosis* (PDB ID 2CGH), *Aquifex aeolicus* (PDB ID: 2EAY) and *Methanococcus jannaschii* (PDB ID: 2EJ9) have been deposited in the PDB but no analyses of these structures have been published.

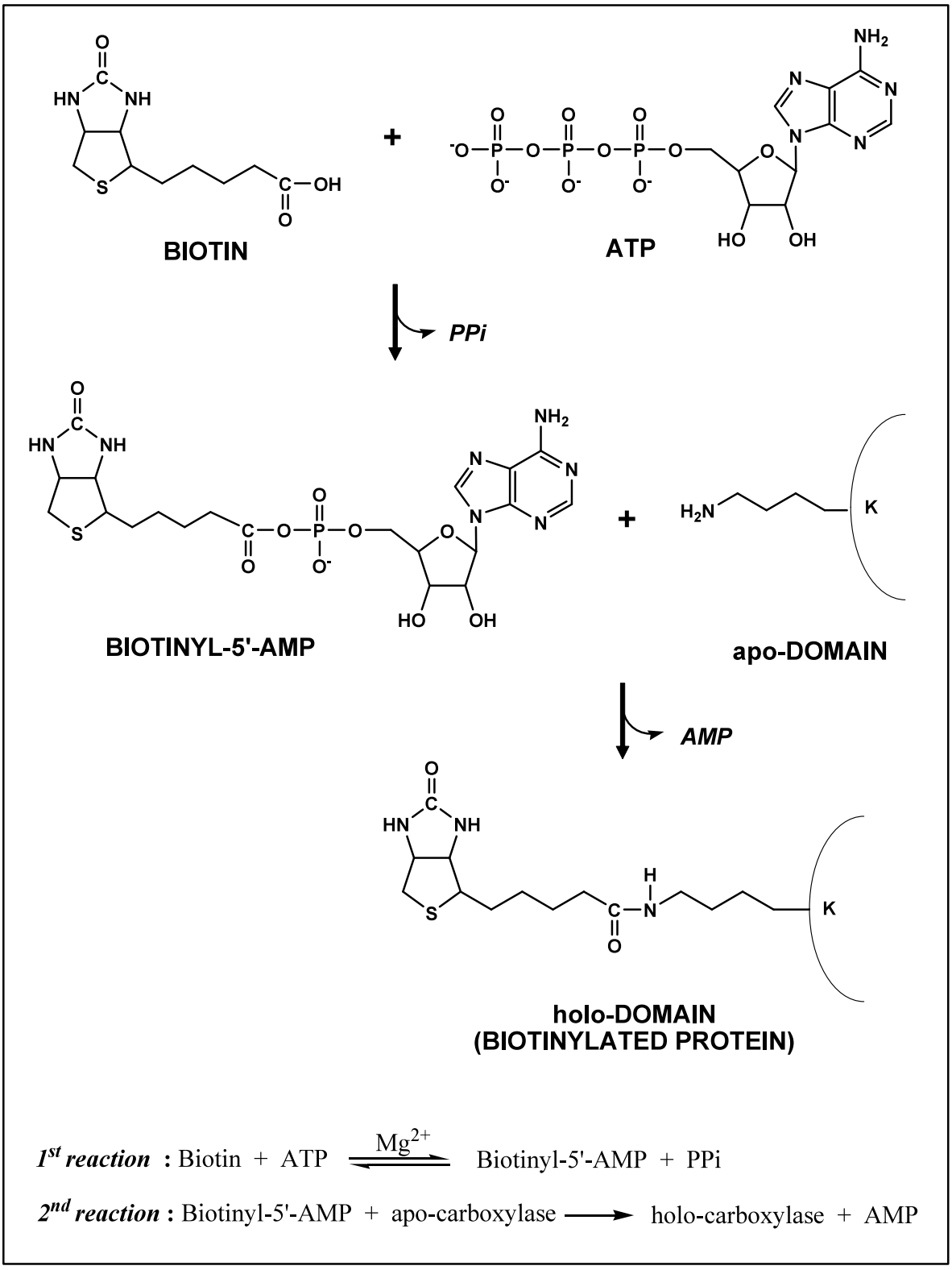

Figure 1.3 : Schematic diagram and equations of two-step biotinylation reaction catalyzed by biotin protein ligase (BPL). K represents lysine in the protein sequence. Figure adapted from (Chapman-Smith and Cronan, 1999b)

1.6.1 *Escherichia coli* BPL (BirA)

E. coli BPL, also known as the biotin inducible repressor A (BirA), is the best characterized BPLs of all species. The monomeric protein of 35.3kDa is encoded by the *bir*A gene (Barker and Campbell, 1981a; Barker and Campbell, 1981b). Besides its role in biotinylation of BCCP, this bifunctional enzyme also acts as a transcriptional repressor, regulating the expression of genes involved in *de novo* biotin synthesis.

The X-ray crystal structures of apoBirA (Wilson *et. al.*, 1992), a BirA-biotin complex (Weaver *et. al.*, 2001) and a BirA-biotinol-5'-AMP complex (Wood *et. al.*, 2006) have been reported. All structures reveal that the BirA monomer is organized in three distinct domains namely the N-terminal, central, and C-terminal domains.

The N-terminal domain of BirA contains a winged helix-turn-helix structure that is responsible for DNA binding and regulation of biotin biosynthesis. BirA switches between a biotin ligase and a transcriptional repressor in response to the intracellular requirement for biotin with the BCCP concentration serving as the indicator. When there is non-biotinylated BCCP present, BirA functions as a biotin ligase. On the contrary, when there is no biotin ligase requirement, biotinyl-5'-AMP acts as a co-repressor that induces dimerization and binding to the bio operator (BioO) to suppress further biotin biosynthesis (Eisenstein and Beckett, 1999; Streaker and Beckett, 2003). Enzymatic and chemical probing of the protein-DNA complex, as well as structural modeling, have shown that each of the DNA binding domains of the holoBirA dimer binds with one of the two 12bp DNA sequences located within the 40bp operator region of the biotin biosynthetic operon (Streaker and Beckett, 1998).

The catalytic site of BirA is located on a solvent-exposed face of the central domain. In apoBirA, the central catalytic domain contains four loops which appear unstructured and disordered (Wilson *et. al.*, 1992). In contrast, three of these loops are visible in the BirA-biotin complex except for a loop composed of residues 212-234. This loop has been shown to be protected from proteolytic digestion as a consequence of biotin or biotinyl-5'-AMP binding (Xu *et. al.*, 1995). Comparison of the apoBirA and BirA-biotin complex structures lead Weaver *et. al*. to propose that the biotin induced disorder to order transition is a prerequisite for dimerization (Weaver *et. al.*, 2001).

It was also noted that one of these poorly ordered loops contains the highly conserved sequence ^{110}GRGRRG^{128} which was initially proposed to function in ATP binding due to its similarity with mononucleotide binding protein kinases (Wilson *et. al.*, 1992). However, kinetic and thermodynamic studies of several mutations in this motif by Kwon and Beckett demonstrated that this sequence is essential for substrate and intermediate binding, not ATP binding (Kwon and Beckett, 2000).

The structure of BirA in complex with biotinol-5'-AMP (Figure 1.4) by Wood *et. al* provided the first crystallographic evidence reporting the nucleotide binding site. It was discovered that there is no preformed binding site for adenylate. Biotin binding induces ordering of the biotin binding loop thereby inducing conformation of the nucleotide binding site. This provides a structural explaination as to why ligands bind in an ordered mechanism. In the binding site, the purine ring of the adenylate stacks on the indole ring of Trp123 to form hydrogen bonds with Asn208 and Phe124. The phosphate group forms three hydrogen bonds with the side chains of Arg118 and Arg121. Other important amino acid residues that interact with the adenylate are 212-223, known as the “adenylate binding loop”, which acts as a loop in covering the bound co-repressor (Laine *et. al.*, 2008). These

Figure 1.4 : Crystal structure of BirA

(a) Crystal structure of BirA dimer.

The right BirA is shown as a solid surface. The left BirA is in ribbon format showing the N-terminal domain (blue) connected by a linker (yellow) to the catalytic domain (purple) and C-terminal domain (red). The bound btnOH-5'-AMP is depicted as spheres coloured by element (PDB ID: 2EWN) (Wood *et. al.*, 2006).

(b) Binding interaction between BirA and btnOH-AMP.

The left panel shows the interaction of btnOH-AMP with the side chains of the core residues in the active site. Hydrogen bonding interactions were shown as green broken lines and the packing interaction of the adenylate binding loop (red residues) is shown as yellow broken line. The indole ring of Trp123 that stacks with the purine ring of the adenylate is shown in orange. The right panel shows the interaction between btnOH-AMP (depicted in ball and stick coloured by element) and BirA in ribbon structure. Trp123 is coloured gold. Diagrams were regenerated by Prof. Andrew Abell.

(A)

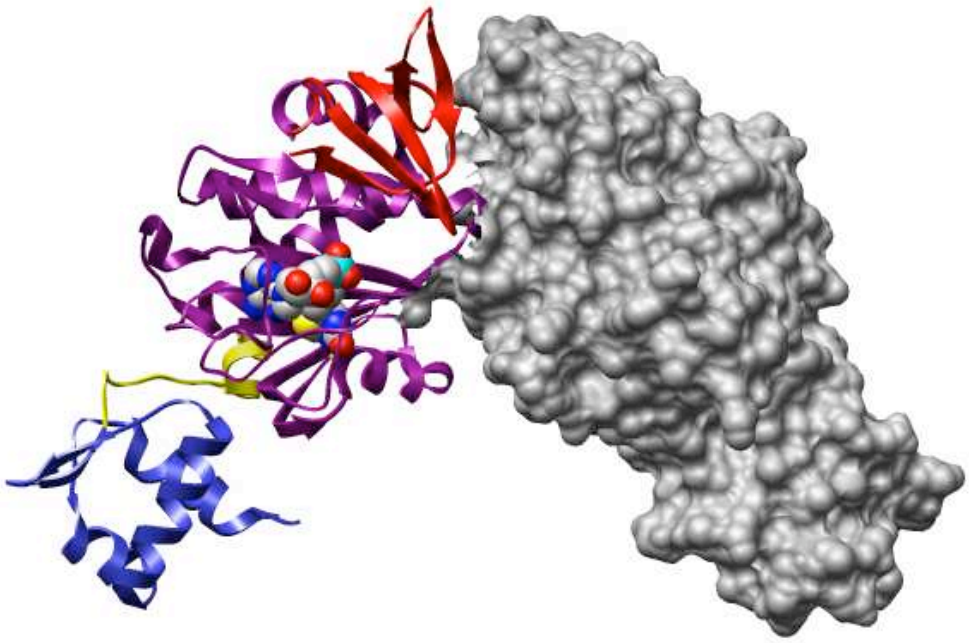

(B)

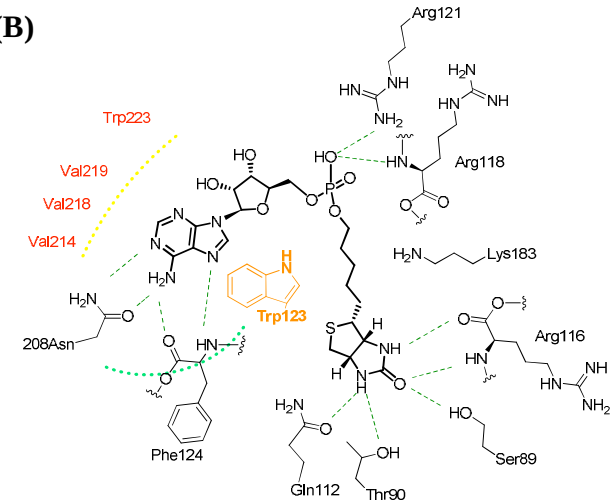
Arg121
Trp223
Val219
Val218
Val214
Arg118
Lys183
Trp123
208Asn
Arg116
Phe124
Gln112
Thr90
Ser89

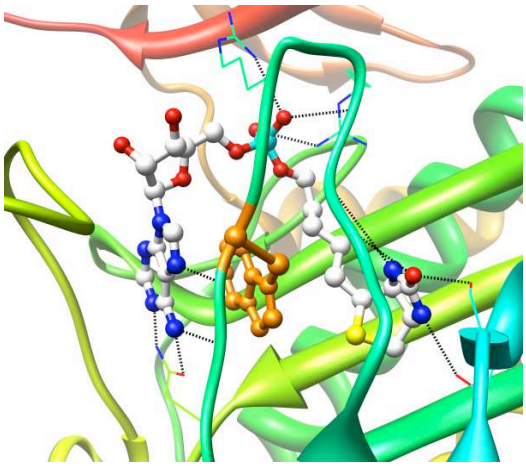

studies agree with mutagenesis studies by Chapman-Smith *et. al.* who postulated that the SH3-like C-terminal domain of BirA modulates the activity at the active site. Their findings indicated that K277 influences the biotinylation of BCCP by BirA whilst residue R317 of this domain interacts with ATP (Chapman-Smith *et. al.*, 2001).

1.6.2 *Pyrococcus horikoshii* BPL

In recent years, an ensemble of BPL structures from the hyperthermophile *Pyrococcus horikoshii* (*Ph*) OT3 has been reported. Significantly, these include *Ph*BPL in its apo-form and in complex with biotin, ADP and biotinyl-5'-AMP (Bagautdinov *et. al.*, 2005). This group has also captured the crystal structure of the enzyme in complex with a biotin acceptor, BCCP (Bagautdinov *et. al.*, 2008). This has provided a wealth of information on the BPL reaction mechanism and substrate recognition.

From these studies, it was shown that the glycine rich biotin-binding pocket has a hydrophobic wall that interacts with the hydrophobic tail and thiophene ring of biotin and a hydrophilic interior that interacts via hydrogen bonding with the biotin carboxyl group and ureido nitrogen atoms. Adjacent to this pocket, separated by a wall of hydrophobic residues, is the solvent-exposed nucleotide binding pocket. The orientation of the adenine ring in this pocket is defined by aromatic interactions between Trp53 and Trp61. The conserved Lys111 is thought to play an essential role in the formation of biotinyl-5'-AMP. According to the proposed reaction mechanism, Lys111 increases the electrophilicity of the α-phosphate group of ATP which leads to the nucleophilic attack by the carboxylic group of biotin.

Whilst both *Ph*BPL and BirA catalyze a conserved reaction mechanism, these two BPLs differ in terms of their molecular size, quarternary structure and amino acid sequence (31% sequence identity). Unlike BirA, *Ph*BPL does not exhibit repression of biotin biosynthesis. The absence of the DNA-binding domain generally contributes to its smaller size. In contrast to BirA, *Ph*BPL is a constitutive dimer with a flexible intersubunit arrangement. However, the PhBPL and BirA dimers are structurally distinct as they employ different dimerisation interfaces (Bagautdinov *et. al.*, 2005).

1.7 EUKARYOTIC BPLS

Mammalian BPL is commonly referred to in the literature as holocarboxylase synthetase (HCS). The human and yeast BPL genes encode proteins of 726 and 690 amino acids respectively, which is about twice the size of the prokaryote BPLs. However, *Arabidopsis thaliana* BPL contains only 367 amino acids (Figure 1.5). Sequence comparisons of BPL proteins have shown that the C-terminal half of the eukaryotic BPLs is highly conserved amongst all BPLs suggesting this segment to be the catalytic domain. Although eukaryotic BPLs catalyze the same biotinylation reaction, they do not exhibit DNA binding activity and thus have no known role in transcriptional regulation (Leon-Del-Rio and Gravel, 1994). This is consistent with biotin metabolism where organisms that obtain biotin exogenously have no need for a repressor function (Chapman-Smith and Cronan, 1999b).

The presence of a large N-terminal domain in human and yeast BPL is not shared in BirA. While there are some sequence similarities within the N-terminal domain of human and yeast BPL (Cronan and Wallace, 1995), the structural and functional properties of this region remain unclear. The truncation studies by Polyak *et. al*. showed that the N-

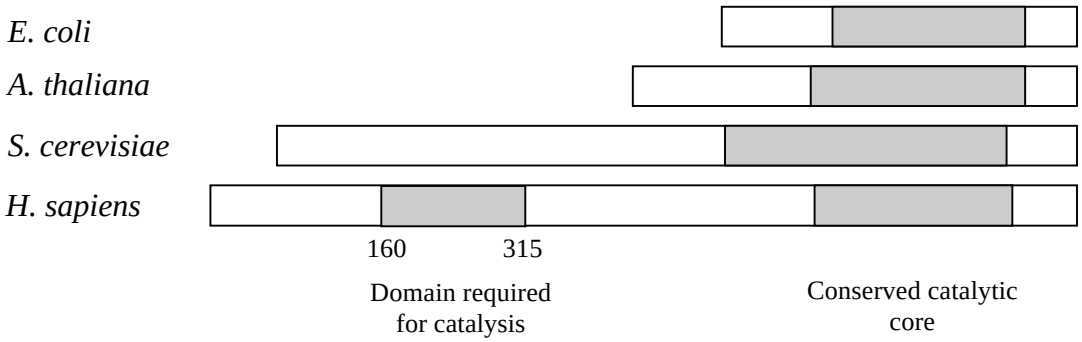

Figure 1.5 : Schematic diagram of the relative length and predicted conserved catalytic core of biotin protein ligases and the N-terminal domain required for catalysis in human BPL.

terminal domain of the yeast BPL is required for catalysis. They observed a 3,500 fold decrease in BPL activity upon the deletion of the N-terminal domain (Polyak *et. al.*, 1999). We first proposed the N-terminal domain functions as a cap over the active site. Campaeu and Gravel demonstrated that removal of the N-terminal domain of human BPL also reduces the enzyme activity (Campeau and Gravel, 2001). This has been substantiated by truncation and mutagenesis studies in our laboratory (Swift, 2003). Consistent with our model, yeast-2-hybrid experiments performed by Lingusa Mayende have shown the two halves of the protein interact (unpublished data). As prokaryotic BPLs do not have this N-terminal extension, it appears that the participation of this region in catalysis is unique to the large eukaryotic BPLs.

1.8 AIMS AND SIGNIFICANCE

1.8.1 Project Aims

The prevalence of multi-drug resistant bacteria is rapidly escalating worldwide. Coupled with a paucity of new antibiotics in the research and development (R&D) pipeline, the world is in a dire need of new antibiotics. However, there has been significant downsizing or withdrawal from early-stage antibiotic R&D by large pharma over recent years. Therefore, early stage research now lies with biotech companies, research institutes and universities.

Here, the project aim is to discover novel drug candidates that have good selectivity and improved antibacterial activity for pathogenic bacteria. We are focusing on the essential metabolic enzyme, BPL as one prospective target for this study. Genetic studies have shown that the activity of this enzyme is essential for bacterial survival. However, the

identification of BPL inhibitors that could serve as drug leads from large-scale compound screening has been limited due to the lack of a high-throughput assay for enzyme activity.

In this project, my aim is to develop a novel assay for high-throughput screening and compound analysis. Compounds identified through *in-silico* screening and rational drug design will be screened with this fluorescence polarization based assay to identify potential BPL inhibitors as new drug leads.

1.8.2 Project Significance

From this project, I will establish technologies for high-throughput screening for inhibitors of bacterial BPL. These inhibitors could be exploited as lead compounds for further development. The FP assay will provide a convenient way for high-throughput compound screening and for data generation to determine structure-activity relationships (SAR) of BPL inhibitors. Information from crystal structures and *in-silico* docking enable us to grow, dock and design virtual derivatives of inhibitors. Therefore, it is feasible to selectively modify the lead compounds into drugs with high specificity towards a target bacterial BPL. It is envisaged that the optimized compounds could potentially be developed into antibiotics.

CHAPTER 2

GENERAL MATERIALS & METHODS

CHAPTER 2 GENERAL MATERIALS AND METHODS

2.1 MATERIALS

2.1.1 General Materials

Material	Supplier
96 well flat bottom black plate	BMG Labtech, Vic, Australia
96 well flat/round bottom clear plate	Nunc, Roskilde, Denmark
Amicon® Centrifugal Filter Devices	Millipore, MA, USA
Regenerated cellulose tubular membrane	Fisher Biotech, Australia
Durapore Membrane Filter	Millipore, MA, USA
Econo-columns (glass) for chromatography	Bio-Rad Laboratories Inc., CA, USA
Econo-Pac (plastic) columns for chromatography	Bio-Rad Laboratories Inc., CA, USA
Griener Lumitrac 600 White 96 well plate	Stennick Scientific, SA, Australia
Minisart syringe filter 0.45 µm and 0.8 µm	Sartorious, Goettingen, Germany
5 mL His-Trap™ HP	Amersham Pharmacia Biotech, CA, USA
Novex® Pre-cast gels	Invitrogen Life Technologies Inc, NY, USA
Nunc MaxiSorpTM flat-bottom 96 well plate	Nunc, Roskilde, Denmark
PD-10 Desalting column	GE Healthcare, Buckinghamshire, England
PVDF membrane (Hybond™-C extra)	Amersham Pharmacia Biotech, CA, USA
X-ray film (Curix ortho HT-G)	Agfa, Belgium

2.1.1 Chemical Reagents

All chemicals and reagents were of analytical grade or higher. Most common laboratory chemicals were purchased from Sigma Aldrich Inc (St Louis, MO, USA) or BDH Chemicals Ltd. (Victoria, Australia). Specialized reagents and their suppliers are listed below.

Reagents	Supplier
1kb and 100bp DNA ladders	New England Biolabs, MA, USA
Agarose, DNA grade	Probiogen Biochemicals, Australia
Avidin from egg white	Sigma, St Louis, MO, USA
Bradford Protein Reagent Concentrate	Bio-Rad Laboratories Inc., CA, USA
Custom oligonucleotides	Geneworks, Adelaide, SA, Australia
Dithiothreitol (DTT)	BioVectra, Canada
Fluorescein-5'-maleimide	Pierce, IL, USA
Glutathione agarose gel	Scientifix, Australia
IPTG	BioVectra, Canada
MOPS / MES SDS running buffer	Invitrogen Life Technologies Inc, NY, USA
Pfu Turbo DNA polymerase	Stratagene, La Jolla, CA, USA
Restriction endonucleases	New England Biolabs, MA, USA
SeeBlue® Plus2 Prestained Protein Marker	Invitrogen Life Technologies Inc, NY, USA
Skim Milk Powder for blocking	Diploma
Streptavidin-HRP conjugate	Chemicon, Australia
T4 DNA ligase	New England Biolabs, MA, USA
Taq DNA polymerase	New England Biolabs, MA, USA
Thermopol Buffer (10x)	New England Biolabs, MA, USA
Thrombin	Sigma, St Louis, MO, USA
VENT DNA polymerase	New England Biolabs, MA, USA

2.1.2 Bacterial Strains

***E. coli* BL21 (B F$^-$ *dcm ompT hsdS*(r_B^- m_B^-) *gal*) :**

For expression of recombinant proteins (Stratagene, La Jolle, CA, USA)

***E. coli* BL21 (hsdS gal (λcIts857) ind1 Sam7 nin5 lacUV5-T7gene1) :**

E. coli BL21 carrying (λDE3) insertion for expression of recombinant proteins using pET expression vector (Stratagene, La Jolla, CA, USA)

***E.coli* DH5α (*sup*EΔ*lac*169 (p80*lacZ*ΔM15) *hsdR17 rec*A1 *end* AA1 *gyr*A96 *thi*-1 *rel*A1) :**

For routine molecular cloning (New England Biolabs, MA, USA)

***E. coli* BM4062 (birA85 *bio*C) :**

For expression of recombinant apo biotin domains (Barker and Campbell, 1981b)

2.1.3 Bacterial Media

Luria Broth (LB) : 1% (w/v) tryptone, 0.5% (w/v) yeast extract, 1% NaCl, adjusted to pH 7.0 with NaOH.

LB agar : LB supplemented with 1.5% (w/v) bacto-agar.

Bacterial selection : Selection of bacteria bearing plasmid was achieved through addition of appropriate antibiotics to both liquid and solid media. Ampicillin was used at 100 μg/mL and kanamycin at 50 μg/mL.

2.1.4 Commercial Kits

Kit	Supplier
BCA Protein Assay Kit	Pierce, IL, USA
QIAprep Miniprep Kit	QIAGEN, GmbH, Germany
QIAquick Gel Extraction Kit	QIAGEN, GmbH, Germany
QIAquick PCR Purification Kit	QIAGEN, GmbH, Germany

2.1.5 Buffers and Solutions

Blocking buffer : 3% (w/v) skim milk powder in TBS, pH7.2

Cell lysis solution : 10% (v/v) β-mercaptoethanol, 2% (w/v) SDS

Coomassie blue stain : 0.2% (w/v) coomassie brilliant blue, 10% (v/v) methanol, 10% (v/v) acetic acid

Coomassie destain : 10% (v/v) methanol, 10% (v/v) acetic acid

DNA loading buffer (6X) : 0.5x Tris-borate-EDTA (TBE) buffer, 40% (v/v) glycerol, 1 mg/mL bromophenol blue

ECL reagent #1 : 100 mM Tris pH 8.5, 2.5 mM luminol, 400 mM courmaric acid

ECL reagent #2 : 100 mM Tris pH 8.5, 0.2% (v/v) H_2O_2

Gel drying solution : 30% ethanol, 10% glycerol

SDS-PAGE loading buffer (5X) : 0.25 M Tris (pH 6.8), 10% (w/v) SDS, 0.5% (w/v) bromophenol blue, 50% (w/v) glycerol

TBS-Tween : TBS, 0.1% (v/v) Tween20

TAE : 40 mM Tris pH 8.2, 20mM sodium acetate, 1 mM EDTA

TBE : 216 g Trizma base, 100 g boric acid, 18.6 g EDTA to 1L with MilliQ H_2O at pH 8.3.

Transfer buffer : 39 mM glycine, 48 mM Tris pH 8.3, 0.037% (w/v) SDS, 20% (v/v) methanol

Transformation Buffer 1 **:** 30 mM KAc, 100 mM RbCl, 10 mM $CaCl_2$, 50 mM $MnCl_2$, 18.7% (v/v) glycerol

Transformation Buffer 2 **:** 10 mM MOPS, 10 mM RbCl, 75 mM $CaCl_2$, 15% (v/v) glycerol

Tris buffer saline (TBS) **:** 25 mM Tris pH 7.5, 150 mM NaCl

2.1.6 Radiochemical

d-[8,9-^{3}H]-biotin were purchased from Amersham Australia, North Ryde, NSW, Australia and Perkin-Elmer, Boston, MA, USA.

2.1.7 Peptide

Custom peptide 85-11 [sequence MAGGLNDIFEAQKIEWHE] was purchased from Auspep Pty. Ltd., Parkville, Victoria, Australia

2.1.8 Primers

All primers were purchased from Geneworks Pty Ltd., Hindmarsh, South Australia. All primers used were of sequencing grade. Endonuclease restriction sites were underlined and mutagenic sequences are shown in bold. Numbers in superscript designate position in the target gene sequence.

Primer Name	Sequence 5' → 3'	Description
B214	5' ATCTAC<u>GGATCC</u>A^{3142}TGAATGGTCAAGCGAGACG^{3161} 3'	PCR oligo for SaPC103
B215	5' ATCTAC<u>GAATTC</u>A^{3451}GTCAGTTGCTTTTTCAATTTCG^{3429} 3'	PCR oligo for SaPC90 & 103
B222	5' ^{3207} GCCAAAAGCAGATAAG**TGC**AATCCAAGTCATATCG ^{3241} 3'	For SaPC S1075C
B223	5' ^{3241} CGATATGACTTGGATT**GCA**CTTATCTGCTTTTGGC ^{3207} 3'	
B224	5' ATCTAC<u>GAATTC</u>A^{3451}GTCAGT**ACA**TTTTTCAATTTCG^{3429} 3'	For SaPC A1148C
B242	5' ATCTAC<u>GGATCC</u>^{3181}AATGTGCATACAAATGCGAACGTTAAGC^{3208} 3'	PCR oligo for SaPC90
B243	5' ^{3257} GGTTCAGTAACTGAAGTC**TGC**GTTAGTGTTGGTGAAACTG ^{3295} 3'	For SaPC K1092C
B244	5' ^{3295} CAGTTTCACCAACACTAAC**GCA**GACTTCAGTTACTGAACC ^{3257} 3'	
B245	5' ^{3262} GTAACTGAAGTCAAGGTT**TGC**GTTGGTGAAACTGTGAAAGC ^{3303} 3'	For SaPC S1094C
B246	5' ^{3303} GCTTTCACAGTTTCACCAAC**GCA**AACCTTGACTTCAGTTAC ^{3262} 3'	
B247	5' ^{3287} GGTGAAACTGTGAAAGCT**TGT**CAGCCGTTGCTAATTACTG ^{3325} 3'	For SaPC N1102C
B248	5' ^{3325} CAGTAATTAGCAACGGCTG**ACA**AGCTTTCACAGTTTCACC ^{3287} 3'	
B249	5' ^{3347} CAATTCAAGCACCATTT**TGC**GGTGTGATTAAACAAG ^{3382} 3'	For SaPC D1122C
B250	5' ^{3382} CTTGTTTAATCACACC**GCA**AAATGGTGCTTGAATTG ^{3347}3'	
B251	5' ^{3413} CAGGCGATTTATTAATC**TGC**ATTGAAAAAGCAACTGAC ^{3451} 3'	For SaPC E1144C
B252	5' ^{3451} GTCAGTTGCTTTTTCAAT**GCA**GATTAATAAATCGCCTG ^{3413} 3'	

2.1.9 Plasmid

pGEX-4T-2 was purchased from GE Healthcare, Buckinghamshire, England.

pGEX-BCCP (Amp^R), a derivative of pGEX-4T-2 was obtained from Dr. Steven Polyak, University of Adelaide.

2.1.10 Computer Software

Data were analysed using GraphPad Prism and Microsoft Excel 2003 software. Images were manipulated with Photoshop version 6. Protein structures were visualized in Chimera. Compounds were docked with Tripos Sybyl 7.2.

2.1.11 Web Resources

NCBI was used to access protein, nucleotide and PubMed databases (http://www.ncbi.nlm.nih.gov/) and the BLAST (Basic Local Alignment Search Tool) databases. The ExPasy Proteomics Tools server (http://au.expasy.org/tools/) provided access to protein prediction (localisation, motif searches, predicted MW and PI) programs and DNA→ Protein Translation programs. Protein structures were downloaded from RCSB Protein Data Bank (http://www.rcsb.org/). Multiple sequence alignments were performed using ClusalW (http://www.ebi.ac.uk/clustalw/).

2.2 GENERAL METHODS

2.2.1 Protein Techniques

2.2.1.1 Preparation of cell lysates

For the preparation of whole cell lysates for SDS-PAGE and Western Blot analysis, cells were lysed in cell lysis buffer. 1 mL of culture was centrifuged at 17,900 x g for 1 minute. Supernatant was discarded and cell pellet resuspended with 40 µL of cell lysis buffer per unit OD. Cell suspension was vortexed, spun and boiled for 5 minutes.

2.2.1.2 Determination of protein concentration

Protein concentration was assayed using either the Bradford Reagent (Bio-Rad Laboratories Inc., CA, USA) or BCA Assay (Pierce, IL, USA) method depending on sample and buffer compatibility. A standard curve of bovine serum albumin (BSA) was generated from 0 to 0.5 mg/mL. For the Bradford assay 10 µL of sample was mixed with 200 µL of 1x Bradford Reagent in a 96 well plate (Falcon). Absorbance at 600 nm wavelength was measured on a microplate reader (Molecular Devices, CA, USA) (Bradford, 1976).

For the BCA assay 20 µL of sample was mixed with 200 µL of BCA working reagent and incubated at 37˚C for 30 minutes. Absorbance at 580 nm was measured on a PolarStar Galaxy microplate reader (BMG Labtech, Vic, Australia) (Smith *et. al.*, 1985). In both instances standard curves were generated and linear regression used to calculate protein concentration using GraphPad Prism.

2.2.1.3 SDS-PAGE electrophoresis and gel staining

Proteins were separated on a 4-12% Bis-Tris polyacrylamide precast gel (Invitrogen) under reducing conditions. Gels were electrophoresed at 180V in 1x MOPS or MES SDS running buffer (Invitrogen), depending on target protein size. Gels were stained for at least 30 minutes with Coomassie Blue stain before destaining overnight with Coomassie destain at room temperature.

2.2.1.4 Western blot analysis

Protein was separated as described in SDS-PAGE electrophoresis and transferred onto a nitrocellulose membrane using a semi-dry transfer unit (Hoefer SemiPhor, Amersham Pharmacia Biotech, CA, USA). Six sheets of Whatman filter paper and the nitrocellulose membrane were pre-soaked in transfer buffer prior to assembly of the gel sandwhich. Protein was transferred for 1 hour at 40 mA per gel. Membrane was soaked with blocking buffer for 1 hour at room temperature and washed 3 times with TBS. Membrane was probed with appropriate detection probe for 1 hour at room temperature and washed 3 times with TBS-Tween (0.1%). For detection, membrane was treated with equal volume of ECL reagent #1 and ECL reagent #2 for 1 minute before being exposed to X-ray film. Film was developed using CURIX 60 X-ray developer (Agfa).

2.2.1.5 MALDI mass spectrometry

Mass Spectrometry was performed at the Adelaide Proteomics Facility, University of Adelaide. Samples were desalted prior to analysis using a ZipTipc18 (Millipore) and eluted in 0.1% trifluoroacetic acid / 60% acetonitrile, following manufacturers instructions. One microliter of each sample was applied to a 600 μm AnchorChip (Bruker Daltonik GmbH, Bremen, Germany) according to the alpha-cyano-4-hydroxycinnamic acid (HCCA)

thin-layer method. MALDI TOF mass spectra were acquired using a Bruker ultralfex II MALDI TOF/TOF mass spectrometer (Bruker Daltonic, GmbH) operating in reflection mode under the control of the flexControl software (version 3.0, Bruker Daltonik GmbH). External calibration was performed using peptide standards (Bruker Daltonik, GmbH) that were analysed under the same conditions. Spectra were obtained at random locations over the surface of the matrix spot. MS spectra were subjected to smoothing, background subtraction and peak detection using flexAnalysis (Version 3.0, Bruker Daltonik GmbH). The spectra and mass lists were exported to BioTools (Version 3.0, Bruker Daltonik GmbH). Here, the MS spectra were submitted to the in-house Mascot database-searching engine (Matrix Science: http://www.matrixscience.com).

2.2.2 Molecular Biology Techniques

2.2.2.1 Agarose gel electrophoresis

Analysis of DNA and separation of DNA fragments was performed using agarose gel electrophoresis. Gel slabs were poured by melting 0.8-2% (w/v) agarose in TAE buffer. Prior to loading into wells, DNA samples were mixed with an appropriate volume of 6x DNA loading buffer. Samples were electrophoresed in TAE buffer at 100-150V and then stained in ethidium bromide solution (1 μg/mL) for 10 minutes followed by destaining in distilled water. DNA was visualised on a UV transilluminator and photographed using a Mitsubishi Video Processor.

2.2.2.2 Preparation of DH5-α competent cells

A single colony picked off a plate was used to inoculate a 2 mL overnight culture of DH5α in Luria Broth. After incubation overnight at 37˚C with rotation, 200 μL was

subcultured into 10 mL of LB and the culture grown until it reached log phase (as indicated by an OD_{600nm} of ~0.6). Five mL of log phase culture was then added to 100 mL pre-warmed LB and incubated for a further 1.5 hours. The culture was split into 4 x 50 mL centrifuge tubes and placed on ice for 5 minutes. Cells were pelleted by centrifugation at 2,000 x g for 5 minutes at 4˚C. The cells were then resuspended in a total of 40 mL of Tranformation Buffer 1 and incubated on ice for 5 minutes, then collected by centrifugation at 2,000 x g for 5 minutes at 4˚C. This was followed by resuspension in Transformation Buffer 2 to a final volume of 4 mL. Cells were chilled on ice for 5 minutes prior to aliquoting and storing at -80˚C until required.

2.2.2.3 Preparation of chemically competent E. coli

A single colony of the required *E. coli* strain was picked and grown overnight in 2 mL LB at 37°C. 600 µL of the overnight culture was subcultured into 50 mL of LB and the culture was grown to log phase (as indicated by an OD_{600nm} of ~0.6). The culture was left on ice for 30 minutes before centrifugation at 2,000 x g for 5 minutes. The cell pellet was resuspended in 30 mL of ice cold 200 mM calcium chloride ($CaCl_2$) and further incubated for 30 minutes on ice. The centrifugation step was repeated and cells resuspended in 5 mL of ice cold 80 mM $CaCl_2$. The cells were left on ice for at least 1 hour before they were used for transformation.

2.2.2.4 Restriction Digest of DNA

Routinely, 1-5 µg of DNA was digested with 1-10 U of restriction enzyme in the appropriate NEB buffer for 2 hours at 37˚C. In the instance of double digests the buffer conditions for the more sensitive enzyme were used (as recommended by NEB). For

cloning, DNA fragments were separated by agarose gel electrophoresis before purification from the excised gel slice using QIAGEN Gel Purification Kit.

2.2.2.5 Ligation of DNA fragments

Ligation was routinely carried out in a total volume of 10 μL containing DNA insert : vector ratio of 3 : 1 (molar ratio), 1x ligation buffer (50 mM Tris-HCl pH 7.5, 10 mM $MgCl_2$, 1 mM ATP, 10 mM DTT) and 2 U of T4 DNA ligase for 1 hour at room temperature.

2.2.2.6 Transformation of competent cells

10 μL of ligation mixture or 1 μL plasmid was added to 100 μL of competent cells and incubated on ice for 30 minutes. This was followed by heat shock treatment at 42˚C for 5 minutes followed by further 5 minutes incubation on ice. Cells were immediately plated onto pre-warmed LB agar plates with appropriate antibiotic selection.

2.2.2.7 Glycerol stocks

For long term storage of *E. coli* strains, equal volumes of an overnight culture and 80% (v/v) glycerol were mixed and stored at -80˚C.

2.2.2.8 Purification of Plasmid DNA

For purification of plasmid DNA, the QAIGEN QIAprep Miniprep Kit was employed according to manufacturer's instructions.

2.2.2.9 Quantification of DNA

DNA was quantified by measuring absorbance at 260 nm using a CARY WinUV Spectrophotometer. A measure of 1 OD_{260} unit is equal to 50 μg/mL.

2.2.2.10 DNA sequencing

Plasmid DNA or PCR products were used as templates for DNA sequencing. A 20 μL reaction containing 200 ng DNA, 100 ng of appropriate primer, 1 μL of BigDye version 3 reaction mix (Perkin Elmer, Applied Biosystems, CA, USA) and 4 μL of 5x sequencing buffer was prepared for sequencing buffer for PCR. The PCR profile consisted of 30 cycles of denaturation at 96˚C for 30 seconds, annealing at 50˚C for 15 seconds and extension at 60˚C for 4 minutes. After thermocycling, 80 μL of 75% (v/v) isopropanol was added to the PCR products, vortexed and left at room temperature for 30 minutes. Precipitated DNA was isolated by centrifugation at 20,800 x g for 20 minutes. The pellet was washed in 75% (v/v) isopropanol followed by centrifugation for 5 minutes at 20,800 x g and dried in a 37˚C heating block. Sequencing was performed by the Molecular Pathology Sequencing Service at the Institue of Medical and Veterinary Science, Adelaide using 3730 Analyser (Perkin Elmer, Applied Biosystems, CA, USA).

2.2.2.11 PCR Protocols

PCR reactions routinely consisted of the following in a 50 μL reaction: 1x ThermoPol Buffer, 250 ng oligonucleotide primers, 100 nM dNTP mixture and 1 U VENT DNA polymerase. Reactions were carried out under the following cycling conditions: 20 seconds denaturation at 92˚C, 20 seconds annealing at 60˚C, 20 seconds extension at 72˚C

2.2.3 In-vitro ^{3}H-biotin biotinylation assay

In-vitro biotinylation assays were carried out as described previously (Chapman-Smith *et. al.,* 1994). Briefly, an *in vitro* biotinylation reaction was performed for 25 minutes at 37°C in a 20 µL reaction mix containing 50 mM Tris pH 8.0, 3 mM ATP, 5.5 mM $MgCl_2$, 10 µM apo-substrate, 0.1 mg/mL BSA, 0.1 µM DTT, 0.5 µM ^{3}H-biotin, 4.5 µM biotin and 100 nM BPL. At completion of the assay aliquots were spotted onto Whatman filter paper pre-treated with 10% TCA and 0.1 mg/mL biotin. Filter papers were washed twice in ice cold 10% TCA and once in ice-cold ethanol (100%) and dried. The filter papers were placed in glass vials and added with 2 mL Optiphase HiSafe Scintillation fluid. Radioactivity measurements were obtained using a Rackbeta Liquid Scintillation Counter (Perkin Elmer, MA, USA). Enzyme kinetic analyses were performed using non-linear regression analyzing tools in GraphPad Prism.

CHAPTER 3

DEVELOPMENT & CHARACTERIZATION OF A HIGH-THROUGHPUT ASSAY FOR *E. COLI BPL*

CHAPTER 3 DEVELOPMENT AND CHARACTERIZATION OF A HIGH-THROUGHPUT ASSAY FOR *E. COLI* BPL

3.1 INTRODUCTION

It has been proposed that BPL is an attractive target for new antibiotics. However, large-scale compound screening has been limited due to the lack of a truly high-throughput assay for the enzyme activity. There are several important considerations when first establishing a high-throughput technology. These include minimal handling and washing steps, the ability to be adapted to robotics and miniaturization, high sensitivity and reproducibility and cost effectiveness. Fluorescence-based assays are an attractive option as they address many of these criteria (Pope *et. al.*, 1999). Additionally, these assays avoid using radioactivity and the high costs and safety issues associated with it. Indeed, fluorescence technologies are now employed in 60% of all high throughput applications (Trinquet and Mathis, 2006). One particularly amenable technique is fluorescence polarization (FP) which was first established ~80 years ago by Perrin (Perrin, 1926). However, its application in high-throughput screening (HTS) has only been realized in recent years after the introduction of high-performance instruments with subnanomolar capabilities in polarization (Sportsman and Leytes, 2000).

FP is a technique that uses plane polarized light for the detection of tumbling motions of fluorescent molecules in solution. Briefly, excitation of the fluorophore occurs with polarised light resulting in preferential excitation of those molecules that have their dipoles parallel to the direction of the polarised light. The polarization value (μ) of a molecule is proportional to the rotational relaxation time determined by viscosity (η),

absolute temperature (T), molecular mass (V) and gas constant (R) where $\mu = 3 \eta V / RT$ (Checovich *et. al.*, 1995). When the temperature and viscosity are held constant, polarization of the emitted light is directly relative to the apparent molecular mass of the flourophore; small molecules that rotate quickly in solution produce a small-polarised signal whereas larger molecules that tumble more slowly exhibit a higher polarization. As the extend of polarization of the emitted light is related inversely to the apparent molecular mass of the fluorophore, this technique can be use for quantitation of changes in molecular mass of target molecules (Checovich *et. al.*, 1995).

Signal detection using polarization is one of the unique features of FP not shared by other conventional fluorimetry methods. Polarization does not change with fluorescence intensity and therefore is not susceptible to the fluorescence background effects. Repeated measurement is also possible with this technique as the measurement of polarization is rapid and has no effect on the sample itself (reviewed in Burke *et. al.*, 2003). However, as with any analytical method, FP has some limitations. The use of FP is generally constrained by the molecular mass of the labeled molecule with 5,000 Da being optimal (Sportsman and Leytes, 2000). Although higher molecular masses can sometimes be measured, this will significantly reduce the detectable polarization shift. This limitation is a function of the lifetime of the fluorophore used (Sportsman and Leytes, 2000). Advances in the chemistry of fluorescent tracers and development of new tracers with shorter lifetimes are expected to expand the range of molecular mass to several hundred thousand Daltons (Terpetschnig *et. al.*, 1995). FP is also affected by quenching caused primarily by compounds that absorb in the visible region of the electromagnetic spectrum. Although this interference is corrected to a certain extent by the ratiometric nature of FP, the noise of measurement that predominates when the intensity is too low leads to poor precision.

A large number of homogeneous assays have now been developed using FP, for example, to measure receptor binding (Rudiger *et. al.*, 2001; Inglis *et. al.*, 2004), protein-protein interaction (Lynch *et. al.*, 1997; Nikolovska-Coleska *et. al.*, 2004; Saldanha *et. al.*, 2006) and the activities of proteases (Schade *et. al.*, 1996; Blommel and Fox, 2005), isomerases (Liu *et. al.*, 2006) and other enzymes (Seethala and Menzel, 1998; Coffin *et. al.*, 2000; Antczak *et. al.*, 2007; Graves *et. al.*, 2008). Recently, this technology has shown remarkable success in HTS of protein-ligand interactions which were used to investigate the potency of various enzymes inhibitors (von Ahsen and Bomer, 2005; Wesche *et. al.*, 2005; Howes *et. al.*, 2006; Lokesh *et. al.*, 2006).

In this chapter, the development of a novel assay system for BPL from *Escherichia coli* (BirA) will be discussed. The fluorescence polarization technology together with a peptide substrate unique for BirA was employed. This assay was validated with enzyme kinetic and statistical analysis. The assay was then employed for inhibition studies of ATP analogues identified through *in-silico* screening. An analogue of the BPL reaction intermediate, biotinol-5'-AMP (btnOH-AMP) was investigated as an enzyme inhibitor and antimicrobial agent.

3.2 SPECIFIC METHODS

3.2.1 Expression and purification of protein

3.2.1.1 E. coli BPL (BirA)

The preparation of homogeneous BirA from *Escherichia coli* was performed as previously described (Chapman-Smith *et. al.*, 2001). Briefly, an overnight culture of *E.*

coli BL21 (λDE3) harbouring the expression plasmid pHBA was grown in LB media supplemented with ampicillin (200μg/ml) and 2% (w/v) glucose then subcultured into fresh media at 1:20 dilution. The culture was grown at 30˚C to an OD_{600} of ~0.6 at which point protein was induced with 0.1mM IPTG for 3 hours. Cells were harvested by centrifugation at 3,000 x *g* at 4˚C for 10 minutes. The cell pellets were washed with ice cold Buffer S (50 mM KPO_4 pH 6.0, 50 mM KCl, 5% glycerol and 0.1 mM DTT). After a second harvesting and washing step, the cell pellets were resuspended in 30 mL of Buffer S. Cells were disrupted by three passages through M110L homogenizer (Microfluidics, USA). Cell lysates were centrifuged at 12,000 x *g* at 4˚C for 25 minutes and filtered through 0.8 μm and 0.45 μm filters.

The filtered protein sample was loaded onto a 50 mL S-Sepharose column that was pre-equilibrated in Buffer S at a flow rate of 5 ml/min. The resin was washed until absorbance at 280 nm returned to baseline. The protein was fractionated using a linear gradient of 0 to 500 mM KCl over 100 minutes, collecting 10 mL fractions. Fractions corresponding with the most prominent peak in the elution profile were pooled and dialyzed overnight at 4˚C against cold Buffer Q (20 mM Tris pH 8.5, 5% glycerol and 1 mM DTT).

The dialysed sample was further purified with a 50 ml Q-Sepharose column pre-equilibrated with Buffer Q at a flow rate of 5 ml/min. The protein was eluted with a gradient of 0 to 400 mM KCl over 40 minutes. Fractions (5 mL) were collected and analyzed by SDS-PAGE. Fractions containing BirA were pooled and dialyzed overnight at 4˚C against cold BirA storage buffer (50 mM Tris pH 8, 100 mM KCl, 5% glycerol, 1 mM EDTA and 1 mM DTT). The purified enzyme was aliquoted and stored at -80˚C prior to use.

3.2.1.2 E. coli BCCP

E. coli BM4062 harbouring pGEX-BCCP (Amp^R) was grown at 30°C overnight in LB media supplemented with ampicillin (200 µg/ml). The overnight culture was subcultured into fresh media at 1: 20 innoculum and grown at 30°C to an OD_{600} of ~0.8. Cultures were transferred to 42°C and incubated for 30 minutes before induction of protein expression with 0.2 mM IPTG. After 3 hours, cells were harvested by centrifugation at 3,000 x *g* for 10 minutes at 4°C. The cell pellets were washed with ice cold TBS pH 8.5 and centrifuged for another 10 minutes. Cell pellets were resuspended in 30 mL TBS pH 8.5 and passed through M110L homogenizer (Microfluidics, USA) three times. The cell lysate was centrifuged at 12,000 x *g* at 4°C for 25 minutes and filtered through 0.8 µm and then 0.45 µm filters.

The filtered cell lysate was loaded onto a 10 mL glutathione agarose column pre-equilibrated in TBS pH 8.5 then washed with 5 column volumes of TBS pH 8.5. The GST-BCCP was cleaved at 37°C for 2 hours with 10 U/mL of thrombin in the presence of 2.5 mM $CaCl_2$. BCCP was eluted with TBS pH 8.5 and treated with PMSF at a final concentration of 1 mM. The sample was concentrated and exchanged into Buffer A (50 mM MOPS pH 7.2, 0.1 mM EDTA and 1 mM DTT) using a spin column with a 3000 MWCO filter (Millipore) before further purified with a 1 mL Resource™ Q column (Amersham Biosciences, Sweden) to resolve the apo and holo domains. DTT (40 mM) was added to the BCCP sample prior to loading onto the column pre-equilibrated in Buffer A. The column was washed and run at 1 mL/min until a baseline absorbance at 600 nm was achieved. The protein was eluted using a gradient of 0 to 400 mM NaCl at 0.5ml/min over 24 minutes. Fractions (0.5 mL) were collected and analysed with SDS-PAGE and

streptavidin blot. Fractions containing apo (*i.e.* streptavin-non reactive) BCCP87 were pooled and dialyzed overnight at 4°C against cold 2 mM ammonium acetate.

3.2.2 BirA assay and fluorescence polarization

96-well black plates (BMG Technologies) were blocked overnight at 4°C with 100 µl of 1% casein dissolved in TBS. Following blocking, plates were dried and stored at 4°C for up to 2 months. For the BirA reaction, a master mix was prepared containing 50 mM Tris pH 8.0, 3 mM ATP, 5.5 mM $MgCl_2$, 8 µM biotin, 0.1 mM DTT, 100 mM KCl, 7 µM peptide 85-11 and 3 µM fluorescein-labeled peptide 85-11. An aliquot of reaction mix, 47.5 µl, was added into each well of the 96-well plates and pre-equilibrated at 37°C for 5 min. The reaction was initiated by the addition of 2.5 µl BirA to a final concentration of 11 nM. After incubation at 37°C for 45 min, the reaction was terminated by the addition of 5 µl of stop solution containing 50 mM EDTA and 13.6 µg avidin (specific binding activity 14 U/mg) per well. The reaction was incubated for a further 10 min at 37°C before the plate was measured for fluorescence polarization using a BMG Laboratories PolarStar Galaxy Plate Reader. The plate reader was set in polarization mode with 485 and 520 nm excitation and emission filters, respectively, and millipolarization units (mP) were calculated, where P is defined as; P = (Int|| - Int^)/(Int|| + Int^) where Int|| = intensity of emission in the plane parallel to excitation (channel 1), and Int^ = intensity of emission in plane perpendicular to excitation (channel 2). The gain was adjusted for channel 1 and 2 using 2.3 µM fluorescein in 50 mM Tris pH 8.0 (55 µL), such that an mP value of 35 was obtained.

3.2.3 Peptide methods

Lyophilised peptide 85-11 (sequence MAGGLNDIFEAQ**K**IEWHE; target lysine for biotinylation in bold) was dissolved in peptide buffer (10 mM Tris pH 7.5, 200 mM KCl, 2.5 mM $MgCl_2$) and the concentration determined by absorbance at 280 nm using the extinction coefficient = 5690 $M^{-1}cm^{-1}$ (Beckett *et. al.*, 1999). The concentration of peptide was then adjusted to 100 µM with peptide buffer. For the fluorescein-labeled peptide (sequence FITC-β alanine – MAGGLNDIFEAQ**K**IEWHE; referred to as fl-85-11) lyophilised peptide was weighed out and dissolved in peptide buffer.

3.2.4 Virtual screening for ATP analogues

Potential ATP analogues were identified through virtual screening. A list of compounds containing adenine was generated from the ZINC database (http://zinc.docking.org/) through substructure search. These compounds were superimposed against biotinol-5'-AMP in the crystal structure of *E. coli* BPL (PDB ID: 2EWN (Wood *et. al.*, 2006)) using Chimera and docked with Sybyl 7.2 which proposed possible binding modes and generated a set of scores for each compound. The compounds within the top 15% of each scoring function (total score, D_score, Potential of Mean Force (PMF) score, G_score and Chemscore) were given a score. These scores were combined into a consensus score (Cscore) which ranged between 0 and 5. The top ranked compounds (Cscore = 5) were identified and selected for visual analysis at the virtual modeling facility. Potential candidates were then purchased for testing. All the compounds were dissolved in DMSO and assayed at the final concentration of 50 µM in 1% (v/v) DMSO.

3.2.5 Disc diffusion assay

Organisms routinely included in microbiology assays were *E. coli* K2495, *E. coli* (*TolC*$^-$) and *S. aureus.* A single colony of interested organism was picked and grown overnight in 2 mL of LB at 37°C with rotation. LB, 1 mL, was inoculated with 10 µL of the overnight culture and grown at 37°C until log phase (OD_{600} of ~0.8). The subculture, 50 µl, was used to inoculate 5 mL of fresh LB. This was grown at 37°C for a further 3 hours at which time the OD_{600} was ~ 1.2. We determined the relationship between OD and cell number to be OD_{600} 1.2 = 3 x 10^8 cells. Cultures were then diluted with LB to contain about 10^4 cells/mL. 300 µl of the inocula were spreaded evenly onto LB agar plates. Dry heat sterilized filter paper discs were soaked in solutions containing test compounds. Erythromycin was employed as a control of *Staphylococcus aureus* and ampicillin was used for *Escherichia coli*. Soaked discs were individually placed onto the agar plate with flame sterilized forceps. Plates were inverted and incubated overnight (18-24h) at 37°C

.

3.2.6 Minimal inhibitory concentration (MIC) assay

Bacterial culture was prepared as described above. The culture grown to an OD_{600} of ~1 and diluted 1:1000 with LB. Log-phase culture (200 µL ~ 10^4 cells) was seeded into 96 well flat bottom clear plates. Compounds were serially diluted (one part in ten dilution) in DMSO before 5 µL of each dilution was added to the respective wells. The plates were incubated at 37°C with constant rotation. The absorbance at 600 nm was measured with a microplate reader (Molecular Devices, CA, USA). Minimal inhibitory concentrations were determined as the lowest concentration inhibiting visible growth after overnight (18-24h) incubation.

3.3 RESULTS AND DISCUSSION

3.3.1 Principle of the assay

The aim of this study was to develop an assay for *E. coli* BPL (BirA) that is suitable for high-throughput screening. Assays for BPL activity have been reported, many of which utilise a common methodology whereby the enzymatic incorporation of radio-labeled biotin onto a suitable protein substrate is measured (Chapman-Smith *et. al.*, 1994; Leon-Del-Rio and Gravel, 1994; Suzuki *et. al.*, 1996; Campeau and Gravel, 2001). The protein is precipitated with trichloroacetic acid, washed to remove unincorporated biotin then protein-bound biotin quantitated by scintillation counting. Whilst these assays have provided excellent kinetic data in the laboratory, multiple handling steps and the requirement for radiolabeled ligand limit its appeal for high-throughput applications. Thus, a new assay system was established in a 96 well format. Here we employed FP to quantitate the enzymatic production of biotinylated product by BPL. As FP relies on changes in molecular mass (Checovich *et. al.*, 1995), peptide 85-11 was investigated. This had the advantage of having a relatively low molecular mass (Mr ≈2500) and is an excellent substrate for BirA (Beckett *et. al.*, 1999). Following the BPL reaction, biotinylated peptide is readily complexed with avidin (Mr = 66 000) due to the extremely high affinity between biotin and avidin. This large molecular mass complex impedes the rotation of the peptide out of the plane of polarized light used for excitation, thus providing a way to measure biotinylated product (holo 85-11). As the 96-well plate can be read directly, the multiple handling and washing steps associated with the radio-label assay are eliminated.

3.3.2 Peptide 85-11 is a suitable BirA substrate

BirA recognises and biotinylates the biotin carboxyl carrier protein (BCCP) subunit of ACC. It is clear from structural (Athappilly and Hendrickson, 1995; Roberts *et. al.*, 1999) and mutagenesis studies (Chapman-Smith *et. al.*, 1999; Polyak *et. al.*, 2001) that BirA recognises the structure adopted by BCCP and specifically attaches biotin onto the target lysine residue that resides in an exposed hairpin loop on the tip of the domain. However, several peptide sequences have been identified that do function as substrates for BirA (Schatz, 1993). Interestingly these bear no sequence identity with the natural substrate. One peptide of particular interest, designated 85-11, is recognised with an affinity equal to that of the natural substrate (Beckett *et. al.*, 1999).

Holo (biotinylated) 85-11 was produced by incubating the peptide overnight with BirA together with biotin, ATP and $MgCl_2$. Mass spectrometry analysis revealed that the molecular mass of the peptide was increased by 226, indicating the attachment of biotin. The BirA reaction was next adapted for FP by the addition of fluorescein-labeled peptide-85-11 (fl-85-11). We observed that it was important to optimise the concentration of fl-85-11 for the plate reader being employed, as variation was noted between different machines. High concentrations of fluorophore were undesirable as this interfered with the FP calculations. In the experiments performed here, the reaction contained 3 μM fl-85-11 and the final peptide concentration was adjusted to 10 μM with non-labeled peptide. Previous studies have shown that at this concentration 85-11 is biotinylated at the same rate as the natural substrate BCCP (Beckett *et. al.*, 1999). Since the K_M for BCCP is 3 μM (Chapman-Smith *et. al.*, 1999; Polyak *et. al.*, 2001) we reasoned that 10 μM would be a saturating concentration of substrate in the BirA reaction. (Determination of the K_M for the peptide was not possible with this assay system as the experiment requires varying amounts of fl-85-11 in the reaction, whereas the assay FP uses a constant fluorescent signal between

samples). Biotinylated product was complexed with avidin for 10 min at 37^{o}C before analysis by FP. Through optimisation of these conditions, > 100 milli polarization unit difference was achievable between apo (unbiotinylated) and holo-peptide.

3.3.3 Development of the assay

The assay was then adapted for steady state kinetic analysis. Standard curves of holo-peptide were performed to ascertain the sensitivity and dynamic range of detection. Here, the final concentration of peptide was adjusted to 10 μM by the addition of apo 85-11, thus ensuring a constant quantity of fluorescence in each well. Following incubation with excess avidin, a linear response was observed between 0 – 6 μM (Figure 3.1). The minimal detection limit was set as a function of the mean for the zero enzyme control plus 3X the standard deviation. Here we routinely calculated ~1 μM holo-peptide as the minimal quantity that could be accurately measured. This is comparable in sensitivity with other published assays (Chapman-Smith *et. al.*, 1994; Leon-Del-Rio and Gravel, 1994; Suzuki *et. al.*, 1996; Campeau and Gravel, 2001). The BirA reaction was then optimised with appropriate enzyme concentrations and time to achieve between 2 and 4 μM product formation (ie < 40% of the total reaction). The assay was routinely performed at 37^{o}C for 45 minutes, at which point the reaction was terminated by the addition of a stop solution containing avidin and EDTA. A 2-fold stoichiometric excess of avidin over biotin and 20-fold excess of EDTA over free Mg^{2+} were effective in terminating the reaction by sequestering these reaction components. Biotin, ATP, $MgCl_2$, avidin and BirA were then systematically removed from the assay to test their effect on BirA activity (Table 3.1). Product formation could only be detected in the complete assay reaction medium, thus demonstrating the specificity of the *in vitro* reaction. As expected, EDTA inhibited the reaction.

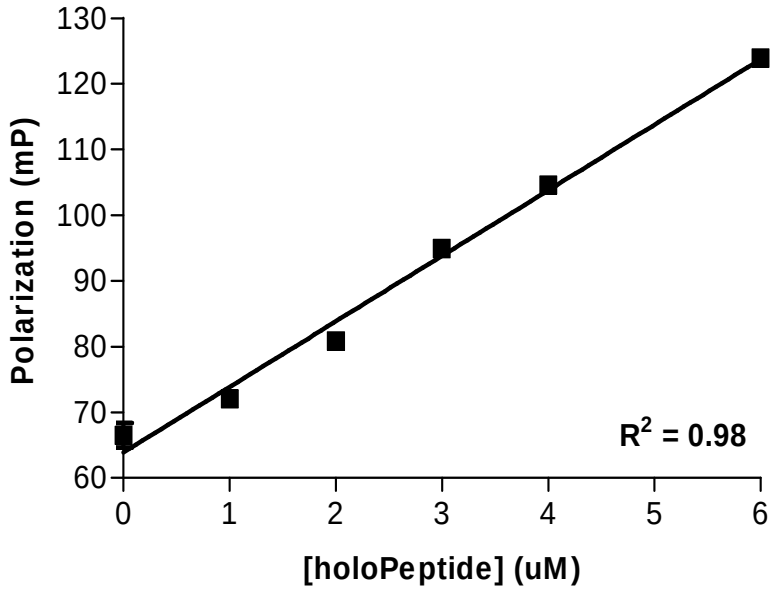

Figure 3.1 : Calibration curve for product formation

Holo (biotinylated) peptide fl-85-11 was prepared by overnight enzymatic biotinylation by BPL. A standard curve of holo peptide concentration vs FP was produced by first varying concentrations of holo and apo fl-85-11 to give a final peptide concentration of 10 μM. Following the addition of a 2-fold excess of avidin over holo-peptide the FP was measured.

Table 3.1 : Effect of removal of reaction components on BirA activity

Reaction conditions	Relative activity[†]
Complete	100 ± 3.65 %
Without ATP	4.7 ± 6.28 %
Without biotin	0 ± 7.7 %
Without $MgCl_2$	4.3 ± 6.4 %
With EDTA	7.4 ± 9.62 %
Without BPL	5.6 ± 8.36 %
Without avidin	3.2 ± 3.42 %

[†] Relative activity was expressed as mean ± SEM, n = 3

3.3.4 Kinetic analysis of BirA

The K_M values for MgATP and biotin were calculated to be 0.25 ± 0.01 mM and 1.45 ± 0.15 μM (Figure 3.2), which are in good agreement with published values (Chapman-Smith *et. al.*, 2001). For routine assays the concentrations of ligands were set at 3 mM ATP and 8 μM biotin. However, the enzyme activity could be readily measured with lower ligand concentrations of either 0.5 X the K_M for MgATP or 2 X K_M of biotin, an important consideration when performing competitive inhibition studies. The nucleotide triphosphate sources that can be utilised by BirA were also investigated. Here ATP, CTP, GTP, ITP, TTP and UTP were included in the reaction as the sole phosphate source (Table 3.2). BirA was most active with ATP, although CTP could also be utilized. The other nucleotides showed no activity.

Figure 3.2 : Kinetic analysis of ligand binding

The activity of BirA was measured over the concentration range of either A) MgATP or B) biotin. The lines represent the non-linear regression to the Michaelis-Menten equation. The apparent K_M for MgATP and biotin were 0.25 ± 0.01 mM and 1.45 ± 0.15 μM respectively.

A

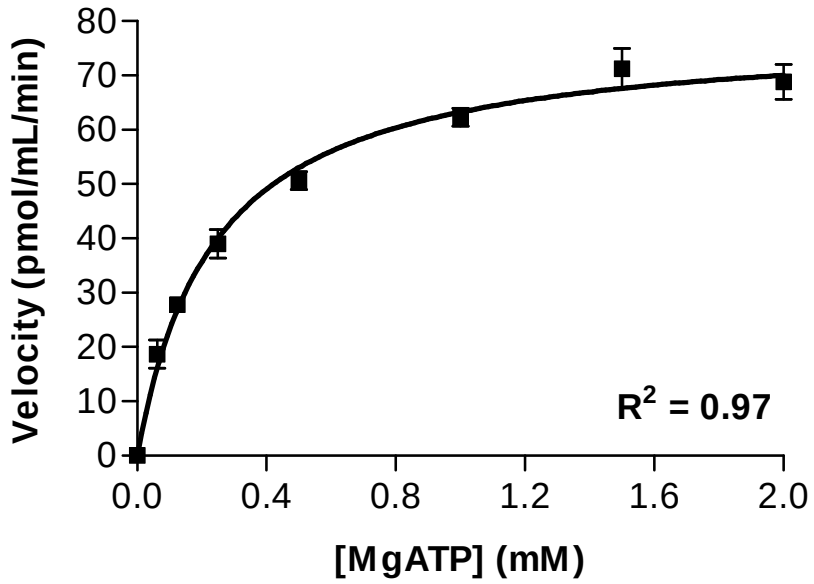
Velocity (pmol/mL/min)
80
70
60
50
40
30
20
10
0
0.0
0.4
0.8
1.2
1.6
2.0
[MgATP] (mM)
R2 = 0.97

B

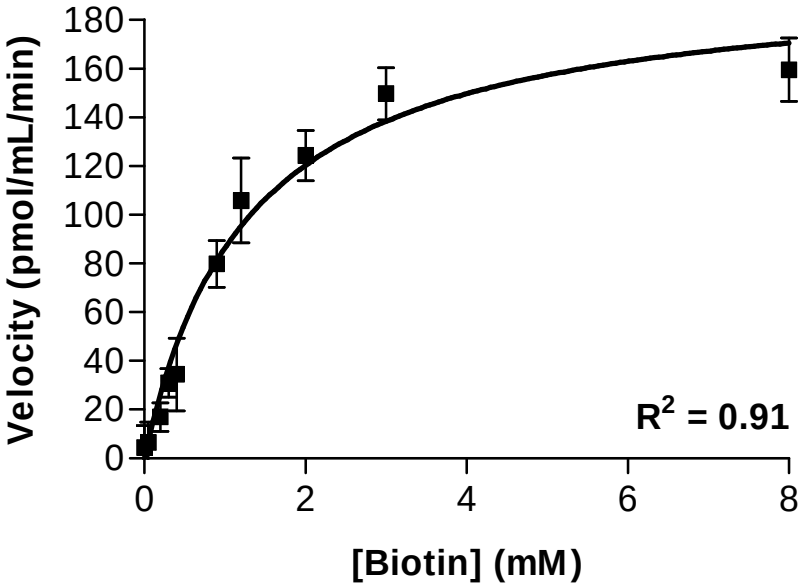
Velocity (pmol/mL/min)
180
160
140
120
100
80
60
40
20
0
0
2
4
6
8
[Biotin] (mM)
R2 = 0.91

Table 3.2 : Activity of E. coli BPL with various nucleotide triphosphates

Nucleotides	Relative activity[†]
Adenosine triphosphate (ATP)	100 ± 5.23 %
Thymidine triphosphate (TTP)	3.2 ± 5.18 %
Cytidine triphosphate (CTP)	12.6 ± 3.36 %
Guanosine triphosphate (GTP)	6.4 ± 5.21 %
Uridine triphosphate (UTP)	2 ± 1.18 %
Inosine triphosphate (ITP)	0 ± 4.15 %

[†] Relative activity was expressed as mean ± SEM, n = 3

3.3.5 Inhibition studies

This assay was further validated with inhibition studies employing the reaction end products, MgAMP and pyrophosphate. As expected, these compounds were able to inhibit BirA activity. MgAMP had an IC_{50} of 8.24 ± 1.75 mM when assayed with 0.5 X the K_M for MgATP (Figure 3.3A). The mechanism of inhibition was further investigated by measuring BPL activity with varying concentrations of both MgATP and MgAMP (Figure 3.3B). As expected, Lineweaver-Burk plots revealed MgAMP to be competitive against MgATP (Figure 3.3C). Pyrophosphate was predicted to inhibit BPL activity through product feedback inhibition of the first partial reaction. Indeed, 0.6 mM pyrophosphate inhibited the enzyme but this could be alleviated by pre-incubation of the reaction mixture with pyrophosphatase (Figure 3.4).

Additionally, the assay was performed in the presence of DMSO. BirA activity was > 90% with 1-2% (v/v) of solvent in the reaction medium, and retained 80% of activity with 5% (v/v) DMSO (Table 3.3). This will be advantageous when screening compound libraries that are commonly solubilized in this solvent. Together these data demonstrated

Figure 3.3 : Inhibition of BirA activity by MgAMP

The activity of BirA was measured with a fixed concentration of MgATP (0.15 μM, ie 0.5X the K_M) and varying concentrations of inhibitor MgAMP. A) The IC_{50} was measured to be 8.24 ± 1.75 mM. B) Competition between MgATP and MgAMP was observed by measuring enzyme activity in varying concentrations of the two reagents. C) Double reciprocal plots of initial velocities with varying concentrations of MgATP and MgAMP. The concentrations of MgAMP used were 0 (■), 5 mM (▲) and 40 mM (●).

A

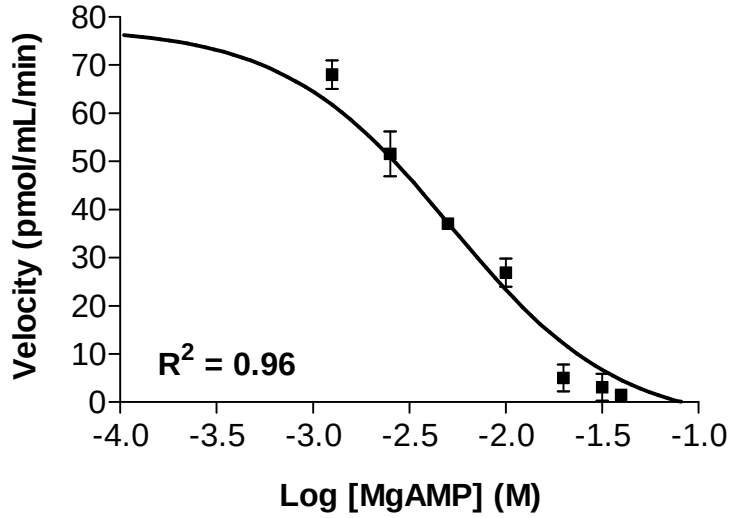
Velocity (pmol/mL/min)
80
70
60
50
40
30
20
10
0
R2 = 0.96
-4.0
-3.5
-3.0
-2.5
-2.0
-1.5
-1.0
Log [MgAMP] (M)

B

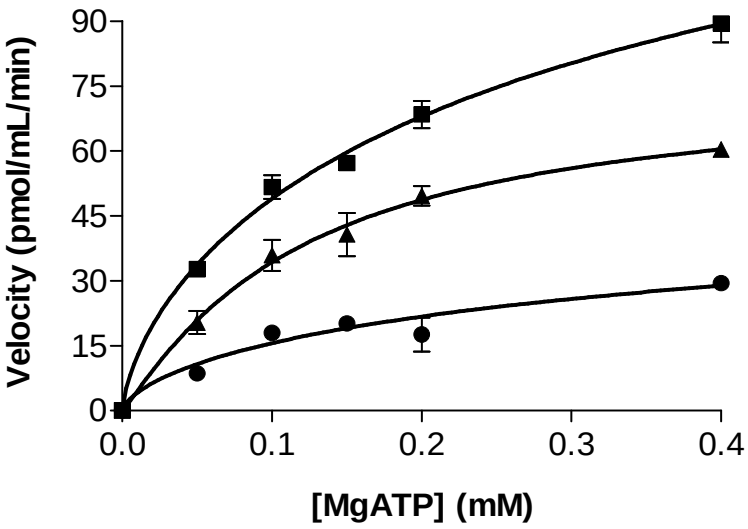
Velocity (pmol/mL/min)
90
75
60
45
30
15
0
0.0
0.1
0.2
0.3
0.4
[MgATP] (mM)

C

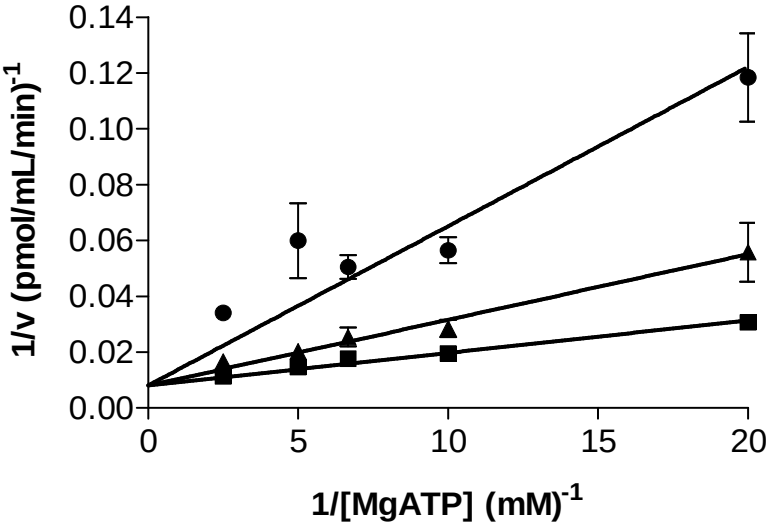
1/v (pmol/mL/min)-1
0.14
0.12
0.10
0.08
0.06
0.04
0.02
0.00
0
5
10
15
20
1/[MgATP] (mM)-1

that this FP-based assay could be employed for high-throughput screening of compound for inhibitors of BirA.

Table 3.3 : Effect of DMSO on BirA activity

DMSO	Relative activity[†]
0 % (v/v)	100 ± 8.8 %
1 % (v/v)	97 ± 1.99 %
2 % (v/v)	88.2 ± 0.64 %
5 % (v/v)	81.3 ± 0.4 %

[†] Relative activity was expressed as mean ± SEM, n = 3

3.3.6 Intra- and inter-assay variation

The results from 30 replicates of apo and holo peptide (ie 0% and 100% of the BirA reaction) were collected to measure intra-assay variation (Table 3.4). The coefficient of variation (CV) was 5.98% for apo- and 2.23% for holo-peptide, indicating good reproducibility. Similarly, data were collected from 30 separate experiments over 3 months for analysis. Again, the CV values were <10% across the data set (8.44% for apo, 6.36% for holo). The Z' value, a measure of data scatter and assay reproducibility (Zhang *et. al.*, 1999), was used to assess the suitability of the assay for high-throughput applications. The results of both intra (0.83) and inter-assay (0.56) analysis were greater than 0.5, thereby indicating the assay is acceptable for high-throughput applications. Taken together, the data implied that the BirA assay was indeed optimized for drug discovery.

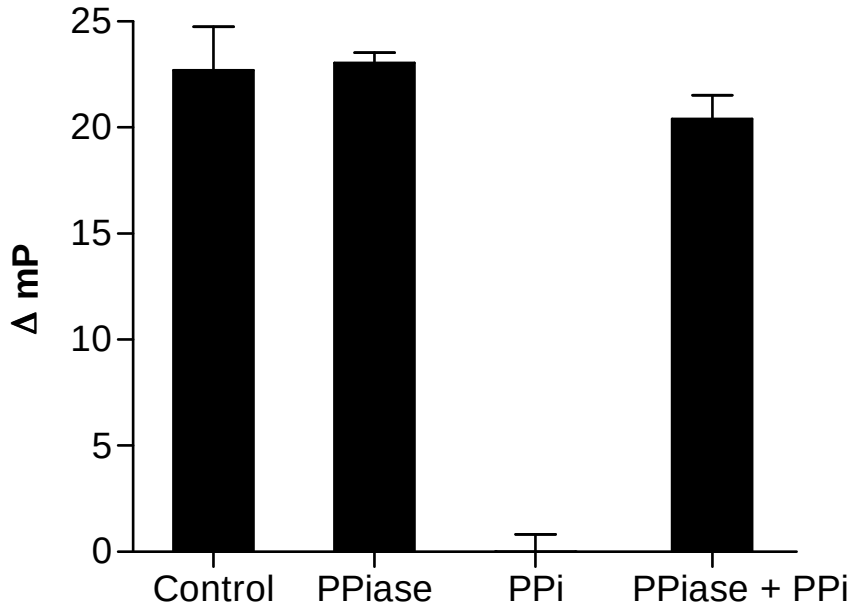

Figure 3.4 : Inhibition of BirA by pyrophosphate

The activity of BirA was measured in the presence of 0.6 mM pyrophosphate (PPi) or pyrophosphatase (PPase). Pyrophosphate inhibited enzyme activity, but this was reversed by pre-incubation of the reaction medium with 1U pyrophosphatase.

Table 3.4 : Statistical analysis of the BirA assay

	Intra-assay		Inter-assay	
% of Reaction	0%	100%	0%	100%
Number of samples	$n = 30$	$n = 30$	$n = 30$	$n = 30$
Mean of data set (mP), μ	67	225	74	214
Std. deviation, σ	± 4	± 5	± 6	± 14
Coefficient of variation (CV)	5.98%	2.23%	8.44%	6.46%
Z' factor	0.56		0.83	

3.3.7 Compound screening for BirA inhibitors

3.3.7.1 ATP analogues

Advances in combinatorial chemistry and high-throughput screening have contributed tremendously to the rapid expansion of chemical databases. Traditional "wet screening" of large chemical libraries, potentially containing millions of unique identities, requires considerable effort and cost. In an attempt to stream-line identification of "hits", computer-based technology, or virtual screening, is gaining increasing acceptance in the discovery process. This technology provides a relatively fast and inexpensive method to identify potential binders as well as enhances the success in identifying novel lead molecules (Walters *et. al.*, 1998; Baber *et. al.*, 2006). Fundamentally, there are two general approaches in virtual screening: 1) receptor based screening, which requires the 3-dimensional (3D) structure of the target protein (reviewed in Lyne, 2002) and 2) ligand-based screening, which identifies compounds based on known ligands or binders (reviewed in Stahura and Bajorath, 2005). Here, the two approaches were synergistically integrated to improve the screening processes. This method enabled rapid scanning and identification of

potential compounds from large databases before these compounds were docked with 3D structures of BPL, thus exploring the ligands' flexibility through various algorithms to provide an accurate ranking of the compounds (reviewed in Khedkar *et. al.*, 2006).

This work employed the existing crystal structure of *E. coli* BirA in complex with btnOH-AMP (Wood *et. al.*, 2006), which was the only bacterial BPL structure defining the nucleotide binding site publicly available at the time I commenced this project. Here, ZINC database was considered as it contained > 18,000,000 available substances. Using a core-based matching approach, this list was reduced to 614 compounds all of which contained an adenine substructure. Each library member was subsequently superimposed and docked against the active site of BirA using Sybyl 7.2. Those poses that had the smallest RMSD to btnOH-AMP were selected for further analysis. The quality of the fit, both chemically and geometrically, for each molecule in the target binding site was determined using Cscore which combines the information from several independent scores to a single measure. This method was found to have significantly improved the reliability and interpretability of the results (Clark *et. al.*, 2002; Baber *et. al.*, 2006). Sixteen of the highest scorers were then identified, from which 7 potential analogues (Cpd B1 - B7) (Figure 3.5) that showed desirable properties from the *in-silico* docking were selected for further analysis. However, due to availability and cost, only 3 (Cpd B1 - B3) of the 7 compounds were obtained. Two additional compounds (Cpd B4a and Cpd B5a) with similar substructure of compound Cpd B4 and Cpd B5 were also purchased.

All the compounds were routinely dissolved in 100% DMSO at the concentration of 5 mM and subsequently diluted to 500 µM in 10% DMSO. However, as discussed earlier, the presence of > 2% (v/v) DMSO reduced BirA activity (Table 3.3). Therefore, taking the effect of DMSO into considerations, this assay was carried out at the final

Figure 3.5 : ATP analogues for BirA

Cpd B1 – B7 were identified through virtual screening whereas Cpd B4a and Cpd B5a were from similar search based on Cpd B4 and Cpd B5 respectively. Only Cpd B1 (Sigma), Cpd B2 (IBScreen), Cpd B3 (IBScreen), Cpd B4a (Sigma) and Cpd B5a (Sigma) were purchased and tested for their effect on BirA activity.

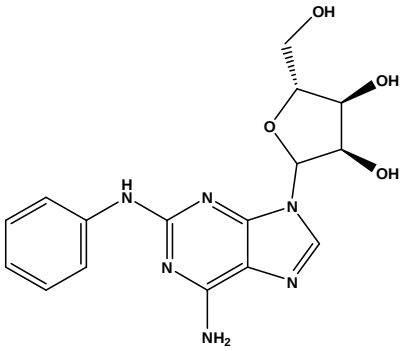

Cpd B1
(ZINC3995405)

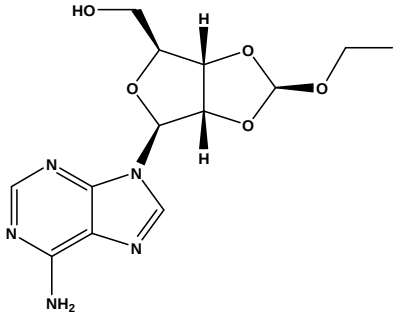

Cpd B2
(ZINC161598)

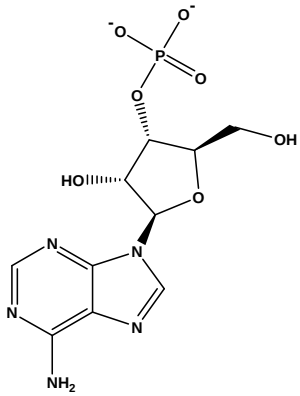

Cpd B3
(ZINC1529188)

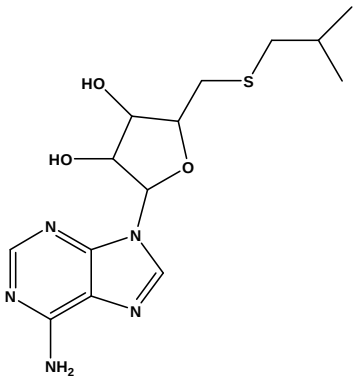

Cpd B4
(ZINC1319992)

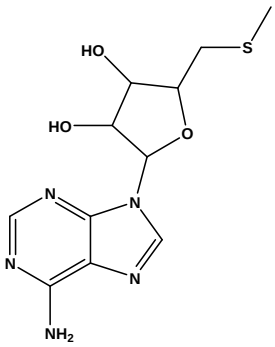

Cpd B4a

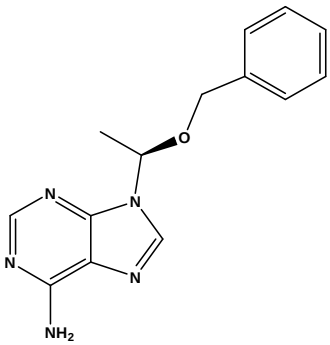

Cpd B5
(ZINC1443593)

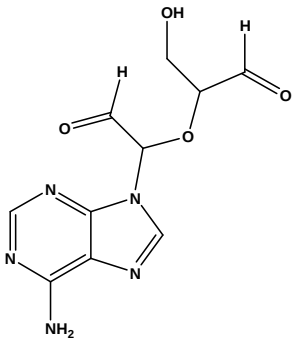

Cpd B5a

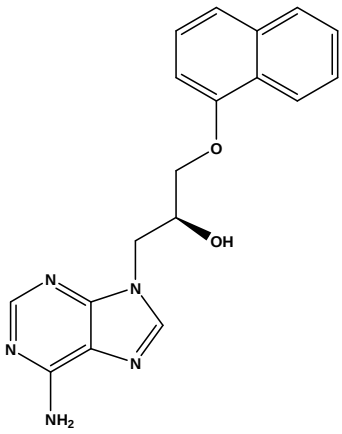

Cpd B6
(ZINC144266)

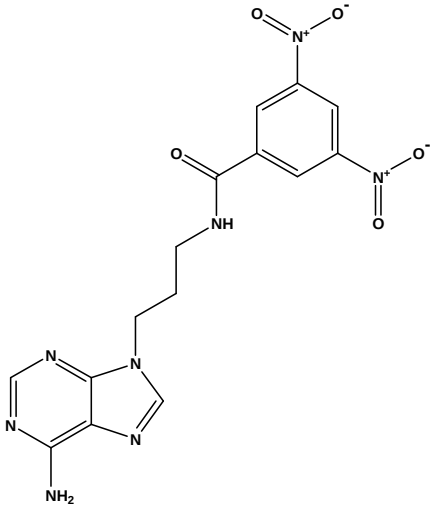

Cpd B7
(ZINC1728051)

compound concentration of 50 µM in 1% DMSO. In a crystal study on Cpd B4a and Cpd B5a by Ms Nicole Pendini at Monash University, both compounds were successfully soaked into the active site of the BirA crystals, showing bound ATP analogues in the ATP binding site (unpublished data). However, these compounds showed poor inhibitory activity (< 10%) and were not good competitors against MgATP (Table 3.5). Similarly, these compounds did not present any anti-bacterial property when tested with disc diffusion assay.

Table 3.5 : Inhibition studies with ATP analogues

ATP analogues	Relative activity[†]
1% DMSO control	100 ± 2.24 %
Cpd B1	95.27 ± 0.19 %
Cpd B2	96.55 ± 0.79 %
Cpd B3	90.58 ± 0.62 %
Cpd B4a	90.97 ± 1.09 %
Cpd B5a	90.25 ± 0.48 %

[†] Relative activity was expressed as mean ± SEM, n = 3

On reflection, the weak inhibitory results were not surprising based on the inhibition studies with MgAMP (see 3.3.5). MgAMP had a high IC_{50} (8.24 ± 1.75 mM) even when tested with 0.15 mM MgATP in the reaction (*i.e.* 0.5 X K_M). Similarly, inhibition assays with adenine further demonstrated that nucleotide analogues are not ideal inhibitors for BPL. The presence of 4.8 mM adenine showed enzyme inhibitory activity by ~50%. Unfortunately, due to the limited compound solubility, I was unable to test the analogues at concentrations exceeding 50 µM. At this point, I decided to perform inhibitor studies with btnOH-AMP to better understand the reaction mechanism.

3.3.7.2 Biotinol-5'-AMP

In the second partial reaction, BPL binds to an apo-biotin domain where the biotin moiety is transferred to the accepting lysine residue. In this reaction, the bond between biotin and AMP of the biotinyl-5'-AMP is hydrolyzed to facilitate biotin transfer onto a biotin domain. Professor John Cronan (University of Illinois) designed and synthesized an analogue of the reaction intermediate, btnOH-AMP, in which he placed a non-hydrolysable carboxyphosphate group between the AMP and biotin moieties. This compound was initially designed to induce BirA dimerization necessary for interaction with DNA. Since btnOH-AMP is non-hydrolysable, we proposed that this compound would also function as a BPL inhibitor. Indeed, this compound had an IC_{50} of 2.5 ± 1.2 μM (Figure 3.6), even when assayed in the presence of saturating concentrations of biotin and MgATP.

BtnOH-AMP was then tested for its anti-bacterial activity against *E. coli* K2495 and *S. aureus*. Interestingly, in the disc diffusion assay, the compound inhibited the growth of *S. aureus* but not *E. coli*. Further testing by Dr. Steven Polyak on a small library of bacteria has indeed shown that the *Staphylococcus* strains (*S. aureus* and *S.epidermitus*) were sensitive to the compound but not the Gram-negative bacteria (*E. coli* K2495, *E. coli* TolC$^-$ strains) nor Gram positive *Bacillus subtilis*. This testing was subsequently verified with clinical isolates of MSSA and MRSA strains by Prof. John Turnidge from the Women's and Children's Hospital, Adelaide. Further characterization of btnOH-AMP as an anti-*S. aureus* agent will be represented in Chapter 4. These experiments provided the first evidence that BPL could indeed be an antibiotic drug target.

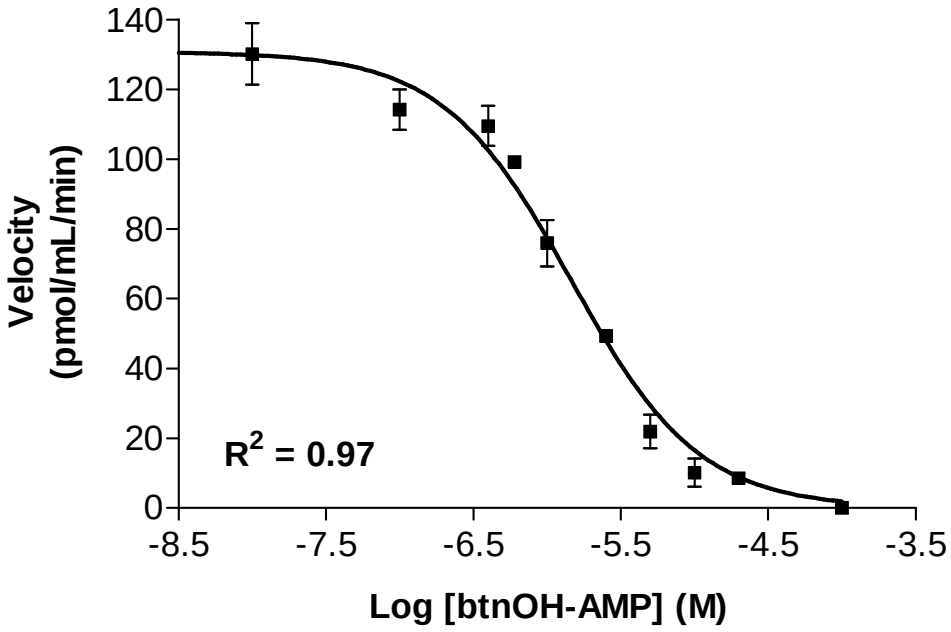

Figure 3.6 : Inhibition of BirA by biotinol-5'-AMP

The activity of BirA was measured with a fixed concentration of biotin at 8 µM in the presence of increasing concentrations of btnOH-AMP. The IC_{50} was measured to be 2.5 ± 1.2 µM (mean ± std. deviation, n = 4)

3.4 CONCLUSION

Here, a simple and robust FP based assay measuring the enzymatic activity of BirA has been developed in a 96-well format. The requirement for radiolabeled ligands (ie. ^{3}H-biotin) as well as the multiple handling and washing steps associated with previous assays for BPL activity (Chapman-Smith *et. al.*, 1994; Leon-Del-Rio and Gravel, 1994; Suzuki *et. al.*, 1996; Campeau and Gravel, 2001) have been eliminated and thus the assay was amendable for the use with robotic automation. The enzymatic properties of BirA were shown to be comparable with published data (Chapman-Smith *et. al.*, 1999 and 2001), thereby validating the assay. Statistical analysis demonstrated that the assay satisfied the criteria for high-throughput applications. Additionally, inhibition studies with MgAMP and pyrophosphate showed that this assay is suitable for high-throughput screening of large compound libraries for inhibitors of *E. coli* BPL as well as for competitive inhibition studies of potential compounds.

In this assay, peptide 85-11 was used as the substrate. This minimal peptide was identified through random screening for BirA substrates. Despite having little resemblance to the biotinylated sequence of BCCP (Figure 3.7), the mass spectrometric analysis of this peptide has shown the same biotin accepting function to that of the natural substrate (Beckett *et. al.*, 1999). Using the stopped-flow traces, the authors demonstrated that from a series of truncated peptides, peptide 85-11 had consistently shown a higher biotinylation rate, comparable to the biotin transfer rate of BCCP. Although it was established that all BPLs reaction are highly conserved among a variety of species, this peptide was not recognized by all BPLs. Recent findings in our laboratory revealed that this peptide was not biotinylated by *S. aureus* BPL (Bird, 2007). Therefore, using peptide 85-11 limits the direct application of the methodology reported here to *E. coli*. Potentially, other peptide substrates could be employed. One such peptide was recently reported as a substrate for

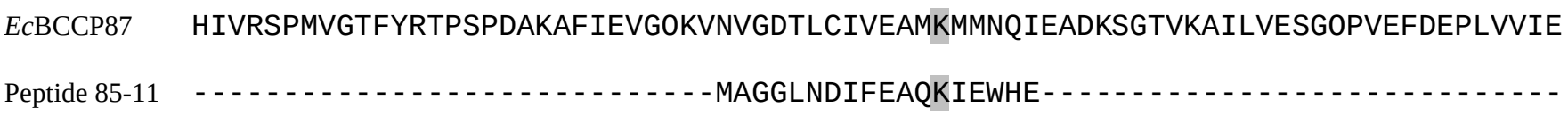

Figure 3.7 : Sequence alignment of *E. coli* biotin domains and minimal peptide 85-11 (Beckett *et. al.*, 1999).

The biotinylated lysine residue was shaded. Sequence comparation showed little similarity between the minimal peptide and the biotin domain.

yeast BPL (Chen *et. al.*, 2007). However, the high K_M (150 µM) is likely to restrict its use in kinetic analysis.

Antagonists of ATP binding have proven to be one of the successes in drug discovery. ATP analogues such as Lavendustin A (Onoda *et. al.*, 1989) and Genistein (Akiyama *et. al.*, 1987) are two such examples. One of the largest drug discovery programmes, the clinical development of protein kinases inhibitors for cancer and other diseases, are directed towards the ATP-binding site (Levitzki and Gazit, 1995; Arora and Scholar, 2005; Bogoyevitch *et. al.*, 2005; Shchemelinin *et. al.*, 2006). This led to our initial proposal that the ATP binding site of BirA could be targeted with small compounds (ATP analogues). In this study, five ATP analogues were identified from the ZINC database and purchased for testing. Crystal structure data showing the bound ATP analogues at the ATP binding site suggested that potential ATP analogues were successfully identified through the *in-silico* screening approach. However, these analogues were found to be weak competitors against the natural ligand (<10% inhibitory activity) even when tested at 50 µM in the presence of 0.15mM MgATP (*i.e.* 0.5 X K_M). In this case, a complementary binding study such as isothermal titration calorimetry (ITC) to the current competitive inhibition assay would definitely provide valuable information for the structure-activity relationship studies.

On the other hand, btnOH-AMP was shown to be a potent inhibitor. This is not unexpected as kinetic analysis demonstrated that the enzyme had a greater affinity for biotin than it does for MgATP. Previous studies have also established that biotin adenylation by BirA is an ordered reaction in which biotin binds first, followed by ATP and subsequently hydrolyzed to form the biotinyl-AMP (Xu and Beckett, 1994). It was later discovered that there is no preformed binding site for adenylate prior to binding of

biotin (Wood *et. al.*, 2006). These circumstances might have given the btnOH-AMP a better chance to compete for the biotin binding site. Interestingly, in the antibacterial assays, this compound only inhibited the *Staphylococcus* strains but neither the *E. coli* nor *Bacillus subtilis.* Although the reason for the selective inhibition is not currently understood, btnOH-AMP is nonetheless a promising lead compound for future antibiotic development especially against *S. aureus*. Therefore, it is critical to have a universal substrate to enable the application of the FP assay for *S. aureus* and other bacterial BPLs. This subject will be discussed in Chapter 4.

CHAPTER 4

ASSAY ADAPTAITION FOR S. AUREUS BPL

CHAPTER 4 ASSAY ADAPTATION FOR *S. AUREUS* BPL

4.1 INTRODUCTION

S. aureus is a clinically significant pathogenic organism. This bacterium has been implicated in a wide range of diseases such as skin infections, endocarditis, osteomyelitis, pneumonia, meningitis, bacteraemia and toxinoses (reviewed in Goldstein, 2007). The methicillin-resistant strain (MRSA) is the major pathogen responsible for nosocomial infection associated with high morbidity and mortality (Cosgrove *et. al.*, 2003). Vancomycin, approved by the FDA in the 1950's, remains one of the primary lines of defense. Not surprisingly, after half a decade of use, resistance has been reported. Newer drugs such as linezolid (FDA approved 2001), daptomycin (FDA approved 2003) and tigecycline (FDA approved 2005) are the current therapies. However, resistance against these has also been discovered (reviewed in Goldstein, 2007). Therefore, new drugs are needed to combat these multi-drug resistant bacteria. In this chapter, btnOH-AMP, which was shown to be an anti-*Staphylococcus* compound, will be further characterized.

In Chapter 3, a convenient, high-throughput FP-based assay for BPL activity was reported. Due to the peptide substrate used, this assay was restricted to *E. coli* BPL (BirA). We also demonstrated that nucleotide analogues were weak BPL inhibitors. Although btnOH-AMP was a potent inhibitor for BirA, this compound only showed antibacterial properties against *Staphylococcus* strains but not *E. coli*. Therefore, I decided that it was necessary to adapt the FP assay for BPL from the pathogenic bacteria *S. aureus* (*Sa*BPL) in order to facilitate further studies. Here we propose to use the biotin domain of *S. aureus* pyruvate carboxylase as the fluorescently labeled substrate. The BPL assay was then performed to characterize the biological properties of *Sa*BPL. Kinetic analyses of ligand

binding were compared with data using the ^{3}H-biotin incorporation assay. This assay was further validated using inhibition studies and statistical analysis. Additionally, biotin analogues were also investigated using this assay.

4.2 SPECIFIC METHODS

4.2.1 Minimal inhibitory concentration assay (MIC)

Bacterial culture was prepared as described in 3.2.6. The culture grown to an OD_{600} of ~1 and diluted 1:1000 with LB. Log-phase culture (200 µL ~ 10^4 cells) was seeded into 96 well flat bottom clear plates. Compounds were serially diluted (one in ten dilution) in DMSO before 5 µL of each dilution was added to the respective wells. The plates were incubated at 37°C with constant rotation. The absorbance at 600 nm wavelength was measured using a microplate reader (Molecular Devices, CA, USA). MICs were read as the lowest concentration inhibiting visible growth after overnight (18-24h) incubation.

4.2.2 Recombinant protein expression and purification

4.2.2.1 SaBPL

The purification of recombinant *Sa*BPL was performed as previously described (Pendini *et. al.*, 2008c). Briefly, an overnight culture of *E. coli* BL21 (DE3) cells harbouring the expression plasmid pET (*S. aureus* BPL-H_6) were grown in 2YT medium supplemented with ampicillin (200µg/ml) then subcultured into fresh media at 1:20 dilution. The culture was grown at 30°C to an OD_{600} of ~0.6. Recombinant protein expression was induced with 1 mM IPTG for 3 hours at 30°C. Cells were harvested by centrifugation at 3,000 x *g* at 4°C for 10 minutes. The cell pellets were washed with ice

cold Ni-NTA Binding Buffer (20 mM Tris–HCl, 0.5 M NaCl pH 7.9, 50 mM imidazole). After a second harvesting and washing step, the cell pellets were resuspended in 60 mL ice-cold Ni-NTA binding buffer containing 0.1 µg/mL lysozyme and 1mM PMSF. Cells were disrupted by three passages through a M110L homogenizer (Microfluidics, USA). Cellular debris was removed by centrifugation at 12,000 x *g* at 4°C for 20 minutes and filtered through 0.8 µm and 0.45 µm filters.

The filtered protein sample was applied onto a 5 mL His-Trap HP column (GE Healthcare) that was pre-equilibrated in Ni-NTA Binding Buffer at a flow rate of 1 ml/min and cycled over the column continuously for 3 hours. The column was washed with 10 column volumes of Ni-NTA Binding Buffer before SaBPL-H_6 was eluted step-wise with Ni-NTA binding buffer containing imidazole at 100 mM, 175 mM and 500 mM. Ten fractions of 1.5 mL for each concentration were collected and the process was monitored with Bradford analysis. Peak fractions were pooled and dialyzed overnight at 4°C against Buffer A (50 mM $NaPO_4$, pH 7.0, 5% (v/v) glycerol, 1 mM EDTA, 1 mM DTT).

The dialysed sample was further purified with a 15 ml SP-Sepharose column pre-equilibrated with Buffer A. The protein was eluted with a gradient of 0 to 400 mM NaCl over 40 minutes with SaBPL-H_6 eluting at ~200 mM NaCl. The fractions containing SaBPL-H_6 were confirmed using SDS-PAGE and ^{3}H-biotin incorporation assay. Fractions containing the enzyme were pooled and dialyzed ovemight at 4°C against cold storage buffer (50 mM Tris-HCl pH 7.5, 5% (v/v) glycerol, 1 mM EDTA and 1 mM DTT). The purified enzyme was aliquoted and stored at -80°C prior to use.

4.2.2.2 Apo SaPC90

Expression of apo-biotin domains was performed in the temperature sensitive *bir*A85$^-$ *E. coli* strain BM4062 (Barker and Campbell, 1981b). The biotin domains were expressed as GST fusion proteins permitting high-level expression and rapid purification by affinity chromatography. Cells were grown in LB media supplemented with 200 µg/ml ampicillin and 10 µM biotin at 30°C to OD_{600} ~0.8. The cultures were then moved to 42^{o}C for another 30 minutes to heat inactivate endogenous BirA before a 3 hour induction with 0.2 mM IPTG. Cells were disrupted by three passages through a M110L homogenizer (Microfluidics, USA) prior to affinity chromatography. The filtered lysate was passed over a 40 ml glutathione-agarose column (Scientifix, Australia) at a flow rate of 2 ml/min. Unbound material was removed by washing with 3 column volumes of TBS pH 8.5. The GST fusions were eluted with 10 mM reduced glutathione in TBS pH 8.5. The GST fusions were then cleaved in solution for 2 hours at 37°C with thrombin digestion buffer (3U thrombin/mg protein, TBS pH8.5, 2.5 mM $CaCl_2$).

Further purification of the apo-domain was carried out by anion exchange chromatography on a 20 ml Q-Sepharose column (GE Healthcare, 3.8 x 2.6 cm). The protein sample was treated with DTT to a final concentration of 40 mM before being loaded onto the pre-equilibrated column in Buffer A (25 mM Tris pH 8.0, 0.1 mM EDTA and 1 mM DTT). Protein was eluted using a gradient of 0% to 25% Buffer B (25 mM Tris pH 8.0, 0.1 mM EDTA, 400 mM sodium chloride and 1 mM dithiothreitol). All washing, loading and elution steps were performed at 5 ml/min. Fractions were analysed by SDS-PAGE and Streptavidin blot to identify holo-domain. Fractions containing *Sa*PC90 were pooled, concentrated with 3 000 molecular weight cut-off protein concentrator (GE Healthcare) and dialysed overnight at 4°C against 2 mM ammonium acetate. The

concentrations of biotin domains were determined using a BCA assay (Pierce Biotechnology) following the manufacturer's instructions.

4.2.3 Protein labeling with fluorescein-5'-maleimide

Mutant *Sa*PC90 domains were labeled with a 15-fold molar excess of fluorescein-5'-maleimide (Pierce Biotechnology) for 2 hours at room temperature. Excess fluorescein was removed using a PD-10 desalting column (GE Healthcare). Labeled protein was concentrated, dialysed against 2mM ammonium acetate and stored at -20^{o}C.

4.2.4 BPL Assay and Fluorescence Polarization

96-well black plates (BMG Technologies) were prepared as described previously in 3.2.2. For the BPL reaction, a master mix was prepared containing 50 mM Tris pH 8.0, 3 mM ATP, 5.5 mM $MgCl_2$, 15 μM biotin, 0.1 mM DTT, 7 μM SaPC90 and 3 μM SaPC90 N1102-Fl. An aliquot of reaction mix, 47.5 μl, was added into each well of the 96-well plates and pre-equilibrated at 37^{o}C for 5 min. The reaction was initiated by the addition of 2.5 μl *Sa*BPL to the final concentration of 360 nM (specific activity = 130 nmol/min/mg). After incubation at 37^{o}C for 30 min, the reaction was terminated by the addition of 4 μl of stop solution containing 50 mM EDTA and 0.1 U/μl avidin (specific binding activity 14 U/mg) per well. The reaction was incubated for a further 10 min at 37^{o}C before the plate was measured for fluorescence polarization using a BMG Laboratories PolarStar Galaxy Plate Reader. The plate reader was set according to previously described in 3.2.2. The gain was adjusted for channel 1 and 2 using 6.5 μM fluorescein in 50 mM Tris pH 8.0 (50 μL), such that an mP value of 35 was obtained.

4.2.5 IC_{50} and K_i for biotin analogues

The FP-based *Sa*BPL assay discussed in this chapter was used to analyze the effect of varying concentrations of biotin analogues on the activity of *Sa*BPL. The data was graphed and analyzed using one side competition curves with GraphPad Prism. This also calculated the concentration of inhibitor that produces half maximal response (IC_{50}). The inhibition constant (K_i) was calculated using the following equation (Cheng and Prusoff, 1973):

$$K_i = \frac{IC_{50}}{1 + \frac{[Biotin]}{K_M}}$$, where [biotin] = 15 µM, K_M = 3.3 µM

4.3 RESULTS AND DISCUSSION

4.3.1 DNA manipulations

The genomic DNA sequence for the methicillin-resistant *S. aureus* strain N315, used to design oligonucleotides for PCR and mutagenesis (shown in 2.1.9), was from GenBank (Genbank accession no. **NC002745**). The DNA encoding *Sa*PC103 was obtained by genomic PCR using oligonucleotides B214 and B215. The DNA encoding *Sa*PC90 was obtained by genomic PCR using oligonucleotides B242 and B215. PCR products were digested with *Bam*HI and *Eco*RI restriction endonucleases and ligated into similarly treated pGEX-4T-2 (GE Healthcare), yielding pGEX-*Sa*PC103 and pGEX-*Sa*PC90 respectively (Figure 4.1). Mutagenesis was performed with the QuikChange® site-directed mutagenesis kit (Stratagene) upon the parent constructs using the oligonucleotides shown in 2.1.9. All constructs were confirmed by DNA sequencing (Institute of Medical and Veterinary Science, Adelaide).

Figure 4.1 : Vector map for pGEX-4T-2 for mutagenesis study

A) Vector map of pGEX-4T-2. Shown in the expanded region is the restriction sites used for cloning of either *Sa*PC103 or *Sa*PC90 sequence into the vector. TEV protease recognition site was as indicated in the diagram.

B) The nucleotide and protein sequence for SaPC103. The unstructured region present outside of the structured biotin domain that underwent proteolysis during thrombin cleavage was highlighted in blue. The minimal functional domain (SaPC90) was generated by truncation of this N-terminal "tail". All constructs were confirmed by DNA sequencing (Institute of Medical and Veterinary Science, Adelaide).

A

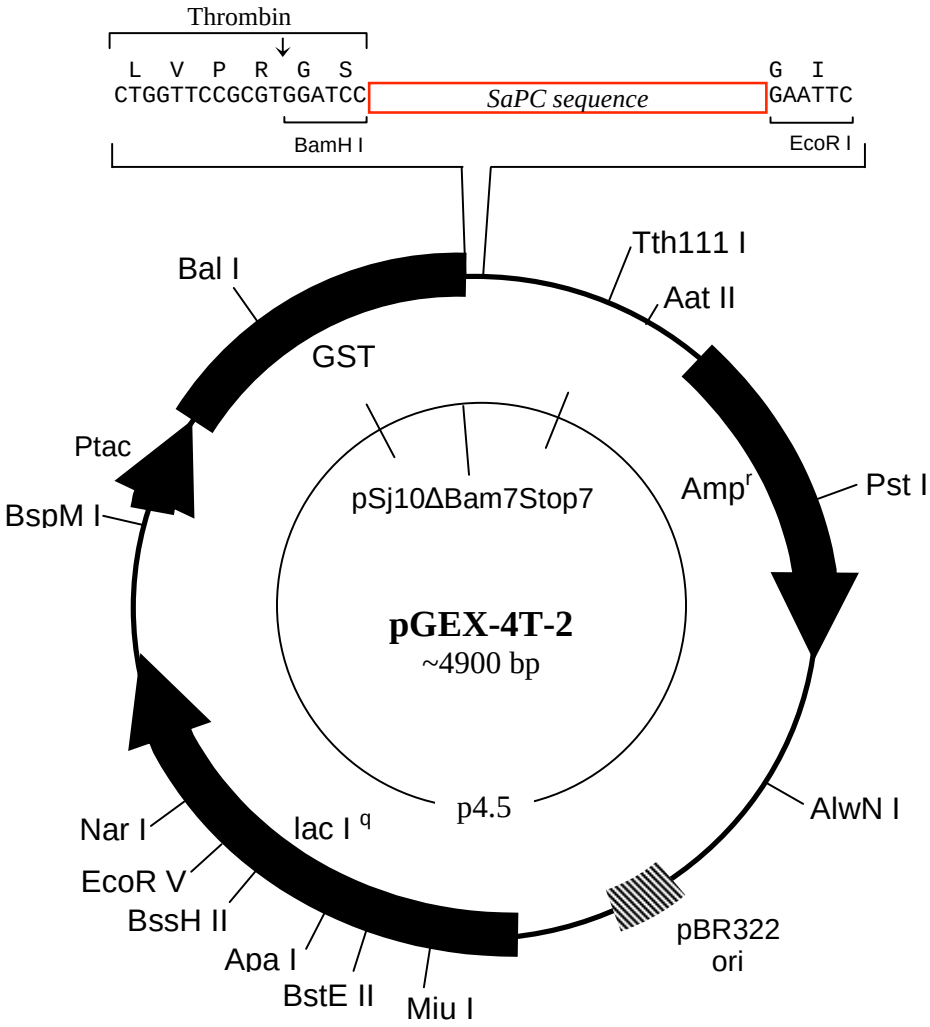

B

```
 M  N  G  Q  A  R  R  I  Y  I  K  D  E  N  V  H  T  N  A  N  V  K
ATGAATGGTCAAGCGAGACGTATTTACATTAAAGATGAAAATGTGCATACAAATGCGAACGTTAAG

 P  K  A  D  K  S  N  P  S  H  I  G  A  Q  M  P  G  S  V  T  E  V
CCAAAAGCAGATAAGAGTAATCCAAGTCATATCGGTGCTCAAATGCCAGGTTCAGTAACTGAAGTC

 K  V  S  V  G  E  T  V  K  A  N  Q  P  L  L  I  T  E  A  M  K  M
AAGGTTAGTGTTGGTGAAACTGTGAAAGCTAATCAGCCGTTGCTAATTACTGAAGCTATGAAAATG

 E  T  T  I  Q  A  P  F  D  G  V  I  K  Q  V  T  V  N  N  G  D  T
GAAACAACAATTCAAGCACCATTTGACGGTGTGATTAAACAAGTAACTGTAAATAATGGTGACACA

 I  A  T  G  D  L  L  I  E  I  E  K  A  T  D  *
ATAGCGACAGGCGATTTATTAATCGAAATTGAAAAAGCAACTGACTGA
```

4.3.2 Characterization of btnOH-AMP as an anti *S. aureus* agent

As discussed in 3.3.7.2, btnOH-AMP was as a potent inhibitor for BPL. However, it has only shown antibacterial effect against *Staphylococcus strains*. This led us to do further characterization on the compound with *Sa*BPL. BtnOH-AMP at various concentrations (between 0 - 150 µM) was tested with liquid cultures of *S. aureus* and *E. coli* K2495. As expected, no inhibition was observed with the *E. coli*. The MIC_{95} for btnOH-AMP was determined to be ~72 µM (Figure 4.2). However, repeated assays consistently showed that the compound does not totally inhibit the bacterial growth even when tested with the compound at higher concentrations. We postulated that the compound could possibly be bacteriostatic.

4.3.3 Mechanism of inhibition of biotinol-5'-AMP

The ^{3}H-biotin incorporation assay, as described in 2.2.2.12, was initially employed for kinetic analysis as there was no FP based assay available for *Sa*BPL at the time. The mechanism of inhibition was investigated by measuring BPL activity with varying concentrations of inhibitor alongside varying concentrations of either biotin or MgATP. Lineweaver-Burk double reciprocal plots (Figure 4.3) indicated that btnOH-AMP behaved as a competitive inhibitor relative to biotin and as a non-competitive inhibitor relative to MgATP (refer to Appendix A). The studies on analogues of tyrosinyl-AMP complexed with tRNA synthetase by Brown *et. al* (1999) provide some insight into this finding. Here, the structural data indicated that most of the core residues in the active site were in contact with the tyrosyl group of the compound but no significant interaction with the adenine ring (Brown *et. al.*, 1999). This finding suggested that the biotin binding site is a promising target for BPL inhibition. Therefore, we propose that biotin analogues could potentially be used as BPL inhibitors. This led us to adapt the FP-based BPL assay for *Sa*BPL.

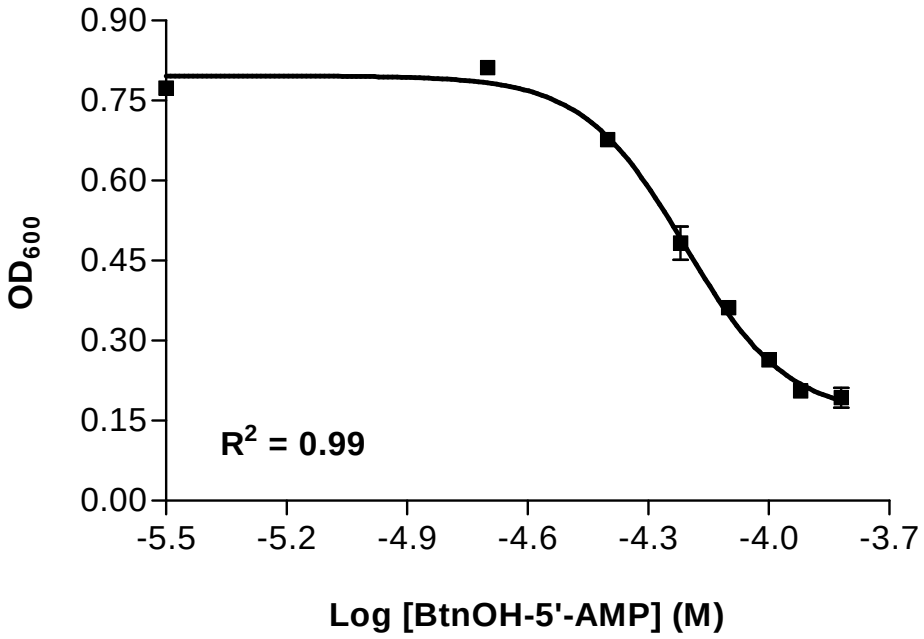

Figure 4.2 : Minimal inhibition concentration for btnOH-AMP

Inhibition curve with increasing concentration (0-150 µM) of btnOH-AMP. MIC_{95} for btnOH-AMP was determined to be ~72 µM (n = 3).

Figure 4.3 : Concentration dependent inhibition of *Sa*BPL by btnOH-AMP and associated double-reciprocal Lineweaver-Burk plots

A) ***BtnOH-AMP competes against ^{3}H-biotin***

Concentrations of btnOH-AMP included in the reaction were 0 nM (■), 20 nM (▲), 100 nM (●) and 200 nM (◆). Left panel shows the velocity plot with different fixed concentrations of btnOH-AMP and varying the concentrations of ^{3}H-biotin. The right panel shows the double reciprocal Lineweaver-Burk plot of initial velocity curves. The lines are seen to intersect at the *y*-axis, indicating competitive inhibition of btnOH-AMP with ^{3}H-biotin.

B) ***BtnOH-AMP competes against MgATP***

Concentrations of btnOH-AMP included in the reaction were 0 nM (■), 50 nM (▲) and 200 nM (●). Left panel shows the velocity plot with different fixed concentrations of btnOH-AMP and varying the concentrations of MgATP. Right panel shows the double reciprocal Lineweaver-Burk plot of initial velocity curves. The lines are seen to intersect beyond the y-axis, indicating non-competitive inhibition of btnOH-AMP with MgATP.

A)

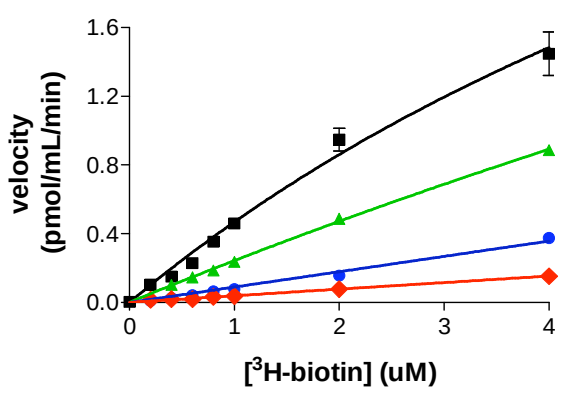
velocity
(pmol/mL/min)
1.6
1.2
0.8
0.4
0.0
0
1
2
3
4
[3H-biotin] (uM)

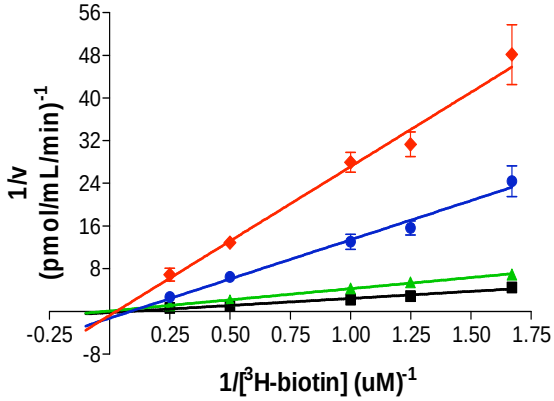
1/v
(pmol/mL/min)-1
56
48
40
32
24
16
8
-8
-0.25
0.25
0.50
0.75
1.00
1.25
1.50
1.75
1/[3H-biotin] (uM)-1

B)

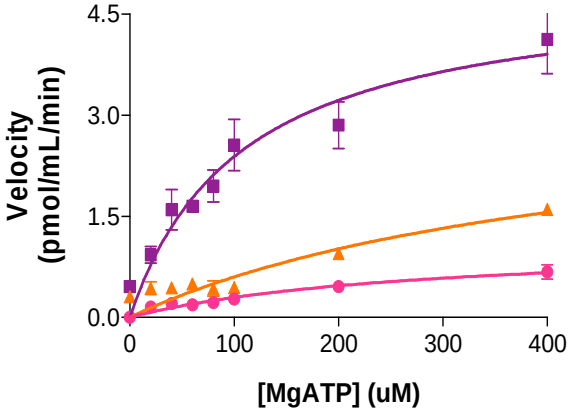
Velocity
(pmol/mL/min)
4.5
3.0
1.5
0.0
0
100
200
300
400
[MgATP] (uM)

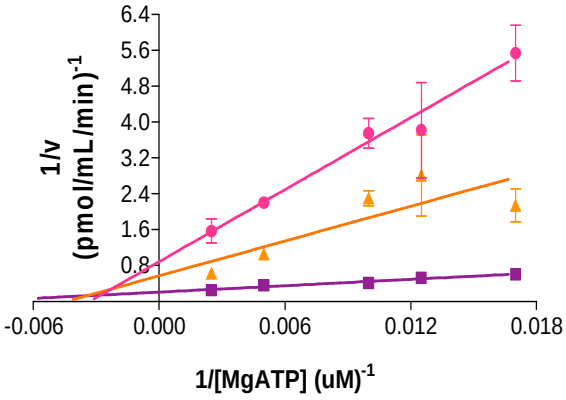
1/v
(pmol/mL/min)-1
6.4
5.6
4.8
4.0
3.2
2.4
1.6
0.8
-0.006
0.000
0.006
0.012
0.018
1/[MgATP] (uM)-1

4.3.4 Principle of the assay

The aim here was to adapt the FP-based *in-vitro* biotinylation assay for BirA discussed in Chapter 3 using a fluorescently labeled biotin domain as the substrate, thereby making the assay universal for a wide range of BPLs. Following the BPL reaction, the biotinylated (holo) domains were complexed with avidin (Mr = 66 000) which has an extremely high affinity for biotin. The increased molecular mass of the complex greatly impedes the rotation and tumbling kinetics of the biotin domain resulting in the emitted light remaining highly polarized relative to the excitation plane. This provided a rapid method to quantitate biotinylated product formation and, thus, BPL activity.

4.3.5 Identify substrate for *Sa*BPL

For the FP-based assay, a fluorescently labeled substrate was required. A small peptide is the ideal substrate for this assay but the attempt to identify a suitable peptide for *Sa*BPL has been unsuccessful (Bird, 2007). Therefore, I decided to adapt this assay using a biotin domain instead. Although the higher molecular mass of the domain (~10 kDa) would reduce the detectable polarization shift, it is still worthwhile to have this assay if the signal is significantly above the background noise (*i.e.* mean for the zero enzyme control plus 3x the standard deviation).

As biotin attachment is made to the side chain of a specific lysine residue, it was important to avoid coupling chemistries that would modify amino groups. Therefore thiol modification of cysteine residues using fluorescein maleimide was employed. *S. aureus* expresses two biotin-dependent enzymes, namely acetyl CoA carboxylase (ACC) and pyruvate carboxylase. The biotin domains of both enzymes were considered as potential substrates. Like the biotin domain from *E. coli* ACC, *S. aureus* ACC (71% sequence

similarity) contains a cysteine residue in close proximity to the biotin accepting lysine. In the biotin domain from *E*. coli ACC this cysteine residue was previously found to be susceptible to disulphide-linked dimer formation and was modified readily by a sulphydryl modifier (Chapman-Smith *et. al.*, 1997). As these findings suggested that thiol modification at this position may interfere with enzymatic biotinylation, we decided to focus upon the pyruvate carboxylase biotin domain (*Sa*PC) that has no pre-existing cysteine residues. This allowed for systematic engineering of a single cysteine residue into the domain structure at specifically selected sites.

The initial study was carried out with the 103 C-terminal residues from *Sa*PC based upon our previous work on the biotin domain from yeast PC (Polyak *et. al.*, 2001). The apo-domain was over-expressed as a GST fusion in the *bir*A85^{-} *E. coli* strain BM4062 (Barker and Campbell, 1980). BM4062 is a temperature sensitive cell line where BPL activity is inactivated at 42°C and, thus, improves the expression of apo domain. The fusion protein was purified using glutathione-agarose chromatography and cleaved with thrombin before further purification. Anion exchange was subsequently employed to resolve apo-biotin domain from any holo-protein, as well as the GST fusion partner. Interestingly, SDS-PAGE analysis revealed three species with molecular mass of approximately 10 000 Da. We proposed that the unstructured regions present outside of the structured biotin domain underwent proteolysis during thrombin cleavage. Mass spectrometry (Figure 4.4) confirmed that the N-terminal "tail" was indeed susceptible to proteolysis. The largest product was determined to be 11 232.4 Da, consistent with the mass expected for *Sa*PC103 (calculated value = 11 231.7 Da). The masses of the two additional species were 10 430.1 Da and 9 513.3 Da, arising from proteolysis between residues R1104 and R1105 (calculated value = 10 429.9 Da) and E1111 and N1112 (calculated value = 9 511.8 Da) respectively. With this data, I re-engineered the substrate

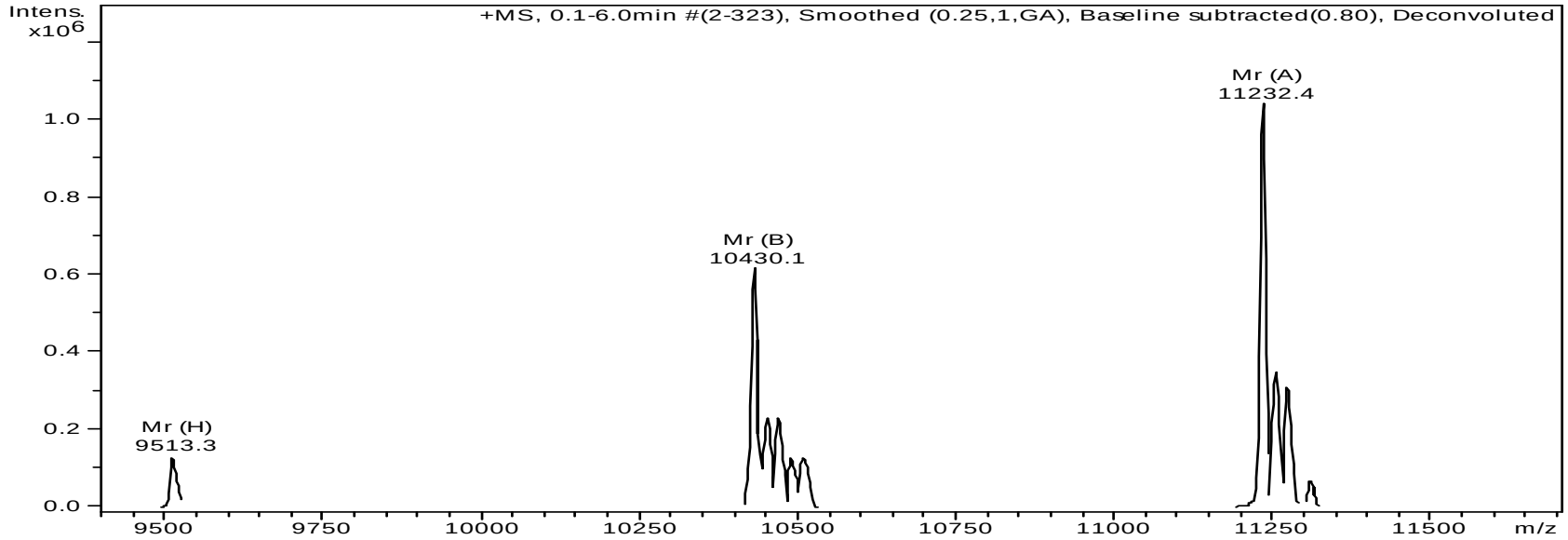

Figure 4.4 : Deconvoluted mass spectra

Three species were detected after thrombin cleavage of *Sa*PC103. The determined molecular mass for each species were indicated in the figure.

based on the minimal proteolytically-stable fragment of 90 amino acid residues (*Sa*PC90) which allows the expression of a more homogenous and stable domain. Additionally, the smaller molecular mass of this domain is advantageous for FP assay.

4.3.6 Mutagenesis and protein labeling

Insertion of a fluorescein label was achieved by engineering a cysteine residue into the biotin domain by site directed mutagenesis followed by reaction with fluorescein-5'-maleimide. Our initial experiments were performed upon holo-*Sa*PC103 with the label introduced in the N- or C-terminal "tails" outside of the structured domain at positions S1075C-Fl and A1148C-Fl respectively. Surprisingly, the apo domains of both constructs were shown to be ~85mP which is not much higher than that of the peptide (~75mP). When complexed with avidin, both constructs produced low FP values (ΔmP = mP (with avidin) – mP (no avidin) = ~ 30 mP). These constructs were unsuitable for BPL assay as the signal to noise ratio was too low. It was hypothesised that the low FP values were due to the mobility of the termini of *Sa*PC103 where fluorescein was attached. Therefore, a series of mutants was created to investigate the optimal positioning of the label within the structured region of the substrate. A set of criteria was taken into consideration to minimize deleterious effects of labeling upon protein folding or substrate recognition by BPL. All amino acid residues targeted for cysteine substitution had solvent exposed side chains and were at least 15Å from the biotin accepting lysine (K1112). This distance was established based on the recent crystal structure of *Pyrococcus horikoshii* BPL-BCCP complex (PDB ID: 2EJG). Additionally amino acid residues required for folding or biotinylation, as identified in our previous mutagenesis studies (Chapman-Smith *et. al.*, 1999; Polyak *et. al.*, 2001), were avoided. Finally, using the crystal structure of holo-SaPC90 (adapted from PDB ID: 3BG5) (Xiang and Tong, 2008), six mutation sites at

various positions across the domain were proposed for investigation. These were S1075, K1092, S1094, N1102, D1122 and E1144 (Figure 4.5).

4.3.7 Analysis of biotin domains as a BPL substrate

4.3.7.1 Analysis of fluorescein placement with holo-domains

The holo-SaPC90 mutants were produced as GST fusion proteins in *E. coli* BL21 cells harbouring the *E. coli* BPL overexpression plasmid pCY216 (Chapman-Smith *et. al.*, 1994) to facilitate biotinylation. Western blot analysis probed with Streptavidin-HRP confirmed all constructs were indeed biotinylated *in-vivo* by *E. coli* BPL (Figure 4.6). Since biotinylation is dependent upon the 3-dimensional structure of the substrate protein, this implied that the cysteine substitutions had not grossly affected the protein structure. All proteins in the mutational series were then prepared in their holo-form for further analysis. Enzymatic biotinylation was driven to completion by overnight incubation of the crude cell lysates at 37°C in the presence of excess ATP and biotin (Chapman-Smith *et. al.*, 1994). Purified holo-domains were then labeled with fluorescein-5'-maleimide, complexed with avidin and assayed by FP. Interestingly, insertion of fluorescein outside the biotin domain at position S1075C-Fl in SaPC90 produced a larger ΔmP value compared with the longer protein *Sa*PC103 (Figure 4.7A). This finding supports our earlier proposal that the long N-terminal tail was highly mobile. For the constructs with the label inserted within the domain structure, results varied markedly (ΔmP = 50 mP to 150 mP) again highlighting the importance of placement for the fluorescein label. Interestingly the construct that produced the largest ΔmP was *Sa*PC90 K1092C. However, when in complex with avidin, there was ~50% quenching of fluorescence (Figure 4.7B) which influenced the measurement of FP. Therefore, this construct was eliminated from further analysis.

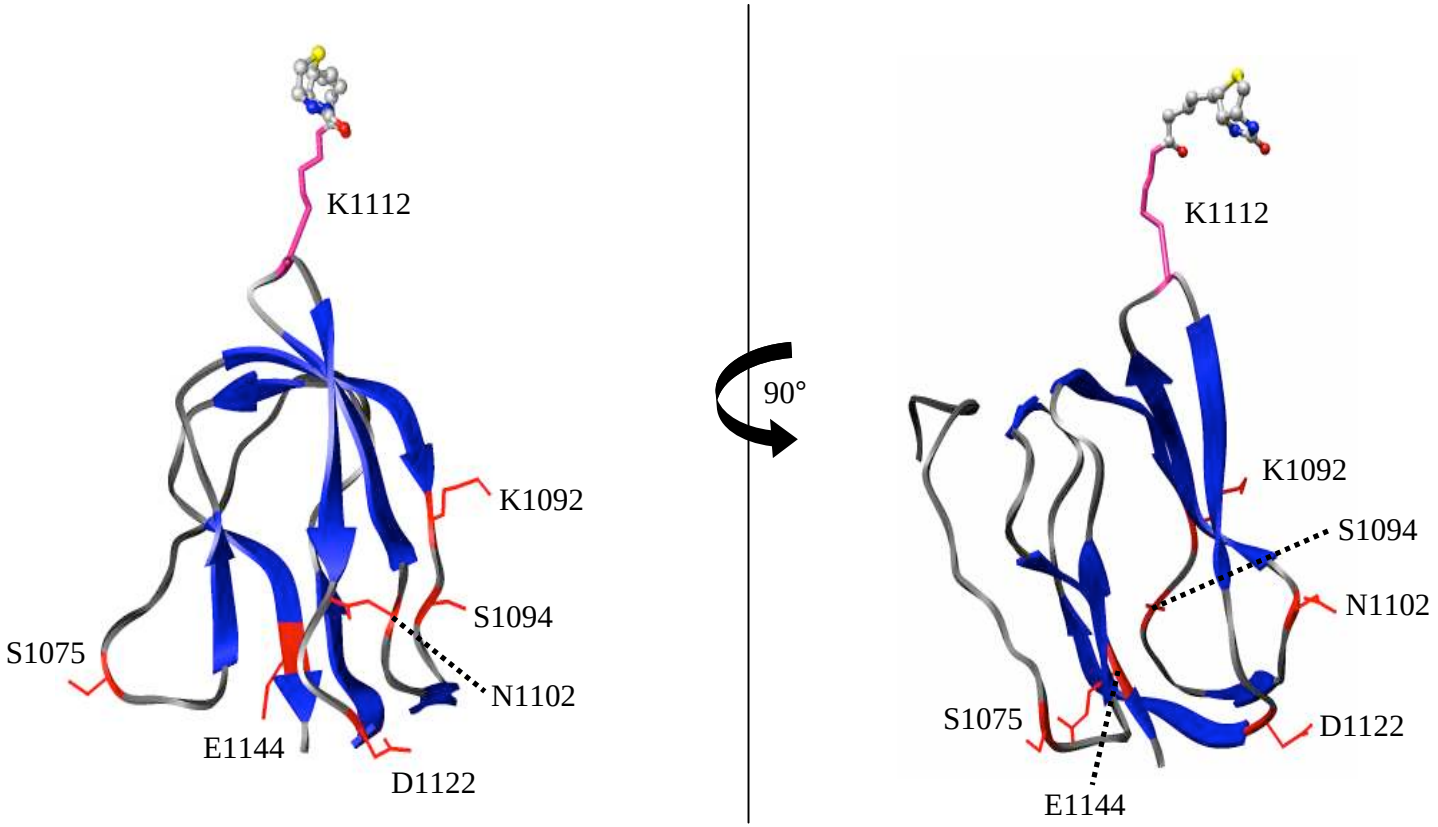

Figure 4.5 : Mutation sites on SaPC90

Crystal structure of the holo-SaPC90 adapted from PDB ID: 3BG5 (Xiang and Tong, 2008). β strands are shown in blue arrows. The biotin moiety, attached to lysine 1112 (pink), is shown as ball and stick. Amino acids selected for cysteine substitution and fluorescein labelling are shown in red. The two panels show the 90° rotation of the structure.

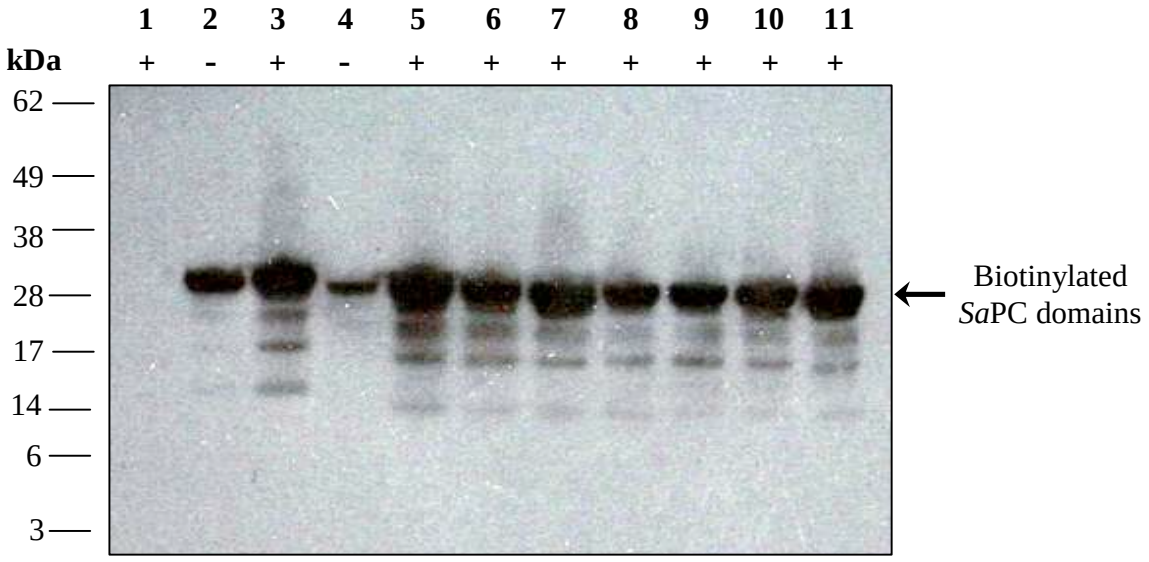

Figure 4.6 : Western blot of *in-vivo* biotinylation

GST-*Sa*PC domains were expressed in BL21 (pCY216) cells. Streptavidin-blot analysis was performed upon crude lysates to detect biotinylated proteins. Cells with parent vector (pGEX-4T-2) were used as negative control. Cells expressing GST-*Sa*PC103 were included as positive controls. The intense bands at ~38kDa were the biotinylated domains indicating truncation and mutations of the domains do not affect the protein activity and folding. Lane 1: Induced parent vector. Lane 2: Uninduced wild-type *Sa*PC103. Lane 3: Induced wild-type *Sa*PC103. Lane 4: Uninduced wild-type *Sa*PC90. Lane 5: Induced wild-type *Sa*PC90. Lane 6: Induced *Sa*PC90 S1075C. Lane 7: Induced *Sa*PC90 K1092C. Lane 8: Induced *Sa*PC90 S1194C. Lane 9: Induced *Sa*PC90 N1102C. Lane 10: Induced *Sa*PC90 D1122C. Lane 11: Induced *Sa*PC90 E1144C.

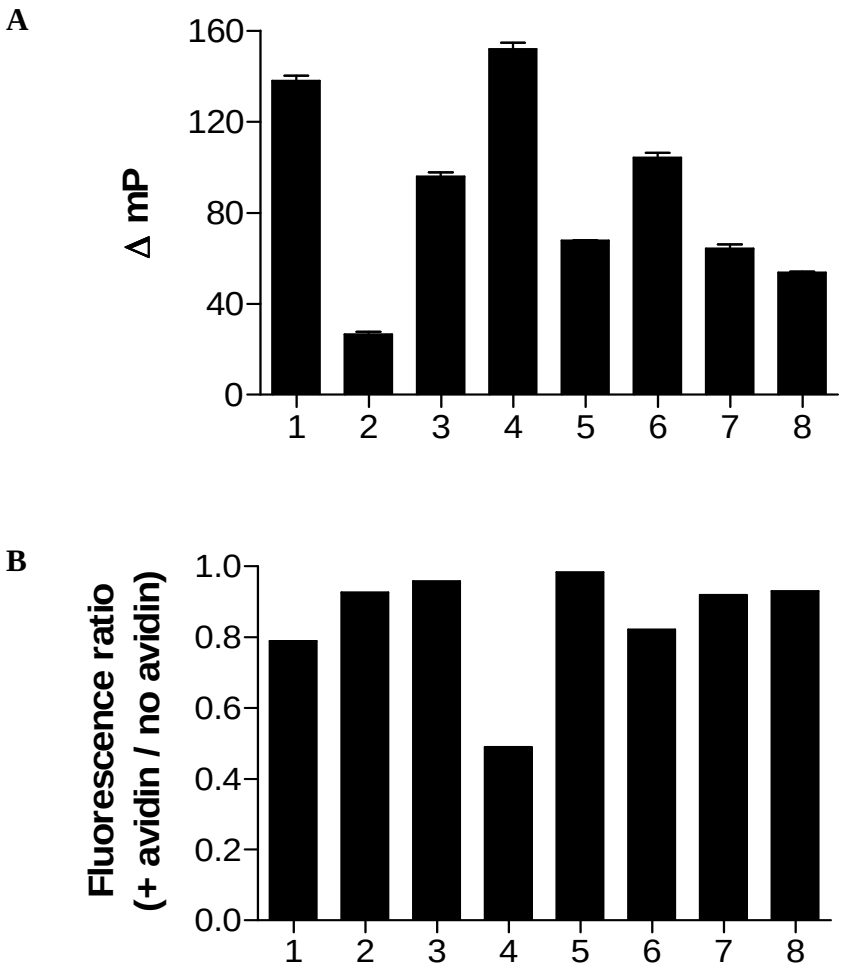

Figure 4.7 : FP with *Sa*PC biotin domain constructs

Constructs investigated here were peptide 85-11 (lane 1), *Sa*PC90 S1075C-Fl (lane 2), *Sa*PC90 S1075C-Fl (lane 3), *Sa*PC90 K1092C-Fl (lane 4), *Sa*PC90 S1094C-Fl (lane 5), *Sa*PC90 N1102C-Fl (Lane 6), *Sa*PC90 D1122C-Fl (lane 7) and *Sa*PC90 E1144C-Fl (lane 8). Panel A shows the ΔmP for each construct tested. Panel B shows the fluorescence ratio for the holo-substrates in the presence or absence of avidin.

Therefore, the two constructs giving the greatest ΔmP (namely SaPC90 N1102C-Fl and SaPC90 S1075C-Fl) were selected for further examination.

4.3.7.2 Kinetic analysis of biotin domains

Apo *Sa*PC90, *Sa*PC90 N1102C-Fl and *Sa*PC90 S1075C-Fl were produced as described in 4.2.3. The protein purity was assessed by SDS-PAGE (Figure 4.8) and the effect of insertion of a fluorescein label on the enzymatic biotinylation was determined. Following labeling of the cysteine mutants, mass spectroscopy confirmed that the major product species (>70%) contained a single fluorescein moiety, as expected. Kinetic analysis with *Sa*BPL was then performed on the wild-type SaPC90 and the fluorescein labeled SaPC90 mutants (*Sa*PC90 N1102C-Fl and SaPC90 S1075-Fl) with our previously reported ^{3}H-biotin incorporation assay (Chapman-Smith *et. al.*, 1994). Determination of the K_M for biotin domains was not possible with the FP-based assay as this methodology requires a constant concentration of the labeled sample (*i.e.* the biotin domain). Both *Sa*PC90 N1102C-Fl (2.78 ± 0.25 μM) and *Sa*PC90 S1075C-Fl (2.90 ± 0.64 μM) gave K_M values in the ^{3}H-biotin incorporation assay that were comparable to that of the non-labeled wild-type domain *Sa*PC90 (1.73 ± 0.22 μM) (Figure 4.9) indicating that the label did not affect enzymatic biotinylation.

Holo protein was obtained by incubating both *Sa*PC90 N1102C-Fl and *Sa*PC90 S1075C-Fl overnight with *Sa*BPL. FP measurements (ΔmP) were obtained after incubation with avidin. Holo *Sa*PC90 N1102C-Fl produced a ΔmP ~75mP, comparable to the previous experiments (Figure 4.7A). In contrast, *Sa*PC90 S1075C-Fl produced a low ΔmP (~9mP). One of the possible reasons for this could be due to the protein instability during purification and labeling. This construct was eliminated from further analysis. Thus, we

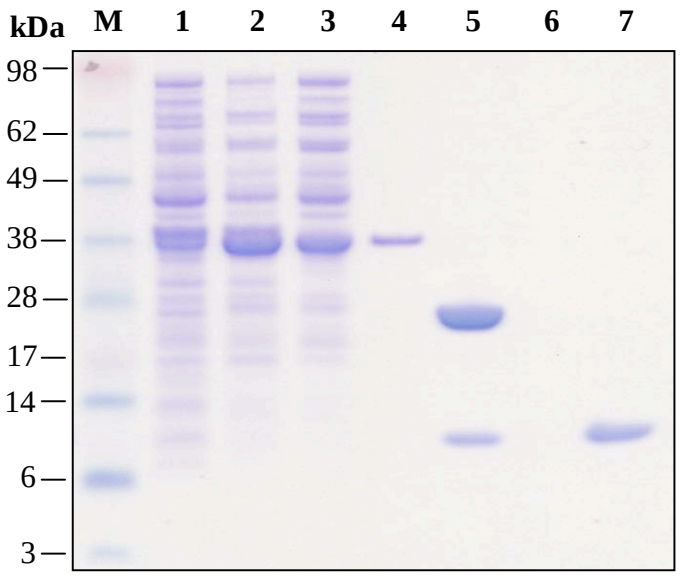

Figure 4.8 : Expression and purification of *Sa*PC90 analysed by SDS-PAGE

Samples were separated on a 4-12% Bis-Tris polyacrylamide gel under reducing conditions. M: SeeBlue Plus 2 prestained molecular mass markers (Invitrogen), Lane 1: crude lysate before induction. Lane 2: Crude lysate after induction with IPTG. Lane 3: Unbound fraction passing through glutathione agarose column. Lane 4: GST-*Sa*PC90. Lane 5: Thrombin cleaved GST-*Sa*PC90. Lane 6: Unbound fraction passing through Q-Sepharose column. Lane 7: Pooled SaPC90 from Q-Sepharose fractions.

Figure 4.9 : Kinetic analysis of biotin domains.

The K_M for various biotin domains were determined by measuring the activity of *Sa*BPL with varying concentrations of substrate using a ^{3}H-biotin incorporation assay (Polyak *et. al.*, 2001). Constructs tested were A) wildtype *Sa*PC90 wild-type, B) *Sa*PC90 S1075C-Fl and C) *Sa*PC90 N1102C-Fl. The graphs represent the non-linear regression to the Michaelis-Menten equation.

A

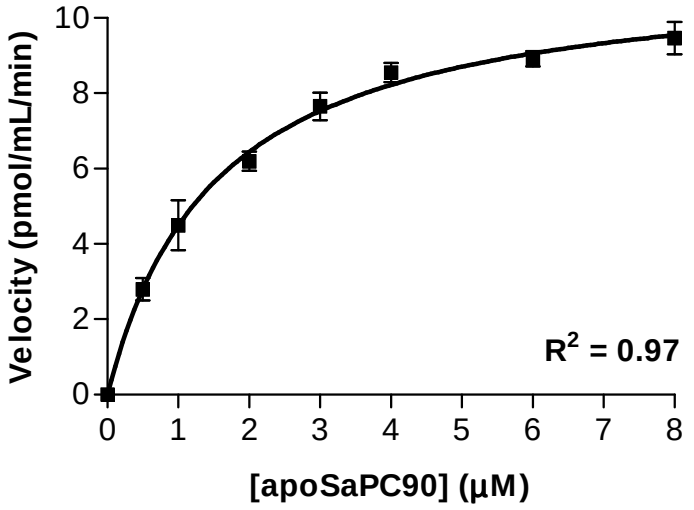
Velocity (pmol/mL/min)
10
8
6
4
2
0
0 1 2 3 4 5 6 7 8
[apoSaPC90] (µM)
R2 = 0.97

B

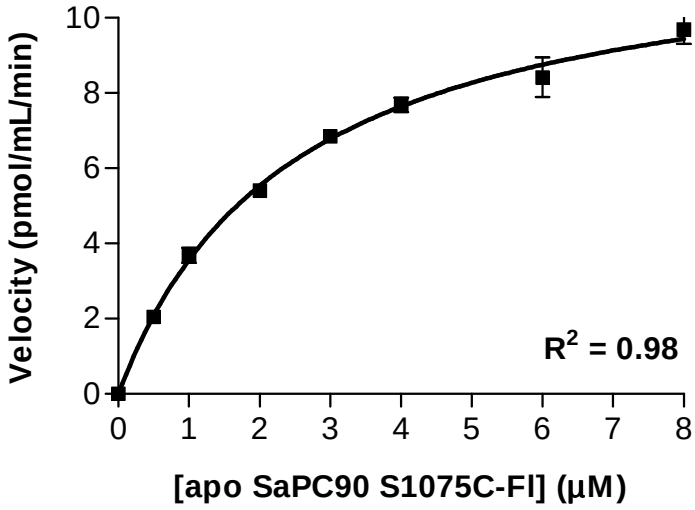
Velocity (pmol/mL/min)
10
8
6
4
2
0
0 1 2 3 4 5 6 7 8
[apo SaPC90 S1075C-Fl] (µM)
R2 = 0.98

C

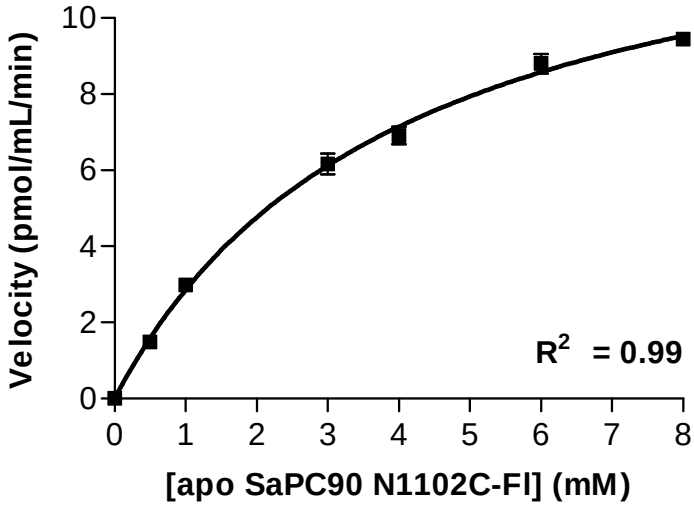
Velocity (pmol/mL/min)
10
8
6
4
2
0
0 1 2 3 4 5 6 7 8
[apo SaPC90 N1102C-Fl] (mM)
R2 = 0.99

concluded that a 90 amino acid domain with the fluorescein label at position 1102 was the optimal substrate.

4.3.8 Development of the assay

The assay was adapted for enzymatic analysis. Standard curves with varying concentrations of holo *Sa*PC90 N1102C-Fl were performed to ascertain the sensitivity and dynamic range of detection. Here, the final concentration of substrate in each well was adjusted to 10 μM with apo *Sa*PC90 N1102C-Fl, thus ensuring a constant level of fluorescence in each well. Following incubation with excess avidin, a linear response was observed between 0 – 10 μM (Figure 4.10). The minimal detection limit was set as a function of the mean for the zero enzyme control plus 3x the standard deviation. Here, ~1 μM holo *Sa*PC90 N1102C-Fl was routinely determined to be the minimal quantity that could be accurately measured. This is comparable in sensitivity with other published assays (Chapman-Smith *et. al.*, 1994; Leon-Del-Rio and Gravel, 1994; Suzuki *et. al.*, 1996; Campeau and Gravel, 2001).

Finally, the *Sa*BPL reaction was optimised for steady state kinetic analysis to achieve between 2 and 4 μM product formation (ie < 40% of the total reaction). The reaction was terminated by the addition of a stop solution containing avidin (*i.e.* 2-fold stoichiometric excess over biotin) and EDTA (*i.e.* 20-fold excess of EDTA over free Mg^{2+}). The specificity of the *Sa*BPL reaction was then established by systematic removal of enzyme, ATP, biotin, $MgCl_2$ and avidin from the assay (Figure 4.11). As expected, removal of any one of these components abolished product formation. The presence of EDTA also terminated the reaction. A range of divalent and monovalent metal ions were substituted for Mg^{2+}. As shown in Table 4.1, substitution of Mg^{2+} by an equimolar

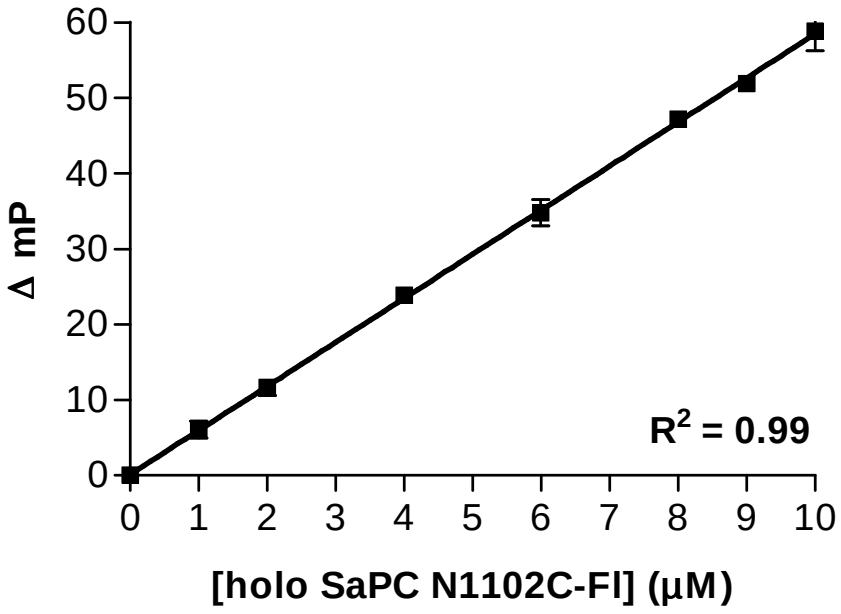

Figure 4.10 : Calibration curve for product formation

A standard curve showing holo *Sa*PC90 N1102C-Fl concentration vs ΔmP. Holo *Sa*PC90 N1102C-Fl was prepared by overnight biotinylation by *Sa*BPL. The concentrations of holo *Sa*PC90 N1102C-Fl were then adjusted with apo *Sa*PC90 N1102C-Fl to give a final substrate concentration of 10 µM.

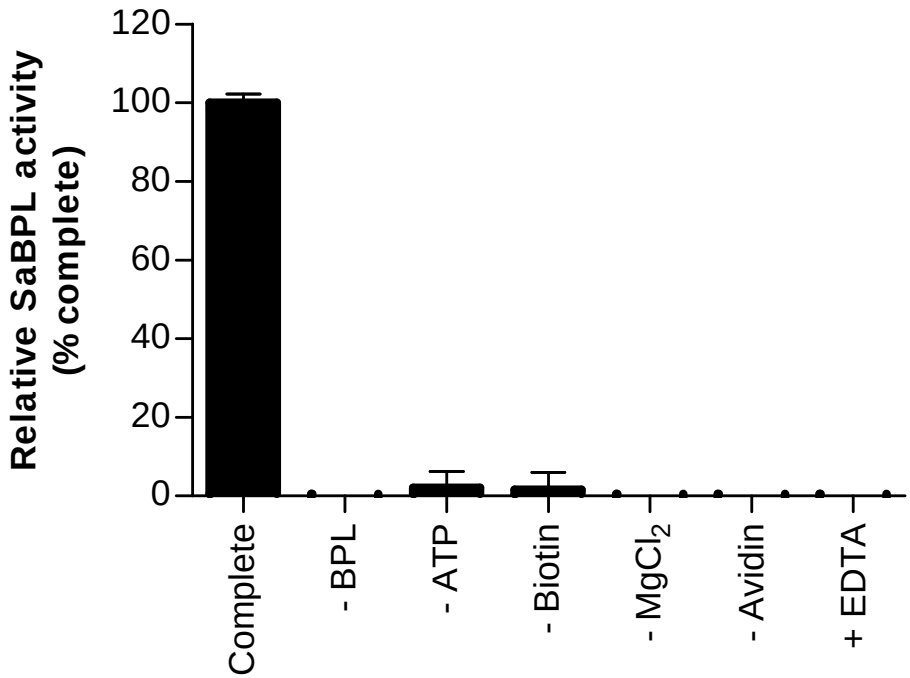

Figure 4.11 : Effect of removing reaction components on *Sa*BPL activity

Percentage activity is based on 100% activity with the complete reaction medium. The concentration of EDTA employed was 11 mM (*i.e.* a 2-fold excess over Mg^{2+}).

concentration of Mn^{2+} resulted in substantial *Sa*BPL activity (24%). However, none of the other metal ions tested reconstituted enzyme activity (< 2%).

Table 4.1 : Activity of *Sa*BPL with 5.5 mM of various metal ions

Metal ions	Relative activity[†]
$MgCl_2$	100 ± 1.8 %
$CaCl_2$	0 ± 0.6 %
$MnCl_2$	24.34 ± 2.2 %
NaCl	0.14 ± 0.8 %
RbCl	1.05 ± 1.3 %
CsCl	1.08 ± 1.8 %

[†] Enzyme activity, expressed relative to the reaction containing 5.5 mM $MgCl_2$, is shown as the mean of 3 experiments ± SEM.

4.3.9 Biological properties of *Sa*BPL

Although all BPLs catalyse the same chemical reaction, factors such as pH, salt and specificity of nucleotide triphosphate source can influence different BPLs (Polyak *et. al.*, 1999). *Sa*BPL activity was measured with a Tris-HCl buffer system between pH 7 – 9.5. Whilst the enzyme was active over this pH range, activity was optimum between pH 8 and 8.5 (Figure 4.12A). Similar optimal pH values have been reported for BPLs from yeast (Polyak *et. al.*, 1999), *Candida albicans* (Pendini *et. al.*, 2008a) and *Pisum sativum* holocarboxylase synthethase (Tissot *et. al.*, 1996). For the BirA reaction, 100-200 mM potassium ions are included (Beckett and Matthew, 1997; Chapman-Smith and Cronan, 1999a). Interestingly, the absence or presence of 200 mM KCl had no effect on *Sa*BPL (Figure 4.12B). Finally, ATP was substituted with various nucleotide triphosphate sources

Figure 4.12 : Biological properties of *Sa*BPL

A) *Sa*BPL activity was measured with Tris-HCl buffer system. The enzyme was active over the range of pH 7 – 9.5 but was optimum between pH 8 and 8.5.

B) *Sa*BPL activity was measured in the presence of 0, 50 and 200 mM KCl. The presence or absence of KCl in the reaction has no effect on enzyme activity.

C) *Sa*BPL activity was measured with the inclusion 3 mM selected nucleotide triphosphates in the reaction medium. The enzyme had the greatest preference for ATP.

A

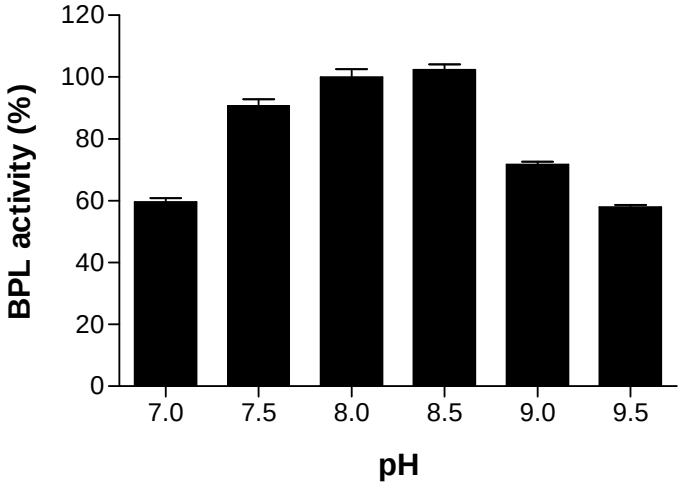
120
100
80
60
40
20
0
BPL activity (%)
7.0
7.5
8.0
8.5
9.0
9.5
pH

B

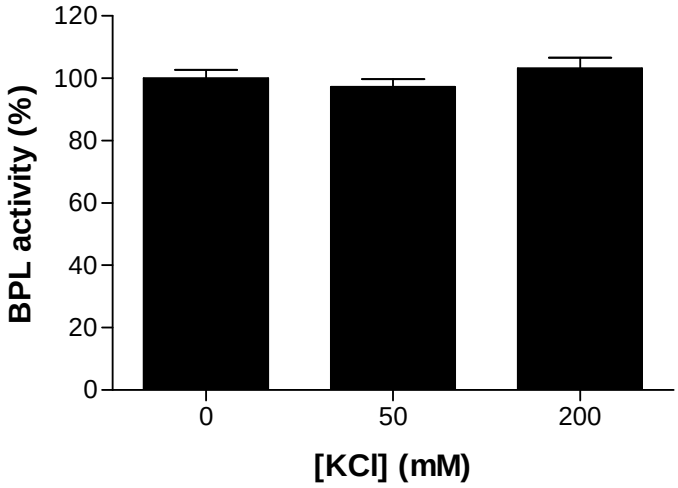
120
100
80
60
40
20
0
BPL activity (%)
0
50
200
[KCl] (mM)

C

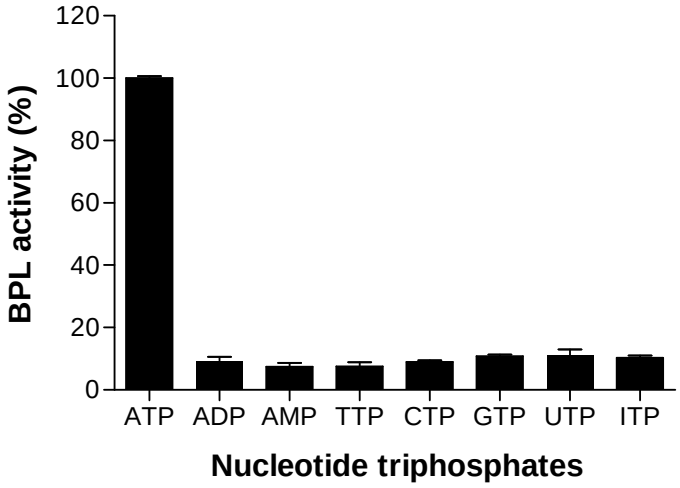
120
100
80
60
40
20
0
BPL activity (%)
ATP
ADP
AMP
TTP
CTP
GTP
UTP
ITP
Nucleotide triphosphates

to investigate specificity. *Sa*BPL had the greatest preference for ATP, as replacement with TTP, CTP, GTP, UTP or ITP yielded < 12% activity (Figure 4.12C).

4.3.10 Kinetic analysis of *Sa*BPL

The assay was then validated by investigating kinetics of ligand binding. K_M values were obtained from the FP assay and compared with the ^{3}H-biotin incorporation assay. The K_M values for both MgATP (68.8 ± 15.4 μM) and biotin (3.3 ± 0.4 μM) (Figure 4.13) differ slightly to that of the ^{3}H-biotin incorporation assay (K_M MgATP = 160 ± 19 μM, K_M biotin =1.1 ± 0.1 μM). This is most likely to be due to the different assay method used. As observed by Chapman-Smith *et. al.* (1999), the K_M of substrates could vary when different assay conditions were used. Different state of reactions during the measurement could potentially contribute to the discrepancy as well. Therefore, for routine assays, the concentrations of ligands were then set at 3 mM ATP and 15 μM biotin.

4.3.11 Inhibition studies

During catalysis, the formation of biotinyl-5'-AMP is accompanied by the release of pyrophosphate. This reaction end product functions as a competitive end point inhibitor relative to MgATP (Polyak *et. al.*, 1999). Thus, the assay was further validated by inhibitor studies using pyrophosphate. Pyrophosphate had an IC_{50} of 7.1 ± 3 mM under standard assay conditions (3 mM MgATP) (Figure 4.14). Additionally, we performed the assay in the presence of DMSO. *Sa*BPL was tolerant of up to 2% DMSO in the reaction medium where it retained 100% of its activity (Table 4.2). DMSO was inhibitory at higher concentrations (90% activity with 3% DMSO, 81% activity with 4% DMSO, 76% activity with 5% DMSO). Together, these data demonstrated that this assay could be employed for *Sa*BPL inhibitor screening and analysis where the compounds are commonly solubilised in this solvent.

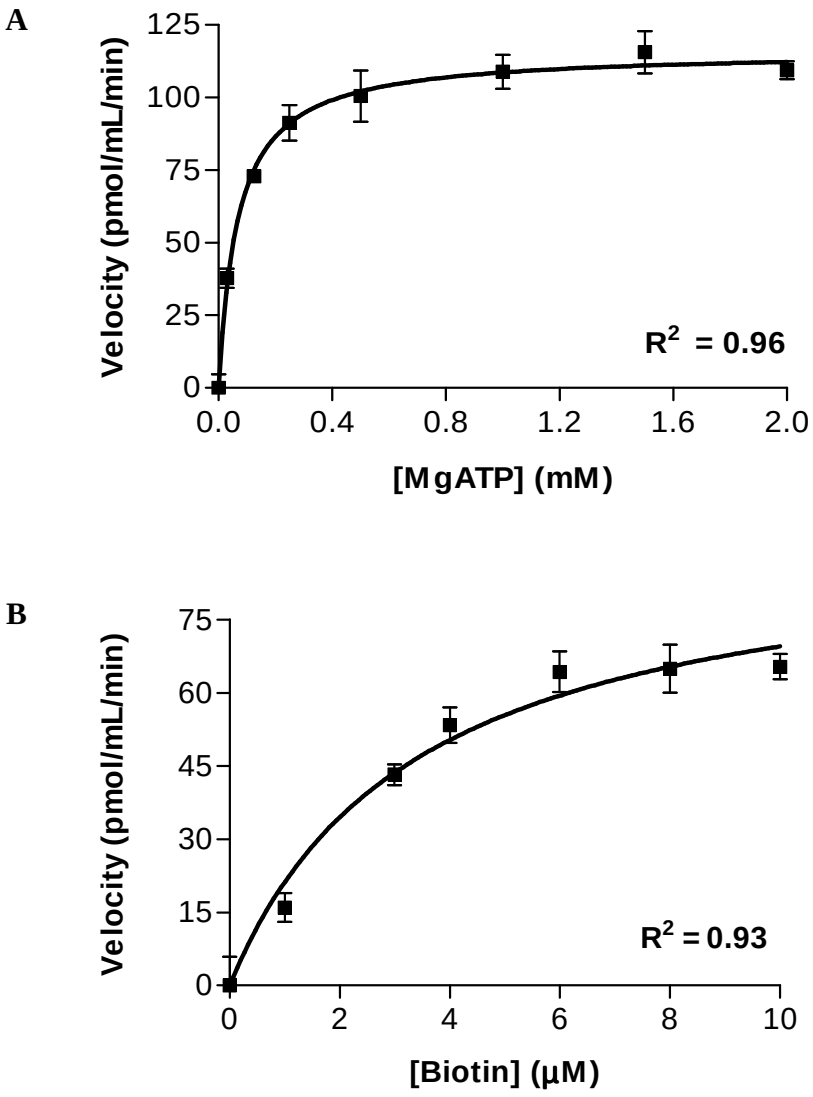

Figure 4.13 : Kinetic analysis of ligand binding

The K_M values for ligands A) MgATP and B) biotin were determined by measuring the activity of *Sa*BPL with varying ligand concentrations. The graphs represent the non-linear regression to the Michaelis-Menten equation.

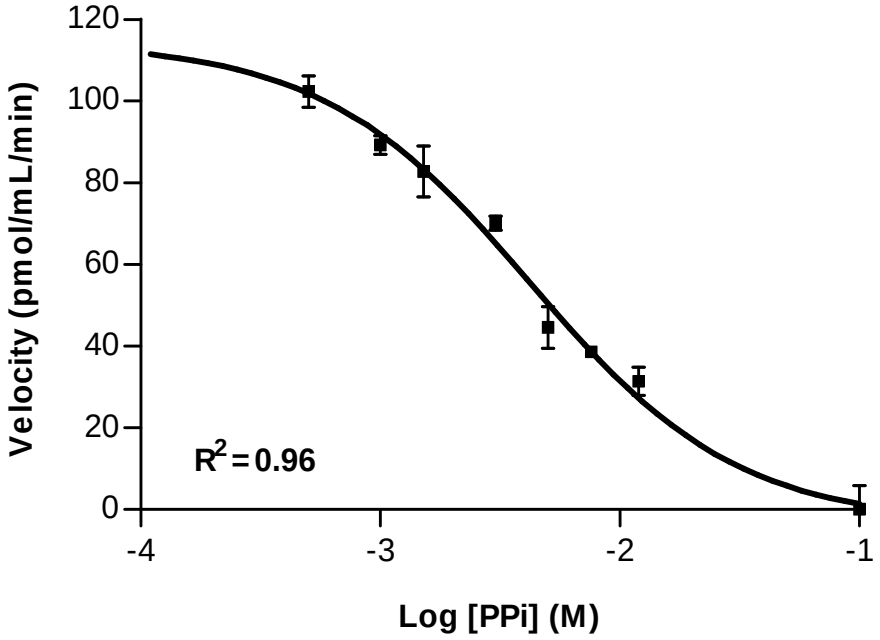

Figure 4.14 : Inhibition of *Sa*BPL activity by pyrophosphate (PPi)

The IC_{50} value for pyrophosphate was determined by measuring the activity of *Sa*BPL with varying concentrations of inhibitor pyrophosphate.

Table 4.2 : Effect of DMSO on *Sa*BPL activity

DMSO	Relative activity[†]
0 % (v/v)	100 ± 9.02 %
1 % (v/v)	97.5 ± 3.65 %
2 % (v/v)	102.8 ± 1.78 %
3 % (v/v)	100.1 ± 7.06 %
4 % (v/v)	81.34 ± 5.28 %
5 % (v/v)	75.94 ± 5.73 %
10 % (v/v)	74.34 ± 4.27 %

[†] Enzyme activity, expressed relative to no DMSO control, is shown as the mean of 3 experiments ± SEM.

4.3.12 Intra- and inter-assay variation

The results from 30 replicates of apo and holo domain (ie 0% and 100% of the *Sa*BPL reaction) were collected to measure intra-assay variation (Table 4.3). The coefficient of variation (CV) was 7.6% for apo- and 2.1% for holo-domain, indicating good intra-assay reproducibility. Similarly, data were collected from 15 separate experiments over 2 months for inter-assay analysis. Again, the CV values were <10% across the data set (7.21% for apo, 3.88% for holo). The Z' factor, a measure of data scatter and assay reproducibility (Zhang *et. al.*, 1999), was used to assess the quality and performance of the assay for high-throughput applications. The results of both intra (0.64) and inter-assay (0.53) analysis were greater than 0.5, thereby indicating the assay is acceptable for high-throughput applications.

Table 4.3 : Statistical analysis of the *Sa*BPL assay

	Intra-assay		Inter-assay	
% of Reaction	0%	100%	0%	100%
Number of samples	n = 30	n = 30	n = 15	n = 15
Mean of data set (mP), μ	85	168	87	169
Std. deviation, σ	± 6.5	± 3.5	± 6.3	± 6.6
Coefficient of variation (CV)	7.63%	2.1%	7.21%	3.88%
Z' factor	0.64		0.53	

4.3.13 Biotin analogues as inhibitors for *Sa*BPL

By employing btnOH-AMP as the lead compound, our collaborators from the School of Chemistry and Physics, University of Adelaide identified a series of potential biotin derivatives through rational drug design. These analogues were synthesized and tested against *Sa*BPL. Preliminary screening of the biotin analogues with ^{3}H-biotin incorporation assay by Dr. Steven Polyak revealed three compounds (Figure 4.15) with good inhibitory activity against *Sa*BPL. Therefore, after the development of the FP-based assay for *Sa*BPL, the IC_{50} and K_i for these compounds were measured. IC_{50} and K_i values provide important information for enzyme inhibitor analysis. IC_{50} represents the concentration of inhibitor that will decrease the enzyme velocity by half in the presence of the competing substrate. The K_i refers to the concentration of the inhibitor required to occupy half of the enzyme sites at equilibrium in the absence of the competitive substrate and thus, is only applicable for competitive inhibitors. As I demonstrated that btnOH-AMP is a competitive inhibitor against biotin, I reasoned that all biotin analogues will behave in the same manner. Therefore, a K_i calculation is appropriate in this scenario.

Figure 4.15 : Structures of *Sa*BPL inhibitors

A) The biotinol-5'-AMP synthesized by Dr. John Cronan. Biotin analogues synthesized for this study that showed good inhibition against *Sa*BPL were B) biotinol, C) biotin acetylene and D) biotin-1,5-triazole-adenosine with a protecting group on the ribose ring

A

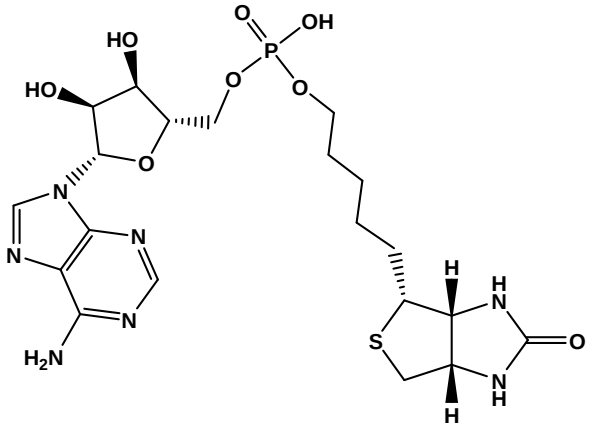
O
OH
P
HO
HO
O
O
O
N
N
N
N
H_2N
H
H
N
S
O
N
H
H

B

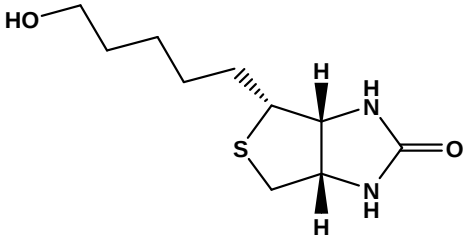
HO
H
H
N
S
O
N
H
H

C

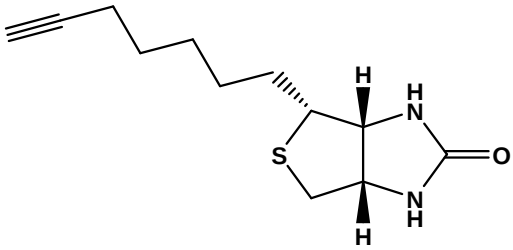
H
H
N
S
O
N
H
H

D

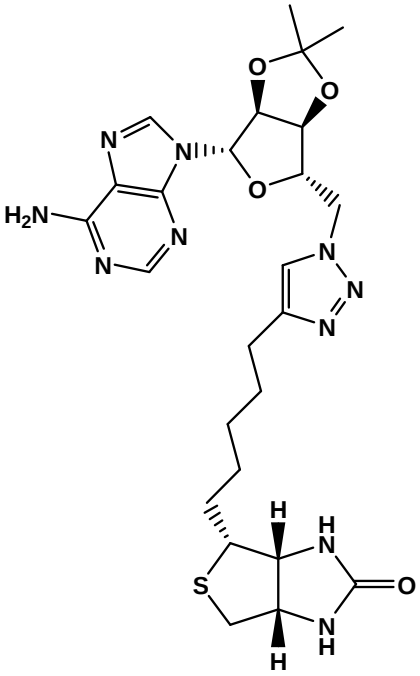
O
O
N
N
O
H_2N
N
N
N
N
H
H
N
S
O
N
H
H

As indicated in Table 4.4, all of the biotin analogues tested showed inhibition activity. However, none of them were as potent as btnOH-AMP. This is consistent with the isothermal titration calorimetry data by Naganathan and Beckett (2007) where both btnOH-AMP and the natural ligand, biotinyl-5'-AMP were shown to bind tighter to BirA with equilibrium dissociation constant of 1.5 X 10^{-9} M and 3.9 X 10^{-11} M respectively compared to biotin (4.3 X 10^{-8} M) (Naganathan and Beckett, 2007). The studies on tyrosyl tRNA synthetases and its inhibitor, tyrosinyl-AMP also provide an explanation for this finding. Here, it was discovered that removal of the adenine moiety from the inhibitor substantially affected the binding (Brown *et. al.*, 1999). This suggested that the presence of the adenine moiety might bear more importance for the inhibitor recognition than its direct binding in the active site.

Considering the high degree of similarity between biotinol and biotin acetylene, it is still unclear as to why biotin acetylene (K_i = 1.16 µM) is a better inhibitor compared to biotinol (K_i = 3.02 µM). The other analogue tested was biotin-1,5-triazole-adenosine with a hydroxyl protecting group on the ribose ring. This compound was a result from the combination of biotin acetylene and an adenosine. These two molecules were linked by a triazole following the reaction of the acetylene and the azide group on the adenosine. Surprisingly, instead of improving the potency, the addition of the adenine moiety had significantly reduced the compounds competitiveness (K_i = 3.34 µM). However, this result is inconclusive as it might be the effect of the protecting group which was added to stabilize the compound in chemical reactions during synthesis. The actual inhibition potential of this compound will need to be confirmed after the removal of this protecting group.

Table 4.4 : IC_{50} and K_i value for compounds tested

Compounds	IC_{50}*	K_i†
Biotinol-5'-AMP	0.23 ± 0.06 µM	0.04 µM
Biotinol	16.76 ± 1.35 µM	3.02 µM
Biotin acetylene	6.44 ± 1.36 µM	1.16 µM
Biotin-1,5-triazole-adenosine (with protecting group)	18.57 ± 6.39 µM	3.34 µM

* IC_{50} was expressed as mean of 3 experiments ± std. deviation.

† K_i value was calculated based on biotin concentration at 15 µM and K_M at 3.3 µM.

4.4 CONCLUSION

Based on published structural data and the inhibition studies presented here, I claim that the biotin binding site is a reasonable target for designing BPL inhibitors. Thus, a series of biotin analogues were synthesized based on the lead compound, btnOH-AMP. This directed approach is a worthwhile effort to establish the structure-activity relationship of biotin analogues and the transition state analogues. Preliminary data suggested that some of these analogues could be considered for further development. As this work requires repeated rounds of enzyme activity analysis, a robust assay for *Sa*BPL was developed by engineering a suitable substrate required for FP. This work demonstrated that precise positioning of a fluorophore into the biotin domain is an important consideration for the assay development. The data presented here provides convenient cues for engineering the substrates required for these assays. The assay performance was then validated through kinetic and inhibition studies. Statistical analysis verified that this assay satisfied the criteria for high-throughput application. Therefore, this assay could also be used for rapid analysis of large compound libraries to identify new chemical classes not related to the known ligands or transition state analogues that function as BPL inhibitors.

Given the highly conserved nature of the protein:protein interaction between BPLs and biotin domains, we propose that the assay reported in this work is adaptable to any isozyme from this important family of enzymes.

A single universal solvent that could quickly and efficiently solubilize compounds was desirable for screening compound libraries. DMSO, a polar solvent that dissolves both polar and non-polar compounds, is one such solvent. This solvent is also miscible in most organic solvents as well as water. Lower toxicity was the other reason for the wide application of this solvent compared to the other members of this class such as dimethylformamide and dimethylacetamide. DMSO was determined to have no effect on most cell lines for up to 0.1% (v/v) while *in-vitro* biochemical assays were more tolerant of 1- 5% (v/v) (Pereira and Williams, 2007). In most cases, the stability and effective concentration of compounds in DMSO was unknown. Hence, these compounds were preferably screened at the highest permissible initial compound concentration which was determined by the tolerance of solvent in the assay. Therefore, it is critical to balance between the maximum compound solubility and the desired concentration for screening which normally determines the success of an assay.

CHAPTER 5

FINAL DISCUSSION & FUTURE DIRECTIONS

CHAPTER 5 FINAL DISCUSSION AND FUTURE DIRECTIONS

5.1 BPL INHIBITORS AS A NEW CLASS OF ANTIBIOTIC

Many drugs that are in clinical use today are enzyme inhibitors. In drug discovery, it is important to understand the target enzyme and, thus, the mechanism of action for a drug. Indeed, this is one of the requirements for obtaining drug regulatory approval by the FDA. Generally inhibitors that bind to a target enzyme impede activity and, thus, upset the cellular metabolic regulation that eventually leads to cell death. Inhibition can be either reversible or irreversible. For irreversible inhibition, the inhibitors usually form covalent bonds and modify key amino acid residues needed for enzymatic activity. Irreversible inhibitors generally are useful tools for studying protein and structure-function relationships but are not as prevalent in the clinic. Reversible inhibitors interact with the enzyme via non-covalent binding and therefore can be easily removed by dilution or dialysis thereby restoring full enzymatic activity (Palmer, 1995). These inhibitors can be further divided into two distinct groups: 1) competitive inhibitors where the inhibitor competes against the natural ligand for the active site and 2) non-competitive (allosteric) inhibitors where the inhibitor binds at a different site on the enzyme, alters the configuration of the active site thereby preventing the binding of ligand.

There are two distinct ligand binding sites in the catalytic domain of all BPLs, namely the nucleotide and biotin binding sites. Initially in this project, I set about targeting the nucleotide binding site. There are several aspects that should be considered when targeting an ATP binding site. As in the case for most drugs that are ATP inhibitors, these must be able to compete against high intracellular ATP concentrations. Furthermore, these inhibitors must be specific and be able to discriminate between the target enzyme and the

2000 other human proteins that utilize ATP (Fischer, 2004; Bogoyevitch *et. al.*, 2005). In this study, ATP analogues were weak BPL inhibitors despite X-ray crystallography data demonstrating binding in the nucleotide site. In contrast, biotin analogues showed more promising results, both in BPL inhibition and in antibacterial assays. Together, this study demonstrated that the biotin binding site is a prospective target for BPL inhibition and that biotin analogues could potentially be developed into a new class of antibiotic.

5.2 PROPOSED UPTAKE MECHANISM OF BIOTIN ANALOGUES

In order to develop the BPL inhibitors reported here into a preclinical lead candidate, chemical optimization is required. The drug design cycle will involve multiple rounds of testing and synthesis, generating a structure-activity relationship series required to identify new compounds with improved properties. An improved MIC could be obtained by one of the several mechanisms. Indentifying compounds that bind tighter to the BPL target and therefore have greater inhibitory activity is one mechanism. Also compounds that can enter the bacteria with greater efficiency could also lead to an improved MIC. Therefore, understanding the mechanism of cellular uptake is an important consideration for future work.

It seems plausible that biotin analogues might be taken into the cell by biotin transport proteins. Biotin is a natural enzyme co-factor required for various metabolic pathways in both prokaryotes and eukaryotes. Despite the ability to synthesize biotin, microorganisms also obtain biotin from exogenous sources. More than 30 years ago, it was suggested that the biotin uptake mechanism in *E. coli* may be independently regulated relative to intracellular biotin biosynthesis (Pai, 1973). Later, Prakash *et. al* (1974) demonstrated that biotin was actively transported into *E. coli* K12 cells (Prakash and

Eisenberg, 1974). These authors also went on to determine the specificity of the biotin transport system by measuring the effect of biotin analogues on biotin uptake. Their finding showed that the biotin transporter was specific for an intact ureido ring where compounds with altered side chains or tetrahydrothiophene ring have little effect. Although not much information on biotin transporter for *Staphylococcus aureus* has been reported, we believe that the cellular uptake of btnOH-AMP into cells could potentially be via this transporter.

The presence of biotin transporter in bacteria was first proposed by Gloeckler *et. al.* (1990). In their study on genes that control the bioconversion of pimelate into dethiobiotin in *Bacillus sphacricus*, the *bioY* gene was implicated in the process. This gene product, whose function was unknown, was postulated to encode a transmembrane protein consisting of four hydrophobic regions constituting transmembrane domains (Gloeckler *et. al.*, 1990). Subsequently an experiment with *Rhizobium etli* showed that the bacteria with mutation in *bioY* exhibited lower biotin uptake compared to the wild-type (Guillen-Navarro *et. al.*, 2005). This provided the first experimental evidence that BioY was indeed a biotin transporter. Comparative genomic analysis reported that the *bioY* gene is widely distributed in all eubacteria and archea and often clustered with biotin metabolism genes (Rodionov *et. al.*, 2002). In a separate experiment Entcheva *et. al* (2002) proposed the involvement of *bioB* gene in biotin synthesis in the nitrogen-fixing bacterium *Sinorhizobium meliloti*. This gene was co-transcribed with another two open reading frames, *bioM* and *bioN* located immediately upstream of the *bioB* gene. Mutations in the *bioM* and *bioN* genes had led to decrease in biotin uptake and, thus, led them to propose that the *bioM* and *bioN* genes encode for the proteins which act as a high-affinity biotin transporter (K_M ~ 2.2 nM) to offset the lack of fully functional biotin synthesis pathway in the bacteria (Entcheva *et. al.*, 2002). However, gene product sequence comparison later

showed that BioB protein was actually similar to the members of BioY family. Hebbeln *et. al* (2007) later confirmed the involvement of these three proteins in biotin transport and provided an explanation for the absence of BioM and BioN in some bacteria. Their findings revealed that single BioY protein in bacteria can indeed function as a high-capacity biotin transporter in the absence of BioM and BioN. However, the presence of the BioM and BioN protein is needed to convert the system into a high-affinity transporter (Hebbeln *et. al.*, 2007). Although the function of this tripartite protein has been established, nothing much else was known of the proteins. The role of each component in the complex requires further studies.

Biotin uptake mechanisms vary extensively in biotin auxotroph species. For *Saccharomyces cerevisiae* and *Schizosaccharomyces pombe,* biotin uptake is mediated by a proton-coupled symporter known as SpVht1p (Stolz, 2003). SpVht1p functions as an active transporter which is optimum at pH 4. In *S. pombe* and *S. cerevisiae,* this transporter has shown high affinity for biotin with K_M values determined to be 0.23 µM (Stolz, 2003) and 0.32 µM (Rogers and Lichstein, 1969) respectively. It was also reported that the rate of biotin uptake of this organism was regulated by the extracellular concentration of biotin. In mammals, biotin is transported across the plasma membrane by the sodium-dependent multivitamin transporter, which is also utilized by two other enzyme cofactors, namely pantothenic acid and lipoic acid (reviewed in Zempleni, 2005). The intestinal uptake of biotin was found to be regulated by ontogeny, extracellular substrate level, protein kinase C and Ca^{2+}/calmodulin-mediated pathway (reviewed in Said, 2004).

The differences in biotin uptake mechanisms between various species could potentially be exploited to design biotin analogues with greater selectivity for pathogenic bacteria.

5.3 ASSAY MINIATURIZATION FOR HIGH-THROUGHPUT SCREENING

Antibiotic discovery and development is a challenging and expensive process that requires long term commitments. Recent trends have shown that many large pharmaceutical companies have restrained, spun off or completely withdrawn from early stage antibacterial research due to the high cost involved, limited life-span of these drugs and relatively unfavourable return (Projan, 2003). However, the alarming rate of the emergence of multi-drug resistant pathogens has compelled researchers to continue research and development to ensure continued availability of novel antibiotics to combat emerging drug resistant strains (Talbot *et. al.*, 2006).

The ever escalating cost of doing "wet" drug screening coupled with the increase in the sizes of compound libraries have prompted miniaturization in HTS. Generally, miniaturization of HTS results in significant benefits such as increased throughput or turnaround, lowered volume which translates into lower cost of both chemical and biological reagents, and reduced space requirements (reviewed in Burbaum, 1998; Mishra *et. al.*, 2008). Miniaturization also allows more samples to be compressed onto one plate and thus enable replication of experiments which minimizes the impact of error and sample-to-sample variation (Gomez-Hens and Aguilar-Caballos, 2007). However, there are two critical factors to consider when employing microfluidics in miniaturized HTS; 1) handling or moving of sample stocks dissolved in organic solvent into miniaturized formats without contamination (reformatting), and 2) capability to dispense identical droplet of bioreagents into microwell plate containing test samples without cross-contamination (Burbaum, 1998).

In this study, a convenient assay system that employs FP technology was developed for the screening of BPL inhibitors. The Z' factor for both the intra- and inter-assays

demonstrated that this assay satisfied the criteria for HTS. The homogenous assay format, coupled with the accessibility of high density microplates (*i.e.* 384 wells) and automated liquid handling devices, will enable the adaptation of this assay into a miniaturized HTS format suitable for screening of large compound libraries. New classes of BPL inhibitors that bear no structural resemblance to the substrates could potentially be discovered through random screening of large diverse libraries. These compounds, both competitive or allosteric inhibitors, could provide valuable leads for further antibiotic development.

5.4 FUTURE DIRECTION

Medicinal enzyme inhibitors are often judged by specificity and potency. Drugs which have high specificity and potency are more attractive as they post fewer side effects and lower toxicity to humans. These criteria are normally determined by the physico-chemical properties of the drug molecules. Minor changes to the parent molecule can potentially alter the potency, specificity and affinity. This is evident in the antibiotic market today that is saturated with compounds derived from parent molecules discovered several decades ago. However, these products often have a short shelf life as resistance mechanisms against the parent molecule, are also effective against its derivatives. For example, bacteria that have acquired beta lactamase to degrade penicillin through horizontal gene transfer are resistant to not only penicillin but closely related analogues. Therefore, new classes of antibiotics may be less prone to resistance as no pre-existing mechanisms are in place.

Modern technologies have greatly assisted drug discovery programmes. The vast range of *in-silico* resources readily available in databases as well as advance visualization software have enabled computational science to integrate biological, chemical and clinical

data (reviewed in Loging *et. al.*, 2007). This approach can facilitate not only rapid identification of potential new drug leads but also to predict potential risks associated with certain molecules. Additionally, the *in-silico* drug optimization software such as CombiGlide (Schrodinger) enables growing of virtual combinatorial molecule libraries. From a lead molecule, a series of derivatives with various core scaffolds or side-chain substitutions can be generated and evaluated relative to the binding affinities towards the targeted enzyme.

Advances in combinatorial chemistry have also contributed tremendously to the changes in drug discovery. Large diverse libraries of compounds can now be synthesized through various systems. One particular new chemical synthesis known as "click chemistry" was introduced by Sharpless and coworkers (2001). Here, drug like molecules were generated quickly and reliably by joining small units together through heteroatom links (C-X-C) (Kolb *et. al.*, 2001). This approach had led to the uprising of target-templated *in-situ* chemistry (reviewed in Kolb and Sharpless, 2003). Therefore, drug discovery that combines *in-silico* screening, new combinatorial chemistry approaches and HTS is a prospective avenue to move this current project towards a new class of antibiotics targeting BPL.

APPENDICES

Appendix A :

Double reciprocal Lineweaver-Burk plot (adapted from Cleland, 1970)

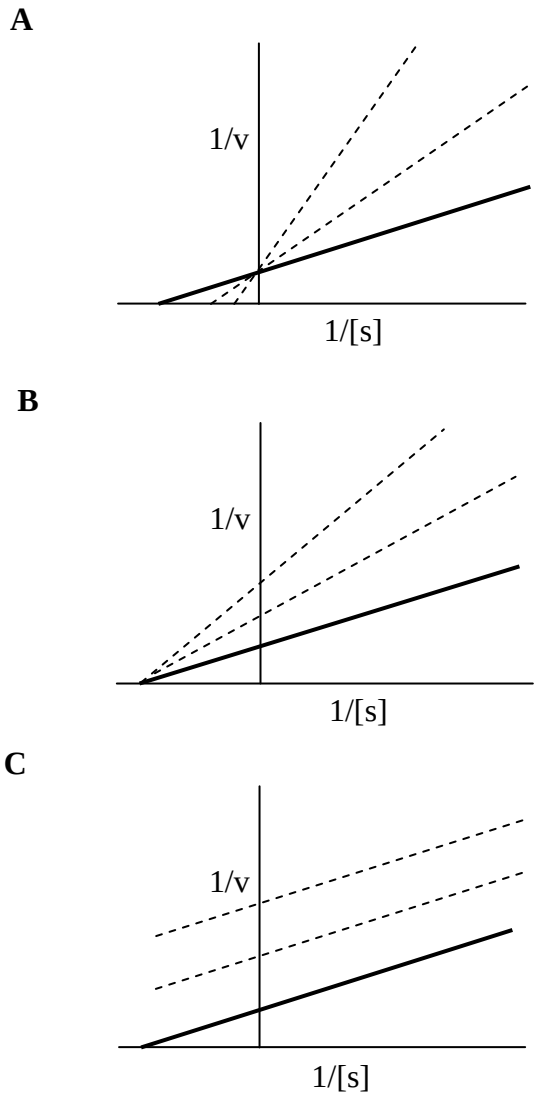

The *x*-axis and *y*-axis represents the reciprocal value of velocity (v) of an enzyme reaction and the substrate concentration ([s]) respectively. Thick lines represent the absence of inhibitor whereas the dotted lines represent the presence of:-

(a) Competitive inhibitor where the lines meet at the *y*-axis,

(b) Non-competitive inhibitor where the lines meet beyond the *y*-axis, and

(c) Uncompetitive inhibitor where the lines are parallel.

Appendix B : Published paper

Ng, B., Polyak, S., Bird, D., Bailey, L., Wallace, J. and Booker, G. (2008)
Escherichia coli biotin protein ligase: characterization and development of a high-throughput assay.
Analytical Biochemistry, v. 376 (1), pp. 131-136, May 2008.

NOTE: This publication is included in the print copy of the thesis held in the University of Adelaide Library.

It is also available online to authorised users at:

http://dx.doi.org/10.1016/j.ab.2008.01.026

REFERENCES

REFERENCES

Akiyama T, Ishida J, Nakagawa S, Ogawara H, Watanabe S, Itoh N, Shibuya M, Fukami Y (1987) Genistein, a specific inhibitor of tyrosine-specific protein kinases. *J Biol Chem* 262: 5592-5595.

Antczak C, Shum D, Escobar S, Bassit B, Kim E, Seshan VE, Wu N, Yang GL, Ouerfelli O, Li YM, Scheinberg DA, Djaballah H (2007) High-throughput identification of inhibitors of human mitochondrial peptide deformylase. *J Biomol Screen* 12: 521-535.

Arora A, Scholar EM (2005) Role of tyrosine kinase inhibitors in cancer therapy. *J Pharmacol Exp Ther* 315: 971-979.

Athappilly FK, Hendrickson WA (1995) Structure of the biotinyl domain of acetyl-coenzyme A carboxylase determined by MAD phasing. *Structure* 3: 1407-1419.

Attwood PV, Wallace JC (2002) Chemical and catalytic mechanisms of carboxyl transfer reactions in biotin-dependent enzymes. *Accounts Chem Res* 35: 113-120.

Baber JC, William AS, Gao YH, Feher M (2006) The use of consensus scoring in ligand-based virtual screening. *J Chem Inf Model* 46: 277-288.

Bagautdinov B, Kuroishi C, Sugahara M, Kunishima N (2005) Crystal structures of biotin protein ligase from *Pyrococcus horikoshii* OT3 and its complexes: Structural basis of biotin activation. *J Mol Biol* 353: 322-333.

Bagautdinov B, Matsuura Y, Bagautdinova S, Kunishima N (2008) Protein biotinylation visualized by a complex structure of biotin protein ligase with a substrate. *J Biol Chem* 283: 14739-14750.

Barker DF, Campbell AM (1980) Use of Bio-Lac fusion strains to study regulation of biotin biosynthesis in *Escherichia coli*. *J Bacteriol* 143: 789-800.

Barker DF, Campbell AM (1981a) The BirA gene of *Escherichia coli* encodes a biotin holoenzyme synthetase. *J Mol Biol* 146: 451-467.

Barker DF, Campbell AM (1981b) Genetic and biochemical characterization of the BirA gene and its product - Evidence for a direct role of biotin holoenzyme synthetase in repression of the biotin operon in *Escherichia coli*. *J Mol Biol* 146: 469-492.

Beckett D, Kovaleva E, Schatz PJ (1999) A minimal peptide substrate in biotin holoenzyme synthetase-catalyzed biotinylation. *Protein Sci* 8: 921-929.

Beckett D, Matthew BW (1997) *Escherichia coli* repressor of biotin biosynthesis. *Methods Enzymol.* 279: 362-376.

Bird DR (2007) Investigation of peptide substrates for biotin protein ligase (Honours thesis) *School of Molecular and Biomedical Science*, University of Adelaide, Adelaide.

Blommel PG, Fox BG (2005) Fluorescence anisotropy assay for proteolysis of specifically labeled fusion proteins. *Anal Biochem* 336: 75-86.

Bogoyevitch MA, Barr RK, Ketterman AJ (2005) Peptide inhibitors of protein kinases - discovery, characterisation and use. *BBA-Proteins Proteom* 1754: 79-99.

Bradford MM (1976) A rapid and sensitive method for the quantitation of microgram quantities of protein utilizing the principle of protein-dye binding. *Anal Biochem* 72: 248-254.

Brown P, Richardson CM, Mensah LM, O'Hanlon PJ, Osborne NF, Pope AJ, Walker G (1999) Molecular recognition of tyrosinyl adenylate analogues by prokaryotic tyrosyl tRNA synthetases. *Bioorgan Med Chem* 7: 2473-2485.

Burbaum JJ (1998) Miniaturization technologies in HTS: How fast, how small, how soon? *Drug Discov Today* 3: 313-322.

Burke TJ, Loniello KR, Beebe JA, Ervin KM (2003) Development and application of fluorescence polarization assays in drug discovery. *Comb Chem High T Scr* 6: 183-194.

Campbell JW, Cronan JE (2001) Bacterial fatty acid biosynthesis: Targets for antibacterial drug discovery. *Annu Rev Microbiol* 55: 305-332.

Campeau E, Gravel RA (2001) Expression in *Escherichia coli* of N- and C-terminally deleted human holocarboxylase synthetase - Influence of the N-terminus on biotinylation and identification of a minimum functional protein. *J Biol Chem* 276: 12310-12316.

Chander Y, Gupta SC, Goyal SM, Kumar K (2007) Perspective - Antibiotics: Has the magic gone? *J Sci Food Agr* 87: 739-742.

Chapman-Smith A, Cronan JE (1999a) The enzymatic biotinylation of proteins: A post-translational modification of exceptional specificity. *Trends Biochem Sci* 24: 359-363.

Chapman-Smith A, Cronan JE (1999b) *In-vivo* enzymatic protein biotinylation. *Biomol Eng* 16: 119-125.

Chapman-Smith A, Forbes BE, Wallace JC, Cronan JE (1997) Covalent modification of an exposed surface turn alters the global conformation of the biotin carrier domain of *Escherichia coli* acetyl-CoA carboxylase. *J Biol Chem* 272: 26017–26022.

Chapman-Smith A, Morris TW, Wallace JC, John E. Cronan J (1999) Molecular recognition in a post-translational modification of exceptional specificity: Mutants of the biotinylated domain of acetyl-CoA carboxylase defective in recognition by biotin protein ligase. *J Biol Chem* 274: 1449–1457.

Chapman-Smith A, Mulhern TD, Whelan F, Cronan JE, Jr., Wallace JC (2001) The C-terminal domain of biotin protein ligase from *E. coli* is required for catalytic activity. *Protein Sci* 10: 2608-2617.

Chapman-Smith A, Turner DL, Cronan JE, Morris TW, Wallace JC (1994) Expression, biotinylation and purification of a biotin domain peptide from the biotin carboxy carrier protein of *Escherichia coli* acetyl-CoA carboxylase. *Biochem J* 302: 881-887.

Checovich WJ, Bolger RE, Burke T (1995) Fluorescence polarization - A new tool for cell and molecular biology. *Nature* 375: 254-256.

Chen I, Choi YA, Ting AY (2007) Phage display of a peptide substrate for yeast biotin protein ligase and application to two-color quantum dot labeling of cell surface protein. *J Am Chem Soc* 129: 6619-6625.

Cheng Y, Prusoff WH (1973) Relationship between the inhibition constant (K_i) and the concentration of inhibitor which causes 50 per cent inhibition (IC_{50}) of an enzymatic reaction. *Biochem Pharmacol* 22: 3099-3108.

Christner JE, Schlesinger MJ, Coon MJ (1964) Enzymatic activation of biotin. *J Biol Chem* 239: 3997-4005.

Clardy J, Fischbach MA, Walsh CT (2006) New antibiotics from bacterial natural products. *Nat Biotechnol* 24: 1541-1550.

Clark RD, Strizhev A, Leonard JM, Blake JF, Matthew JB (2002) Consensus scoring for ligand/protein interactions. *J Mol Graph Model* 20: 281-295.

Cleland WW (1970) Steady State Kinetics. *The Enzymes* 2: 1.

Climent I, Rubio V (1986) ATPase activity of biotin carboxylase provides evidence for initial activation of HCO_3^- by ATP in the carboxylation of biotin. *Arch Biochem Biophys* 251: 465-470.

Coffin J, Latev M, Bi XH, Nikiforov TT (2000) Detection of phosphopeptides by fluorescence polarization in the presence of cationic polyamino acids: application to kinase assays. *Analytical Biochemistry* 278: 206-212.

Cosgrove SE, Sakoulas G, Perencevich EN, Schwaber MJ, Karchmer AW, Carmeli Y (2003) Comparison of mortality associated with methicillin-resistant and methicillin-susceptible Staphylococcus aureus bacteremia: A meta-analysis. *Clin Infect Dis* 36: 53-59.

Cronan JE (1990) Biotination of proteins *in-vivo* - A post-translational modification to label, purify and study proteins. *J Biol Chem* 265: 10327-10333.

Cronan JE, Wallace JC (1995) The gene encoding the biotin-apoprotein ligase of *Saccharomyces cerevisiae*. *Fems Microbiol Lett* 130: 221-229.

Dakshinamurti K, Chauhan J, Ebrahim H (1987) Intestinal absorption of biotin and biocytin in the rat. *Bioscience Rep* 7: 667-673.

du Vigneaud V, Hofmann K, Melville DB (1942) On the structure of biotin. *J Am Chem Soc* 64: 188-189.

Eisenstein E, Beckett D (1999) Dimerization of the *Escherichia coli* biotin repressor: Co-repressor function in protein assembly. *Biochemistry* 38: 13077-13084.

Entcheva P, Phillips DA, Streit WR (2002) Functional analysis of *Sinorhizobium meliloti* genes involved in biotin synthesis and transport. *Appl Environ Microb* 68: 2843-2848.

Fischer PM (2004) The design of drug candidate molecules as selective inhibitors of therapeutically relevant protein kinases. *Curr Med Chem* 11: 1563-1583.

Gerdes SY, Scholle MD, Campbell JW, Balazsi G, Ravasz E, Daugherty MD, Somera AL, Kyrpides NC, Anderson I, Gelfand MS, Bhattacharya A, Kapatral V, D'Souza M, Baev MV, Grechkin Y, Mseeh F, Fonstein MY, Overbeek R, Barabasi AL, Oltvai ZN, Osterman AL (2003) Experimental determination and system level analysis of essential genes in *Escherichia coli* MG1655. *J Bacteriol* 185: 5673-5684.

Gloeckler R, Ohsawa I, Speck D, Ledoux C, Bernard S, Zinsius M, Villeval D, Kisou T, Kamogawa K, Lemoine Y (1990) Cloning and characterization of the *Bacillus sphaericus* genes controlling the bioconversion of pimelate into dethiobiotin. *Gene* 87: 63-70.

Goldstein FW (2007) Combating resistance in a challenging, changing environment. *Clin Microbiol Infec* 13: 2-6.

Gomez-Hens A, Aguilar-Caballos MP (2007) Modern analytical approaches to high-throughput drug discovery. *Trac-Trend Anal Chem* 26: 171-182.

Graves TL, Zhang Y, Scott JE (2008) A universal competitive fluorescence polarization activity assay for S-adenosylmethionine utilizing methyltransferases. *Anal Biochem* 373: 296-306.

Guillen-Navarro K, Araiza G, Garcia-de los Santos A, Mora Y, Dunn MF (2005) The *Rhizobium etli* bioMNY operon is involved in biotin transport. *Fems Microbiol Lett* 250: 209-219.

Hebbeln P, Rodionov DA, Alfandega A, Eitinger T (2007) Biotin uptake in prokaryotes by solute transporters with an optional ATP-binding cassette-containing module. *Proc Natl Acad Sci USA* 104: 2909-2914.

Howes R, Barril X, Dymock BW, Grant K, Northfield CJ, Robertson AGS, Surgenor A, Wayne J, Wright L, James K, Matthews T, Cheung KM, McDonald E, Workman P, Drysdale MJ (2006) A fluorescence polarization assay for inhibitors of Hsp90. *Analytical Biochemistry* 350: 202-213.

Inglis SR, Stojkoski C, Branson KM, Cawthray JF, Fritz D, Wiadrowski E, Pyke SM, Booker GW (2004) Identification and specificity studies of small-molecule ligands for SH3 protein domains. *J Med Chem* 47: 5405-5417.

Jitrapakdee S, Wallace JC (2003) The biotin enzyme family: Conserved structural motifs and domain rearrangements. *Curr Protein Pept Sc* 4: 217-229.

Khachatourians GG (1998) Agricultural use of antibiotics and the evolution and transfer of antibiotic resistant bacteria. *Can Med Assoc J* 159: 1129-1136.

Khedkar SA, Malde AK, Coutinho EC (2006) *In-silico* screening of ligand databases: Methods and applications. *Indian J Pharm Sci* 68: 689 - 696.

Knowles JR (1989) The mechanism of biotin dependent enzymes. *Annu Rev Biochem* 58: 195-221.

Kogl F, Tonis B (1936) Uber das Bios-Problem. Darstellung von krystallisiertem biotin aus Eigelb. *Z Physiol Chem* 242: 43-73.

Kolb HC, Finn MG, Sharpless KB (2001) Click chemistry: Diverse chemical function from a few good reactions. *Angew Chem Int Edit* 40: 2004-2021.

Kolb HC, Sharpless KB (2003) The growing impact of click chemistry on drug discovery. *Drug Discov Today* 8: 1128-1137.

Kwon K, Beckett D (2000) Function of a conserved sequence motif in biotin holoenzyme synthetases. *Protein Sci* 9: 1530-1539.

Laine O, Streaker ED, Nabavi M, Fenselau CC, Beckett D (2008) Allosteric signaling in the biotin repressor occurs via local folding coupled to global dampening of protein dynamics. *J Mol Biol* 381: 89-101.

Lampen JO, Bahleb GP, Peterson WH (1941) The occurence of free and bound biotin. *J Nutr* 23: 11-21.

Lane MD, Lynen F (1963) The biochemical function of biotin VI. Chemical structure of the carboxylated active site of propionyl carboxylase. *Proc Natl Acad Sci U S A* 49: 379-385.

Leon-Del-Rio A, Gravel RA (1994) Sequence requirements for the biotinylation of carboxyl-terminal fragments of human propionyl-CoA carboxylase alpha-subunit expressed in *Escherichia coli*. *J Biol Chem* 269: 22964-22968.

Levitzki A, Gazit A (1995) Tyrosine kinase inhibition - An approach to drug development. *Science* 267: 1782-1788.

Levy SB (1998) The challenge of antibiotic resistance. *Sci Am* 278: 46-53.

Levy SB (2005) Antibiotic resistance - The problem intensifies. *Adv Drug Delivery Rev* 57: 1446-1450.

Liu Y, Jiang J, Richardson PL, Reddy RD, Johnson DD, Kati WM (2006) A fluorescence polarization-based assay for peptidyl prolyl cis/trans isomerase cyclophilin A. *Anal Biochem* 356: 100-107.

Loging W, Harland L, Williams-Jones B (2007) High-throughput electronic biology: mining information for drug discovery. *Nat Rev Drug Discov* 6: 220-230.

Lokesh GL, Rachamallu A, Kumar GDK, Natarajan A (2006) High-throughput fluorescence polarization assay to identify small molecule inhibitors of BRCT domains of breast cancer gene 1. *Anal Biochem* 352: 135-141.

Lynch BA, Loiacono KA, Tiong CL, Adams SE, MacNeil IA (1997) A fluorescence polarization based Src-SH2 binding assay. *Anal Biochem* 247: 77-82.

Lyne PD (2002) Structure-based virtual screening: An overview. *Drug Discov Today* 7: 1047-1055.

Mazel D, Davies J (1999) Antibiotic resistance in microbes. *Cell Mol Life Sci* 56: 742-754.

McAllister HC, Coon MJ (1966) Further studies on the properties of liver propionyl coenzyme A holocarboxylase synthetase and the specificity of holocarboxylase formation. *J Biol Chem* 241: 2855-2861.

McDevitt D, Payne DJ, Holmes DJ, Rosenberg M (2002) Novel targets for the future development of antibacterial agents. *J Appl Microbiol* 92: 28S-34S.

McMahon RJ (2002) Biotin in metabolism and molecular biology. *Annu Rev Nutr* 22: 221-239.

Melville DB, Moyer AW, Hofmann K, Vigneaud VD (1942) The structure of biotin: The formation of thiophenevaleric acid from biotin. *J Biol Chem* 146: 487-492.

Mishra KP, Ganju L, Sairam M, Banerjee PK, Sawhney RC (2008) A review of high throughput technology for the screening of natural products. *Biomed Pharmacother* 62: 94-98.

Murtif VL, Samols D (1987) Mutagenesis affecting the carboxyl terminus of the biotinyl subunit of transcarboxylase - Effects on biotinylation. *J Biol Chem* 262: 11813-11816.

Naganathan S, Beckett D (2007) Nucleation of an allosteric response via ligand-induced loop folding. *J Mol Biol* 373: 96-111.

Nikolovska-Coleska Z, Wang RX, Fang XL, Pan HG, Tomita Y, Li P, Roller PP, Krajewski K, Saito NG, Stuckey JA, Wang SM (2004) Development and optimization of a binding assay for the XIAP BIR3 domain using fluorescence polarization. *Anal Biochem* 332: 261-273.

Onoda T, Iinuma H, Sasaki Y, Hamada M, Isshiki K, Naganawa H, Takeuchi T, Tatsuta K, Umezawa K (1989) Isolation of a novel tyrosine kinase inhibitor, Lavendustin A, from *Streptomyces griseolavendus. J Nat Prod* 52: 1252-1257.

Pai CH (1973) Biotin uptake in biotin regulatory mutant of *Escherichia coli*. *J Bacteriol* 116: 494-496.

Palmer T (1995) Understanding enzymes. *Prentice Hall*, 128-151

Payne DJ, Gwynn MN, Holmes DJ, Pompliano DL (2007) Drugs for bad bugs: confronting the challenges of antibacterial discovery. *Nat Rev Drug Discov* 6: 29-40.

Pendini NR, Bailey LM, Booker GW, Wilce MC, Wallace JC, Polyak SW (2008a) Biotin protein ligase from *Candida albicans*: Expression, purification and development of a novel assay. *Arch Biochem Biophys* 479: 163–169.

Pendini NR, Bailey LM, Booker GW, Wilce MCJ, Wallace JC, Polyak SW (2008b) Microbial biotin protein ligases aid in understanding holocarboxylase synthetase deficiency. *BBA-Proteins Proteom* 1784: 973-982.

Pendini NR, Polyak SW, Bailey L, Booker GW, Wallace JC, Wilce MCJ (2008c) Purification, crystallization and preliminary crystallographic analysis of biotin protein ligase from *Staphylococcus aureus*. *Acta Cryst.* F64: 520–523.

Pereira DA, Williams JA (2007) Origin and evolution of high throughput screening. *Brit J Pharmacol* 152: 53-61.

Perrin F (1926) Polarization de la lumiere de fluorescence. Vie moyenne de molecules dans letat excite. *J Phys Radium* 7: 390-401.

Polyak SW, Chapman-Smith A, Brautigan PJ, Wallace JC (1999) Biotin protein ligase from *Saccharomyces cerevisiae* - The N-terminal domain is required for complete activity. *J Biol Chem* 274: 32847-32854.

Polyak SW, Chapman-Smith A, Mulhern TD, Cronan JE, Jr., Wallace JC (2001) Mutational analysis of protein substrate presentation in the post-translational attachment of biotin to biotin domains. *J Biol Chem* 276: 3037-3045.

Pope AJ, Haupts UM, Moore KJ (1999) Homogeneous fluorescence readouts for miniaturized high-throughput screening: theory and practice. *Drug Discov Today* 4: 350-362.

Prakash OM, Eisenberg MA (1974) Active transport of biotin in *Escherichia coli* K-12. *J Bacteriol* 120: 785-791.

Projan SJ (2003) Why is big Pharma getting out of antibacterial drug discovery? *Curr Opin Microbiol* 6: 427-430.

Reche P, Li YL, Fuller C, Eichhorn K, Perham RN (1998) Selectivity of post-translational modification in biotinylated proteins: The carboxy carrier protein of the acetyl-CoA carboxylase of *Escherichia coli*. *Biochem J* 329: 589-596.

Roberts EL, Shu NC, Howard MJ, Broadhurst RW, Chapman-Smith A, Wallace JC, Morris T, Cronan JE, Perham RN (1999) Solution structures of apo and holo biotinyl domains from acetyl coenzyme A carboxylase of *Escherichia coli* determined by triple-resonance nuclear magnetic resonance spectroscopy. *Biochemistry* 38: 5045-5053.

Rodionov DA, Mironov AA, Gelfand MS (2002) Conservation of the biotin regulon and the BirA regulatory signal in eubacteria and archaea. *Genome Res* 12: 1507-1516.

Rogers T, Lichstein HC (1969) Characterization of the biotin transport system in *Saccharomyces cerevisiae. J Bacteriol* 100: 557-564.

Rudiger M, Haupts U, Moore KJ, Pope AJ (2001) Single molecule detection technologies in miniaturized high throughput screening: Binding assays for G protein-coupled receptors using fluorescence intensity distribution analysis and fluorescence anisotropy. *J Biomol Screen* 6: 29-37.

Said HM (2004) Recent advances in carrier-mediated intestinal absorption of water-soluble vitamins. *Annu Rev Physiol* 66: 419-446.

Saldanha SA, Kaler G, Cottam HB, Abagyan R, Taylor SS (2006) Assay principle for modulators of protein-protein interactions and its application to non-ATP competitive ligands targeting protein kinase A. *Anal Chem* 78: 8265-8272.

Samols D, Thornton CG, Murtif VL, Kumar GK, Haase FC, Wood HG (1988) Evolutionary conservation among biotin enzymes. *J Biol Chem* 263: 6461-6464.

Schade SZ, Jolley ME, Sarauer BJ, Simonson LG (1996) BIODIPY-alpha-casein, a pH-independent protein substrate for protease assays using fluorescence polarization. *Anal Biochem* 243: 1-7.

Schatz PJ (1993) Use of peptide libraries to map the substrate specificity of a peptide-modifying enzyme - A 13 residue consensus peptide specifies biotinylation in *Escherichia coli*. *Bio-Technology* 11: 1138-1143.

Seethala R, Menzel R (1998) A fluorescence polarization competition immunoassay for tyrosine kinases. *Anal Biochem* 255: 257-262.

Shchemelinin I, Sefc L, Necas E (2006) Protein kinase inhibitors. *Folia Biologica* 52: 137-148.

Shenoy BC, Paranjape S, Murtif VL, Kumar GK, Samols D, Wood HG (1988) Effect of mutations at Met-88 and Met-90 on the biotinylation of Lys-89 of the Apo 1.3s subunit of transcarboxylase. *Faseb J* 2: 2505-2511.

Shenoy BC, Xie Y, Park VL, Kumar GK, Beegen H, Wood HG, Samols D (1992) The importance of methionine residues for the catalysis of the biotin enzyme, transcarboxylase - Analysis by site-directed mutagenesis. *J Biol Chem* 267: 18407-18412.

Smith PK, Krohn RI, Hermanson GT, Mallia AK, Gartner FH, Provenzano MD, Fujimoto EK, Goeke NM, Olson BJ, Klenk DC (1985) Measurement of protein using bicinchoninic acid. *Anal Biochem* 150: 76-85.

Sportsman JR, Leytes LJ (2000) Miniaturization of homogeneous assays using fluorescence polarization. *Drug Discov Today*: 27-32.

Stahura FL, Bajorath M (2005) New methodologies for ligand-based virtual screening. *Curr Pharm Design* 11: 1189-1202.

Stolz J (2003) Isolation and characterization of the plasma membrane biotin transporter from Schizosaccharomyces pombe. *Yeast* 20: 221-231.

Streaker ED, Beckett D (1998) Coupling of site-specific DNA binding to protein dimerization in assembly of the biotin repressor biotin operator complex. *Biochemistry* 37: 3210-3219.

Streaker ED, Beckett D (2003) Coupling of protein assembly and DNA binding: Biotin repressor dimerization precedes biotin operator binding. *J Mol Biol* 325: 937-948.

Suzuki Y, Aoki Y, Sakamoto O, Li X, Miyabayashi S, Kazuta Y, Kondo H, Narisawa K (1996) Enzymatic diagnosis of holocarboxylase synthetase deficiency using apo-carboxyl carrier protein as a substrate. *Clin. Chim. Acta* 251: 41-52.

Swift R (2003) Domain mapping and functional analysis of human biotin protein ligase (Honours thesis) *School of Molecular and Biomedical Science,* University of Adelaide, Adelaide.

Talbot GH, Bradley J, Edwards JE, Gilbert D, Scheld M, Bartlett JG (2006) Bad bugs need drugs: an update on the development pipeline from the Antimicrobial Availability Task Force of the Infectious Diseases Society of America. *Clin Infect Dis* 42: 1065-1065.

Terpetschnig E, Szmacinski H, Lakowicz JR (1995) Fluorescence polarization immunoassay of a high-molecular-weight antigen based on a long-lifetime Ru-ligand complex. *Anal Biochem* 227: 140-147.

Thanassi JA, Hartman-Neumann SL, Dougherty TJ, Dougherty BA, Pucci MJ (2002) Identification of 113 conserved essential genes using a high-throughput gene disruption system in *Streptococcus pneumoniae. Nucleic Acids Res* 30: 3152-3162.

Tissot G, Job D, Douce R, Alban C (1996) Protein biotinylation in higher plants: Characterization of biotin holocarboxylase synthetase activity from pea (*Pisum sativum*) leaves. *Biochem J* 314: 391-395.

Trinquet E, Mathis G (2006) Fluorescence technologies for the investigation of chemical libraries. *Mol Biosyst* 2: 380-387.

von Ahsen O, Bomer U (2005) High-throughput screening for kinase inhibitors. *Chembiochem* 6: 481-490.

Walters WP, Stahl MT, Murcko MA (1998) Virtual screening - An overview. *Drug Discov Today* 3: 160-178.

Weaver LH, Kwon K, Beckett D, Matthews BW (2001) Corepressor-induced organization and assembly of the biotin repressor: a model for allosteric activation of a transcriptional regulator. *Proc Natl Acad Sci U S A* 98: 6045-6050.

Wenzel RP (2004) The antibiotic pipeline - Challenges, costs, and values. *New Engl J Med* 351: 523-526.

Wesche H, Xiao SH, Young SW (2005) High throughput screening for protein kinase inhibitors. *Comb Chem High T Scr* 8: 181-195.

Wilson KP, Shewchuk LM, Brennan RG, Otsuka AJ, Matthews BW (1992) *Escherichia coli* biotin holoenzyme synthetase biorepressor crystal-structure delineates the biotin-binding and DNA-binding domains. *P Nat Acad Sci USA* 89: 9257-9261.

Wood HG (1977) Biotin Enzymes. *Ann. Rev. Biochem* 46: 385-413.

Wood ZA, Weaverl LH, Brown PH, Beckett D, Matthews BW (2006) Co-repressor induced order and biotin repressor dimerization: A case for divergent followed by convergent evolution. *J Mol Biol* 357: 509-523.

Xiang S, Tong L (2008) Crystal structures of human and *Staphylococcus aureus* pyruvate carboxylase and molecular insights the carboxyltransfer reaction. *Nature Struct. Mol. Biol.* 15: 295–302.

Xu Y, Beckett D (1994) Kinetics of biotinyl-5'-adenylate synthesis catalyzed by the *Escherichia coli* repressor of biotin biosynthesis and the stability of the enzyme-product complex. *Biochemistry* 33: 7354-7360.

Xu Y, Johnson CR, Beckett D (1996) Thermodynamic analysis of small ligand binding to the *Escherichia coli* repressor of biotin biosynthesis. *Biochemistry* 35: 5509-5517.

Xu Y, Nenortas E, Beckett D (1995) Evidence for distinct ligand-bound conformational states of the multifunctional *Escherichia coli* repressor of biotin biosynthesis. *Biochemistry* 34: 16624-16631.

Zempleni J (2005) Uptake, localization, and noncarboxylase roles of biotin. *Annu Rev Nutr* 25: 175-196.

Zhang JH, Chung TDY, Oldenburg KR (1999) A simple statistical parameter for use in evaluation and validation of high throughput screening assays. *J Biomol Screen* 4: 67-73.